ABSTRACT

TAGGART, MATTHEW. Surface Shading, Soil Temperature, and Soil Moisture Effects on Soil C Loss in a Temperate Peatland. (Under the direction of Joshua Heitman).

Histosols are a huge reservoir for C, covering < 1% of the world's land surface but holding up to 12% of total soil C. Thorough comprehension of factors controlling the rate of soil C loss from peatlands is critical for proper management of these C sinks. Three experiments evaluated how formerly cultivated, warm-climate Histosols undergoing restoration efforts might respond to increasing water content via water table re-establishment and decreases in soil temperatures via vegetative shading. We compared temperature and soil CO_2 efflux differences from intact soil cores, collected from Juniper Bay, under three levels of light reduction in a greenhouse: 0%, 70%, and 90%. Soil in full sun was consistently warmer and showed higher efflux rates than 70% and 90% shade treatments: 4.132, 3.438, and 2.054 μmol CO_2 m^{-2} s^{-1}, respectively. Shade treatments reached peak efflux rates at similar water potential, -2 to -4 kPa. A field experiment at Juniper Bay subjected in-situ soil to full sun, 70% light reduction, and light reduction from naturally occurring herbaceous vegetation. Shade treatment effects on soil temperature and C mineralization were evident throughout the growing season. Vegetation shade effects on soil temperature were greatest in August and September when soil under vegetation was 5°-11°C cooler than unshaded soil. Soil CO_2 efflux was correlated strongly with soil temperature; daily efflux rates were consistently highest from unshaded soil. Efflux across treatments showed a strong seasonal correlation to soil moisture, increasing as soil dried in response to water table decline. Soil water potential was unaffected by shade treatment, suggesting temperature effects were solely responsible for efflux differences between treatments. C mineralization response to temperature and moisture was verified with lab incubations of soil material at 25° and 37°C for three moisture ranges. Temperature sensitivity of soil organic matter decomposition rates are often described by Q_{10} values calculated with the Arrhenius equation. Incubations showed a temperature/moisture

interaction suggesting decomposition was more temperature sensitive in wet soil ($0.40\ m^3\ m^{-3}$) than dry soil ($0.15\text{-}0.16\ m^3\ m^{-3}$), Q_{10} 2.55 and 1.64, respectively. All results confirm surface shading has a strong influence on soil temperatures and C mineralization rates. Thoughtful management of vegetative shading in mitigated peatlands may be an effective strategy for slowing soil C losses and promoting soil C sequestration.

Surface Shading, Soil Temperature, and Soil Moisture Effects on Soil C Loss in a Temperate Peatland

by
Matthew J. Taggart

A thesis submitted to the Graduate Faculty
of North Carolina State University
in partial fulfillment of the
Requirements for the Degree of
Master of Science

Soil Science

Raleigh, North Carolina

2010

APPROVED BY:

_____	_____
Michael R. Burchell II	Michael J. Vepraskas

_____
Joshua L. Heitman
Chair of Advisory Committee

BIOGRAPHY

Matthew Taggart was born to Larry and Jean Taggart in Butler, Pennsylvania on May 31, 1982. He was raised with his older sister, Amy, and twin brother, Chris, in the small town of Slippery Rock. Spending the majority of his childhood in the woods with his siblings, Matt developed a love for the outdoors at an early age. He graduated from Slippery Rock High school in 2001 and received his Bachelor of Science in environmental geosciences from Slippery Rock University in 2007. In the fall of 2007 Matt was admitted to the North Carolina State University soil science program. He has since worked under the guidance of Dr. Joshua Heitman.

ACKNOWLEDGMENTS

I owe an enormous debt of gratitude to my advisor, Dr. Josh Heitman, for taking me under his wing just as my hopes for a 'funded' research project were beginning to wane. His encouragement and support were central to my success in research and academics. My committee members', Dr. Michael Vepraskas and Dr. Mike Burchell, assistance with interpretation of my results and impeccable proof-reading were invaluable for helping me write a scientifically sound document. I would also like to thank Adam Howard and Chris Niewoehner for their assistance in the lab and field. Their willingness to help with logistics, labor, and anything else I needed always exceeded my expectations. Consuelo Arellano was enormously helpful with all my statistical analyses. She took many hours out of her schedule to help analyze the vast amounts of data collected over my three experiments. I also owe thanks to Dan Bowman and Tom Sauer for generously lending equipment I would have otherwise been without.

Finally, I'd like to thank my wonderful fiancée, Diana, and my family. Diana has been my rock since we moved to Raleigh and her steadfast support has been beyond compare. My parents, Larry and Jean, have always encouraged me to do my best and I hope I've made them proud. There are many others to whom I owe my gratitude. Thank you.

TABLE OF CONTENTS

LIST OF TABLES

LIST OF FIGURES

Chapter 1: Literature Review

Introduction

Soil is the third largest reservoir of carbon in the biosphere, holding an estimated 1456 Pg C (Schlessinger, 1977). With approximately twice the C capacity of the atmosphere (750 Pg C), soil has the potential for storing excess atmospheric C and mitigating the effects of global climate change. An important factor of soil C sequestration is mean residence time of the stored C, with longer residence times more favorable for sequestration. Raich and Schlessinger (1992) estimated turnover rates for soil C varied between 10 yr in tropical grasslands and 490 and 520 yr in tundra and swamps and marshes, respectively. These values suggest cold and/or wet soils have the highest potential for storing and holding atmospheric C and should therefore receive a significant proportion of research interest.

Cold and/or wet soils have increased soil C storage potential for one of two reasons; oxygen availability or metabolism kinetics. When soils flood, pores fill with water and oxygen is displaced. Aerobic microbes soon use all available O_2 and conditions become anaerobic or reduced. Under reducing conditions, soil organic matter decomposition is much less efficient and slows dramatically (Atlas and Barth, 1981 and Mitsch and Gosselink, 1993). In cold soils, microbial decomposition again slows drastically. The Arrhenius equation, originally used to describe chemical reaction rates, has also been used to describe microbial decomposition (Wiant, 1967). Essentially, microbial decomposition increases or decreases by a certain magnitude for every 10°C increase or decrease in temperature. Where microbial decomposition is significantly limited by O_2 availability and low temperatures, soil C deposits exceed losses and soil C is stored.

When soil C deposition exceeds loss for thousands of years, the potential for development of Histosols is high. Histosols are soils containing more than 12 to 20% organic carbon (depending

on clay content) within the upper 40 cm and are saturated with water for 30 days or more in normal years of precipitation (Soil Survey Staff, 1992). These highly organic soils cover a little over 1% of the global land area but estimates suggest almost 23% of global soil C (Eswaran, et al., 1993). Also referred to as peatlands, Histosols are normally found in northern latitudes where cool soil temperatures limit soil organic matter (SOM) oxidation, which leads to an accumulation of SOM (Everett, 1983). A smaller percentage of Histosols can be found in mid-latitude temperate climates where a high water table or tidal influences create reducing conditions conducive to organic matter accumulation. In the United States, the majority of these temperate Histosols are located in Minnesota, Wisconsin, Michigan, Florida, Louisiana, and North Carolina (NRCS, 2009). To date, the majority of research focuses on Histosols located in areas of mesic and colder soil temperature regime e.g. (Dinsmore et al., 2009; Gorham, 1991; Kettridge and Baird, 2007). Consequently, more research regarding warm-climate Histosols is needed to understand the global soil C pool.

The nearly 600,000 ha of Histosols of North Carolina are almost entirely restricted to the Lower Coastal Plain and tidewater region (Lilly, 1981). Organic soils in the lower coastal plain primarily develop where flat topography, wide interstream divides, and clay lenses combine to create areas of poor drainage with a seasonal high water table at or very near the surface (Lilly, 1981) for a large portion of the year. Wetlands found on these upland interstream divides are called Pocosins, a word thought to come from the Eastern Algonquin language for “swamp on a hill” (Tooker, 1899).

Carolina Bays

Inland Histosols of North Carolina are not exclusive to the interstream divides of the Lower Coastal Plain. They can also be found in the interior of Carolina bays (Daniels et al., 1984). Carolina bays are unique geologic features found along the Atlantic seaboard from New Jersey to

Florida. These northwest to southeast oriented elliptical depressions range in size from less than one to 3,600 ha and are of unknown origin (Prouty, 1952). Today, few pristine bays remain intact; the majority have been logged, drained, and used for agronomic production (Kirkman et al., 1996). Drainage and conventional agriculture can have significant impact on the topography of a Carolina bay.

One of the most profound impacts of draining Carolina bays for agriculture is sinking of the land surface via primary and secondary subsidence. The loss of buoyant force after drainage leads to sinking, i.e., primary subsidence. Secondary subsidence decreases land surface elevations due to microbial decomposition of soil organic matter, loss by fire, and shrinking (Terzaghi, 1943). Of primary importance to C budgeters is the loss of C due to organic matter decomposition. Ewing and Vepraskas (2006) evaluated the rates of subsidence in a Carolina bay 15, 20, and 30 years after drainage. They estimated that primary and secondary subsidence decreased the land surface by approximately 121 cm after 30 years of drainage. Secondary subsidence was responsible for one-third of the total subsidence and occurred at a rate between 1.7 and 2.8 cm yr^{-1}. While secondary subsidence cannot be easily separated into its main components of oxidation and shrinkage (Ewing and Vepraskas, 2006), it can be assumed that the losses due to C oxidation are significant. These researchers suggest that subsidence, and therefore oxidative C loss, could be decreased by restoring the water table to near-surface levels outside the growing season. Efforts to further reduce C loss could entail restoring the wetland and keeping the water table high indefinitely.

Depressional wetlands, such as Carolina bays, have been recognized for performing high value functions including wildlife habitat, surface water storage, and water quality improvement (Whigham, 1999). The high value functions inherent to depressional wetlands have created some demand for disturbed Carolina bays as attractive wetland mitigation sites. For example, 16 of 20

bays were deemed fit for and restored to previous function in a non-industrialized management area of South Carolina (Barton, 2008). With the high likelihood for restoration of more Carolina bays, it remains important to understand how soil C mineralization will respond in these organic soils.

Land Use Change and C Loss

Land use change has a large impact on vegetation and microclimate, two soil forming factors. Effects of land clearing and deforestation on soil have been documented (Lewis, 1998; Lal and Cummings, 1979; Grace et al., 2006; Fearnside and Barbosa, 1998; Cunningham, 1963) in addition to impacts of secondary succession and reforestation (Bautista-Cruz and Castillo, 2005; Belsky et al., 1989; Guo and Gifford, 2002; Mathes and Schriffer, 1985; Post and Kwon, 2000). Results generally indicate a loss of soil carbon and increased soil temperatures following deforestation and soil C sequestration and decreased soil temperatures during secondary succession and reforestation.

Lewis (1998) compared subsurface soil temperatures in forested and cleared areas of Vancouver Island. Soil temperatures were logged at 30 to 60 cm below the soil surface for 1 yr. The coolest temperatures were observed at sites with a high water table and a full tree canopy. Sites with no tree cover and deep water tables had ground surface temperatures 1 to 2°C warmer than the coolest sites.

Observed temperature differences between forested and cleared sites can be an order of magnitude greater in tropical climates. Lal and Cummings (1979) evaluated soil temperature changes after three methods of land clearing in Nigerian lowland forest: slash, slash and burn, and bulldozing. Peak daytime soil temperature at 1 cm depth were 25° to 20°C warmer in the bulldozed and slashed sites compared to an intact reference forest. Soil temperature differences

were attenuated with depth in the profile. At 5 cm, the bulldozed and slashed sites were 12° and 10°C warmer, respectively.

The influence of a mature forest on soil and microclimate were detailed by Belskey et al. (1989). The researchers measured total solar radiation and soil temperature at 5 and 10 cm to quantify soil and microclimate differences between forest sites and adjacent grassland in semi-arid savanna in Kenya. A single day measurement showed solar radiation was reduced by as much as 65% under the tree canopy. Soil temperature differences between forested and grassland sites varied during the 2 yr experiment. Initially, grass coverage was between 50% and 70% and soil temperature at 5 cm was 32° to 34°C. When grass coverage increased to 90% to 100%, soil temperatures dropped to 28° to 30°C. Soil temperatures were lowest under tree canopy, 23° to 25°C.

Cunningham (1963) observed increases in soil temperature in addition to significant losses of soil C after deforestation. Mean daily soil temperature at 7.5 cm under bare soil was 6°C higher than those soil temperatures observed in a forested reference, and 11°C higher than soil under total sunlight elimination. Soil C decreased most rapidly in the fully exposed soil, from 1.8% to 1.4% total organic carbon (TOC) within 3 mo of clearing. Soil C decreased less rapidly where the soil was completely shaded and soil temperatures were lowest, from 1.8% to 1.6%. During the 3 yr experiment, TOC decreased to a minimum of 1.05% in the fully exposed site and 1.5% in the fully shaded site.

Research regarding land use change on soil temperature and C dynamics has generally focused on deforestation and C loss. The literature summarized above shows that loss of vegetation can lead to increased soil temperatures and decreases in soil C stocks. More information is needed to describe how reforestation and vegetation establishment will affect the soil and whether

decreases in soil C loss with time should be expected. Unfortunately, vegetation reestablishment is a much slower process than deforestation, which may explain the gap in the literature.

Laboratory Incubations

A multitude of laboratory experiments have been performed to elucidate the individual and combined effects of temperature and soil moisture on soil C mineralization (Asada and Warner, 2005; Bowden et al., 1998; Fang and Moncrieff, 2001; Fang et al., 2005; Ilstedt et al., 2000; Reichstein et al., 2000; Reichstein et al., 2005; Yuste et al., 2007; Zak et al., 1999). Temperature effects on C mineralization are typically reported as a Q_{10} value, often calculated with the Arrhenius equation. Q_{10} is a temperature coefficient used to describe the rate of change of a chemical or microbiological process in response to a 10°C increase in temperature. Optimum soil moisture content for peak C mineralization rate and the response of mineralization to dryer and wetter conditions are often reported to characterize soil moisture effects. Both temperature and soil moisture effects are critical to understanding how the soil C storage dynamic of Carolina bays will be affected by restoration.

Reichstein et al. (2005) incubated eight mineral soil and eight organic soil intact cores for 90 d. Two moisture treatments were applied, a wet treatment where soil moisture remained constant (-10 kPa for mineral soil and -30 kPa for organic soil) and a dry-rewet treatment where cores were allowed to dry from -10 to -160 kPa (mineral soil) and -40 to -155 kPa (organic soil). Incubation temperature followed a diurnal cycle from 7 to 23°C. The researchers found a positive correlation between CO_2 evolution and soil temperature with a Q_{10} value of 2.7, or a 2.7 fold increase in C mineralization for every 10°C temperature increase. Raich and Schlessinger (1992) reviewed measured rates of soil respiration and calculated a median Q_{10} value of 2.4.

Bowden et al. (2005) evaluated moisture and temperature effects by incubating mineral soil material and material from the overlying, highly organic Oi horizon. Five moisture treatments, 20%, 40%, 60%, 80% and 100% water holding capacity (WHC), were applied and the soil material was incubated at 9°, 12.5°, 16.5°, 20°, or 25°C for 48 h. C mineralization was evaluated by measuring CO_2 efflux rates. A positive relationship between efflux and temperature was observed from both soil materials, with much higher total respiration rates from the organic material than the mineral soil. Q_{10} values at 50% WHC were 2.39 for mineral soil and 2.03 for organic material. For the mineral soil, the highest rates of C mineralization were observed at 60% WHC. Efflux was less sensitive to moisture in the mineral soil than in the organic one. Maximum efflux occurred at nearly 80% WHC from the organic material.

Reichstein et al. (2000) designed a long term, 104 d, incubation to test C mineralization temperature sensitivity of soil material from an Oa-Oe and an A horizon. Soil material was brought to 60% WHC and incubated at 5°, 15°, and 25°C. Material from both the Oa-Oe layer and A-horizon showed a positive relationship between temperature and C respiration. Calculated Q_{10} values were 2.5 and 2.8, respectively.

Fang and Moncrieff (2001) incubated intact soil cores to evaluate temperature and moisture effects on C mineralization. Incubation temperature began at 10°C and was incrementally increased in 3°C steps to a maximum of 40°C. The cores were then cooled to 10°C with the same incremental approach. Three soil moisture treatments were applied: volumetric water content of 40-50%, 30%, or 20%. Very little moisture effect was observed during the 120 day incubation because "inhibition of soil moisture content on CO_2 efflux is significant only at its lower end (dry soil) or higher end (wet soil)". Respiration rate increased exponentially with temperature and Fang and Moncrieff (2001) used 10 different models for calculating Q_{10}. Their Q_{10} values ranged from 1.5 at 30° C to 8.8 at 10°C. The authors concluded the Arrhenius model provided the best estimate for Q_{10}.

Ilstedt et al. (2000) designed a study to determine ideal soil water content for soil C respiration in mineral and organic soils. Three mineral soils and a highly organic soil (LOI 95.6% w w^{-1}) were incubated at 20°C. While optimum respiration rates were achieved at similar WHC (43 to 48%), respiration in the mineral soil decreased much more dramatically than in the organic soil when soil moisture reached air dry or saturation. The researchers concluded soil moisture limits soil respiration less in organic soils than in mineral soils.

Results from nearly all laboratory incubations investigating temperature effects on soil C mineralization agree that it is a temperature dependent process. Disagreement arises when attempting to describe the magnitude of response to changes in temperature, or Q_{10}. Most incubations focus on a mineral soil or specific substrate. Many incubations probing temperature influence on peatlands focus on the Oi horizon rather than the less abundant Oa horizon. Q_{10} can vary widely, so it becomes important to determine site specific Q_{10} when investigating temperature effects on C mineralization.

Field Experiments Controlling Microclimate

A variety of less standardized experiments have been conducted to further investigate environmental impacts on C loss in more complex, 'realistic' environments. Some researchers have conducted soil warming experiments in the field to simulate the anticipated effect of global climate change (Bridgham et al., 1999; Harte et al., 1995; Lukewille and Wright, 1997; Peterjohn et al., 1994; Tingey et al., 1996) while others have used shading to reduce solar radiation and cool the soil (Cunningham, 1963; Shaver and Jonasson, 1999).

Several methods of raising soil temperature can be found in the literature. One of the more common methods is the use of heating cables, both buried and on the surface. Lukewille and Wright (1997) effectively raised the soil temperature of a 400 m^2 forested plot 3° to 5°C above

ambient by placing electric heating cables 10 cm apart below the litter layer. Soil temperature was monitored via thermocouples was affected as deep as 30 cm. The affect of warming on C loss was not evaluated for this experiment.

Peterjohn et al. (1994) buried electric heating cables in a similar experiment. The cables were placed at a depth of 10 cm at 20 cm spacings and successfully increased soil temperature to 5°C above ambient. The unavoidable soil disturbance that accompanied the heating cable placement resulted in an artificial CO_2 efflux increase. The researchers found that CO_2 efflux increased exponentially with increasing soil temperature and estimated the annual soil C flux may increase from 712 g m^{-2} to 1250 g m^{-2} in response to a 5°C rise in soil temperature. A potential problem with the soil cable heat source is that it does not replicate the natural system. The primary source of heat input to the soil, solar radiation, enters at the soil-atmosphere boundary. A buried heating cable creates a zone of artificially high soil temperature closest to the cable that cannot be avoided.

Harte et al. (1995) used overhead infrared radiators to better replicate the downward heat flux of solar radiation. The infrared heaters contributed an additional 15 W m^{-2} to the soil surface and increased soil temperatures by as much as 6° at 5 cm and 3.3°C at 25 cm. Peak temperature differences between heated and control plots were observed near the soil surface at midday when light intensity was highest. Harte et al. noticed that: (1) the heaters raised soil temperatures most in areas of lowest soil moisture, (2) the infrared heaters accelerated soil water loss via evaporation in dryer plots and transpiration in wetter plots, and (3) vegetative cover affected the temperature difference between heated and control plots. The latter point is especially significant because the researchers found that vegetative cover may have a greater influence than soil moisture on soil response to heating.

Bridgham et al. (1999) used a method similar to Harte et al. (1995) for their soil warming experiment. Infrared lamps were placed to add an additional 191 W m^{-2} or 78 W m^{-2} to a bog and fen soil. Two years of data showed the highest infrared treatment produced soil temperatures at 15 cm 3° and 2.2°C warmer than the control from May to October. No significant temperature difference was recorded during the winter months.

Cunningham (1963) studied the impact of clearing a tropical forest soil on physical and chemical properties. In this study, he subjected the soil to three exposure treatments: full sun, 50% shade, and 100% shade. For 50% shade, Cunningham constructed a set of wooden frames covered with 2.5 cm aluminum strips with 2.5 cm spacing 46 cm above the soil surface. Full shade was achieved by covering the frames with aluminum sheeting perforated to permit rainfall. Daily maximum temperature was recorded at 7.5 cm. Mean maximum daily soil temperature had a positive correlation with light intensity; full sun > 50% shade > full shade. Values were 38°, 32°, and 27°C, respectively.

Problem Statement

Wetland restoration and the subsequent secondary vegetative succession can significantly change soil temperature, moisture, and carbon dynamics. The former two have been shown to strongly influence C respiration on an individual and interacting basis. There are a number of soil factors that complicate moisture and temperature effects, including soil type (mineral vs. mucky), landscape position, vegetation, bulk density, and others. The majority of research relating temperature and moisture effects to C storage in Histosols focuses on those found in mesic and colder soil temperature regimes. The lack of abundant Histosols in warmer climates has resulted in a deficiency in the literature explaining how these warmer, and often muckier, soils will respond to changes in soil water and temperature. The impetus for my work was to gauge how the soil C

dynamic of drained and farmed organic soils in Carolina bays will respond to water table re-establishment and reductions in total solar irradiance that often accompany restoration.

Research Objectives and Thesis Organization

The objectives of this investigation were to: (1) evaluate how decreasing solar irradiance accompanying simulated secondary succession will affect soil temperature and moisture in a thermic Histosol, (2) determine how soil CO_2 respiration will respond to changes in soil temperature controlled by reductions in total solar irradiance, and (3) observe water table effects on CO_2 respiration rates.

Three experiments were used to achieve these general objectives. The first two, a greenhouse study and field study, were conducted to subject the soil of interest to microclimate conditions controlled largely by solar irradiance intensity (Chapter 2). During a third study, laboratory incubations were performed to gather temperature and moisture effects on soil CO_2 respiration in the absence of complicating environmental factors (Chapter 3). Chapter 4 provides a summary of the previous chapters and general conclusions based on this work.

REFERENCES:

Asada, T. and B.G. Warner. 2005. Surface peat mass and carbon balance in a hypermaritime peatland. Soil Sci. Soc. Am. J. 69:549-562.

Barton, D.B., D.M. Andrews, and R.K. Kolka. 2008. Evaluating hydroperiod response in restored Carolina bay wetlands using soil physiochemical properties. Restor. Ecol. 16:668-677.

Bautista-Cruz, A. and R.F. del Castillo. 2005. Soil changes during secondary succession in a tropical montane cloud forest area. Soil Sci. Soc. Am. J. 69:906-914.

Belsky, A.J., R.G. Amundson, J.M. Duxbury, S.J. Riha, A.R. Ali, S.M. Mwonga. 1989. The effects of trees on their physical, chemical, and biological environments in a semi-arid savanna in Kenya. J. Appl. Ecol. 26:1005-1024.

Bowden, R.D., K.M. Newkirk, G.M. Rullo. 1998. Carbon dioxide and methane fluxes by a forest soil under laboratory-controlled moisture and temperature conditions. Soil Biol. Biochem. 30:1591-1597.

Bridgham, S.D., J. Pastor, K. Updegraff, T.J. Malterer, K. Johnson, C. Harth, and J. Chen. 1999. Ecosystem control over temperature and energy flux in northern peatlands. Ecol. Appl. 9:1345-1358.

Cunningham, R.K. 1963. The effect of clearing a tropical forest soil. J. Soil. Sci. 14:334-345.

Daniels, R.B., H.J. Kleiss, S.W. Buol, H.J. Byrd, and J.A. Phillips. 1984. Soil systems in North Carolina. North Carolina Agricultural Research Service Technical Bulletin No. 181. North Carolina State Univ., Raleigh, NC.

Dinsmore, K.J., U.M. Skiba, M.F. Billett, and R.M. Rees. 2009. Effect of water table on greenhouse gas emissions from peatlands mesocosms. Plant Soil 318:229-242.

Eswaran, H., E. Van Den Berg, and P. Reich. 1993. Organic carbon in soils of the world. Soil Sci. Soc. Am. J. 57:192-194.

Everett, K.R. 1983. Histosols. p. 1-53 *In* L.P. Wilding, N.E. Schmeck, and G.F. Halls (ed.) Pedogenesis and Soil Taxonomy, II. Elsevier, Amsterdam.

Ewing, J.M. and M.J. Vepraskas. 2006. Estimating primary and secondary subsidence in an organic soil 15, 20, and 30 years after drainage. Wetlands 26:119-130.

Fang, C. and J.B. Moncrieff. 2001. The dependence of soil CO_2 efflux on temperature. Soil Biol. Biochem. 33:155-165.

Fang, C., P. Smith, J.B. Moncrieff, and J.U. Smith. 2005. Similar response of labile and resistant soil organic matter pools to changes in temperature. Nature 433:57-59.

Fearnside, P.M. and R.I. Barbosa. 1998. Soil carbon changes from conversion of forest to pasture in Brazilian Amazonia. Forest Ecol. Manag. 108:147-166.

Gorham, E. 1991. Northern peatlands: role in the carbon cycle and probable response to climatic warming. Ecol. Appl. 1: 182-195.

Grace, J.M., R.W. Skaggs, and D.K. Cassel. 2006. Soil physical changes associated with forest harvesting operations on an organic soil. Soil Sci. Soc. Am. J. 70:503-509.

Guo, L.B. and R.M. Gifford. 2002. Soil carbon stocks and land use change: a meta analysis. Glob. Change Biol. 8:345-360.

Harte, J., M.S. Torn, F. Chang, B. Feifarek, A.P. Kinzig, R. Shaw, and K. Shen. 1995. Global warming and soil microclimate: results from a meadow-warming experiment. Ecol. Appl. 5:132-150

Ilstedt, U., A. Nordgren, and A. Malmer. 2000. Optimum soil water for soil respiration before and after amendment with glucose in humid tropical acrisols and a boreal mor layer. Soil Biol. Biochem. 32:1591-1599.

Kettridge, N. and A. Baird. 2007. In situ measurements of the thermal properties of a northern peatland: Implications for peatland temperature models. J. Geophys. Res. 112: 1-12.

Kirkman, L.K., R.F. Lide, G. Wein, and R.R. Sharitz. 1996. Vegetation changes and land-use legacies

of depression wetlands of the western coastal plain of South Carolina. Wetlands 16:564-576.

Lewis, T. 1998. The effect of deforestation on ground surface temperatures. Global Planet Change. 18:1-13.

Lal, R. and D.J. Cummings. 1978. Clearing a tropical forest soil. I. Effects on soil and micro-climate. Field Crop Res. 2:91-107.

Lilly, J.P. 1981. The blackland soils of North Carolina: their characteristics and management for agriculture. North Carolina Agricultural Experiment Station. Bulletin 270. North Carolina State Univ. Raleigh, NC.

Lükewille, A. and R.F. Wright. 1997. Experimentally increased soil temperature causes release of nitrogen at a boreal forest catchment in southern Norway. Glob Change Biol. 3:13-21.

Mathes, K. and T.H. Schriffer. 1985. Soil respiration during secondary succession: influence of temperature and moisture. Soil Biol. Biochem. 17:205-211.

Peterjohn, W.T., J.M. Melillo, P.A. Steudler, K.M. Newkirk, F.P. Bowles, and J.D. Aber. 1994. Responses of trace gas fluxes and N availability to experimentally elevated soil temperatures. Ecol. Appl. 4:617-625.

Post, W.M. and K.C. Kwon. 2000. Soil carbon sequestration and land-use change: processes and potential. Glob. Change Biol. 6:317-328.

Prouty, W.F. 1952. Carolina bays and their origin. Geol. Soc. Am. Bull. 63:167-224.

Raich, J.W. and W.H. Schlesinger. 1992. The global carbon dioxide flux in soil respiration and its relationship to vegetation and climate. Tellus. 44B:81-99.

Reichstein, M., F. Bednorz, G. Broll, and T. Kätterer. 2005. Does the temperature sensitivity

of decomposition of soil organic matter depend upon water content, soil horizon, or incubation time? Glob. Change Biol. 11:1754-1767.

Reichstein, M., J. Subke, A.C. Angeli, and J.D. Tenhunen. 2000. Temperature dependence of carbon mineralisation: conclusions from a long-term incubation of subalpine soil samples. Soil Biol. Biochem. 32:947-958.

Schlesinger, W.H. 1977. Carbon balance in terrestrial detritus. Ann. Rev. Ecol. Syst. 8:51-81.

Shaver, G.R. and S. Jonasson. 2007. Response of arctic ecosystems to climate change: results of long-term field experiments in Sweden and Alaska. Polar Res. 18:245-252.

Soil Survey Staff. 2006. Keys to Soil Taxonomy, 10th ed. USDA-Natural Resources Conservation Service, Washington, DC.

Terzaghi, K. 1943. Theoretical Soil Mechanics. John Wiley & Sons, Inc., New York.

Tingey, D.T., B.D. McVeety, R. Waschmann, M.G. Johnson, D.L. Phillips, P.T. Rygiewicz, and D.M. Olszyk. 1996. A versatile sun-lit controlled-environment facility for studying plant and soil processes. J. Environ. Qual. 25:614-625.

Tooker, W.W. 1899. Adapted Algonquian Term "Poquosin". Am. Anthropol. 1:162-170.

USDA – National Resources Conservation Service. 2009. Histosols map. Available at http://soils.usda.gov/technical/classification/orders/histosols_map.html (verified 29 Sep. 2009). USDA-NRCS Washington, DC.

Whigham, D.F. 1999. Ecological issues related to wetland preservation, restoration, creation and assessment. Sci. Total Environ. 24:31-40.

Wiant, H.V. 1967. Influence of Temperature on the Rate of Soil Respiration. Journal of Forestry 65:489-490.

Yuste, J.C., D.D. Baldocchi, A. Gershenson, A. Goldstein, L. Mission, and S. Wong. 2007. Microbial soil respiration and its dependency on carbon inputs, soil temperature and moisture.

Glob. Change Biol. 13:2018-2035.

Zak, D.R., W.E. Holmes, N.W. MacDonald, and K.S. Pregitzer. 1999. Soil temperature, matric potential, and the kinetics of microbial respiration and nitrogen mineralization. Soil Sci. Soc. Am. J. 63:575-584.

Chapter 2: Greenhouse Mesocosm Study and Field Site Study

Introduction

Within the conterminous United States, the majority of Histosols are found in the Northern, formerly glaciated states of Minnesota, Michigan, Wisconsin, Maine, and New York (Bridgham et al., 2001). A smaller, yet still significant, percentage of Histosols can be found in the southern United States were the water table is close to the soil surface for enough of the growing season to favor C accumulation over oxidation. Florida, Louisiana, and North Carolina combined have 28% of all mapped Histosols in the lower 48 states (Bridgham et al., 2001). North Carolina alone has over 600 000 ha of Histosols (Lilly, 1981) that cover approximately 4.4 percent of the total state land area.

The majority of research regarding temperature and moisture effects on C mineralization in Histosols comes from northern regions where they are of greater spatial extent. The result is a deficiency in the literature describing temperature and moisture effects on warm-climate Histosols. While they share the same order classification, organic soils differ a great deal from Minnesota to Florida. Parent material, structure, texture, temperature regime, climate, vegetation, and microbial communities can all vary quite widely (Table 2.1). We assert that these differences are vast enough to warrant separate examination of warm- and cool-climate Histosols.

Of particular interest is understanding how reductions in total solar irradiance (TSI) accompanying vegetation establishment can affect the soil temperature regime and soil C dynamic in warm-climate Histosols. As detailed in Chapter 1, Carolina bays often contain Histosols at their center. Carolina bays that have been drained and used for agronomic production are more commonly being used as wetland mitigation banks (Barton et al., 2008), having native hydrology and vegetation restored. It becomes vitally important from a C budgeting aspect to understand how

restoring hydrology and vegetation will control C mineralization, the main pathway of soil C loss, in these unique soils. Vegetation establishment could decrease soil temperatures by attenuating total sunlight reaching the soil surface. Soil C mineralization, a temperature dependent process, would decrease in turn. A more thorough discussion of merits for investigating warm-climate Histosols can be found in Chapter 1.

Two experiments were conducted to evaluate the direct effect of total solar irradiance (TSI) intensity on soil temperature and moisture and TSIs indirect effect on soil C respiration in an organic soil. Secondary succession in mitigated Carolina bays will cause increased shading of the soil surface with the appearance of successive plant communities. The focus of this study is to estimate how decreasing TSI will affect near surface soil temperatures and soil CO_2 efflux in a Carolina bay Histosol.

The soil used for the following experiments was chosen for a number of reasons: (1) comparatively few studies have been conducted on Histosols in thermic temperature regimes, (2) thermal properties of Histosols and mineral soils differ dramatically and may respond differently to TSI differences, and (3) the Ponzer soils (Loamy, mixed, dysic, thermic Terric Haplosaprists) (Soil Survey Staff, 2008) are commonly found in the interior of mitigated Carolina bays and a better understanding of soil C storage dynamics may improve restoration of wetland functions.

The first study, conducted from 13 June 2008 to 12 Sept. 2008, subjected intact core mesocosms to various levels of TSI reduction in a greenhouse. A complimentary field experiment was carried out from 31 Mar. 2009 to 10 Sept. 2009. In each experiment soil temperature and soil CO_2 efflux were measured directly. Soil water status and TSI were monitored in both experiments to give further insight to changes in soil respiration.

The objectives of the greenhouse mesocosm experiment were to: (1) observe the influence of TSI reduction on soil material temperature, (2) monitor temperature effects on CO_2 efflux, and (3) evaluate soil water influence on CO_2 efflux. A greenhouse housed the mesocosms, which eliminated precipitation input and allowed strict soil moisture control.

Objectives for the field experiment were similar to those of the greenhouse study: subject soil plots to various degrees of TSI reduction and (1) compare soil temperatures between treatments, (2) detect soil CO_2 efflux differences among and between shade treatments, and (3) observe soil moisture influence on soil CO_2 respiration under natural moisture variation associated with the seasonally fluctuating water table.

Materials and Methods

Site Description

A field study was conducted at Juniper Bay (34°30'29" N; 79°01'29" W) approximately 13 km south of Lumberton, NC in Robeson County. Cores for the greenhouse mesocosm experiment were collected from the same location. Mean annual precipitation at Juniper Bay is 478 mm with maximum and minimum mean monthly temperatures (1971-2000) of 32°C in July and -1°C in January (NOAA, 2002). Juniper Bay was ditched and drained from 1966 to 1972 for agronomic production (Ewing, 2003). The site was purchased by NCDOT as a wetland mitigation site, and cropping ceased in 2000. In 2002 the ditches were filled and native hydric vegetation regrew from the soil seedbank.

The soils within Juniper Bay are similar to those found in the majority of Carolina bays. The perimeter of the bay is characterized by a sandy rim, higher in elevation than the interior of the bay. The interior of the bay is mapped as Ponzer muck (Loamy, mixed, dysic, thermic Terric

Haplosaprists) (Soil Survey Staff, 2008). Liming and plowing during agricultural production have resulted in an approximately 20 cm deep granular surface horizon overlying undisturbed, structureless muck. Ewing and Vepraskas (2006) determined TOC, bulk density, and particle size distribution for a typical profile at Juniper Bay (Table 2.2). We measured near surface (0 to 5 cm) bulk density at the field site using the core method (Blake and Hartge, 1986). Bulk density ranged from 0.51 Mg m^{-3} to 0.79 Mg m^{-3} with a mean of 0.69 Mg m^{-3}. TOC of soil samples collected from the field site varied from 11.09% to 36.84% with a mean of 25.74%. TOC within the top 7.6 cm was determined by the NCSU Dept. of Soil Science analytical services laboratory with a dry combustion CHA analyzer (Perkin Elmer, San Jose, CA).

Greenhouse Mesocosm Experiment

On 6 June 2008, 12 intact soil cores were collected from Juniper Bay using 20 cm diameter x 20 cm long schedule 40 polyvinyl chloride (PVC) pipe with beveled edges to minimize disturbance during sampling. The PVC pipe served as an extraction device and holding container for the duration of the experiment. Cores were collected from two depths, 0 to 20 cm and 25 to 45 cm. The 0 to 20 cm layer (hereafter referred to as 'topsoil') was the granular surface horizon while the 25 to 45 cm layer ('subsoil') was undisturbed, structureless muck. The intact cores were transported to the NCSU Method Road greenhouse complex where they remained for approximately 3 mo. The columns were capped at the bottom by a 20 cm diameter PVC socket coupling caulked to a 25 cm^2 PVC sheet (Fig. 2.1). Filter sand filled the coupling sockets, providing a solid base for the soil material in the PVC cores while also allowing uniform water distribution from beneath. A static water table 17.5 cm from the soil mesocosm surface was maintained for the first 90 d of the experiment. Thereafter, the water table was removed and the mesocosms were permitted to dry for 45 d.

Vented 4 L Nalgene containers were converted to Mariotte bottles and used to control water table height. Vinyl tubing (6.35 mm i.d.) connected the Mariotte bottles to the mesocosms with quick-disconnect fasteners in between so the mesocosms and Martiotte bottles could be separated for measurements and maintenance. The Mariotte bottles were covered with foil to reduce the solar radiation load and minimize diurnal temperature fluctuation of the water table. Vertically oriented clear acrylic tubing was affixed to a T-joint in the plumbing to show the height of water in the mesocosms.

The twelve mesocosms were arranged in a split-plot randomized complete block design (Fig. 2.2). Three factors were applied: percent light reduction, presence of a water table, and original core depth within the soil profile (topsoil vs. subsoil). Percent light reduction was applied at three levels: 0% (full sun), 70%, and 90% to simulate the range in light intensity reaching the soil surface. Havens (1998) reported as little as 2% of total solar radiation reached the soil surface under a dense stand of Atlantic cedar while 25% of TSI reached the soil under a loblolly pine canopy. The aforementioned shade treatments were chosen to simulate a very thick tree canopy (90%) and one that allowed some dappled sunlight (70%).

To achieve the desired light reduction, mesocosms were covered by shade tents. Four tents were constructed of 5x5 cm lumber and were sized to shade two mesocosms: 60 cm wide x 90 cm long x 90 cm tall. Greenhouse shade cloth, certified for 70% and 90% shade, was used to achieve the desired percentage of light reduction. Frames were covered with a single layer of shade cloth on all sides. Shade cloth on each end was rolled up 20 cm to facilitate air movement and prevent air stagnation in the tents. Mesocosms subjected to full sun treatment were not placed under shade tents. Two LI200X pyranometers (LI-COR, Lincoln, NE) recorded total solar irradiance throughout the experiment to verify actual TSI reaching the mesocosm surfaces. One pyranometer remained in

full sun while the second was periodically moved between the 70 and 90 treatments. TSI was read each minute and an hourly average was recorded by a CR10 data logger (Campbell Scientific, Logan, UT).

Soil material temperature was measured at three depths within each mesocosm: 2.5, 7.6, and 14 cm. Type T thermocouples were permanently installed through the side of the columns, caulked into place, and connected to the data logger. The logger recorded temperature each minute and was programmed to calculate an hourly average for the output. The thermocouples could be disconnected from the mesocosms for maintenance and measurements.

Monitoring soil temperature within the mesocosms served multiple purposes. First, mesocosm soil temperature could be used to verify shade treatment was having an effect on soil temperature. Second, we could use soil temperature to help explain efflux differences between the shade treatments. Third, knowing soil temperature within the mesocosm profiles allowed a comparison between experiment and in-situ profile temperature trends.

Moisture content was monitored using a mass balance method. Mesocosms were disconnected from their respective Mariotte bottles and thermocouple leads and weighed periodically with a 16 kg ± 0.1g digital balance (Mettler-Toledo, Columbus, OH). Column mass fluctuation was assumed to be entirely attributed to changes in water content.

Three platinum-tipped redox probes (Wafer et al., 2004) were installed in each mesocosm following removal of the imposed water tables. Probes were placed at 2.5, 15, and 19 cm. Redox potential measurements were made using a portable volt meter and saturated calomel (mercury containing) electron probe. Redox potential was measured concurrently with mesocosm mass and CO_2 efflux.

CO_2 efflux was the primary response variable measured throughout the experiment. Efflux was measured using a LI-6200 portable photosynthesis analyzer with a 6000-09 soil respiration chamber (LI-COR). The LI-6200 is a field portable infrared gas analyzer with dynamic chamber closed-loop plumbing. A PVC collar was permanently inserted 2 cm into the surface of each mesocosm, onto which the soil chamber was placed during efflux measurements. The collar minimizes soil disturbance from chamber placement, which can increase microbial activity and cause artificially high efflux measurements (Norman et al., 1997). Measurements for each mesocosm were conducted as follows. Ambient atmospheric CO_2 was measured with the LI-6200. The soil chamber was then placed on the collar and the CO_2 concentration within the chamber was drawn down below ambient by one-half the total estimated increase of CO_2 after the 100 s measurement interval. This drawdown minimized potential measurement error attributed to changes in CO_2 concentration gradient between the soil and atmosphere. Four efflux values, generated during each 100 s measurement interval, were later averaged and recorded.

SAS (V. 9.1; Cary, NC) was used to analyze the efflux data. We used the mixed model procedure to conduct analysis of variance for main effects and interactions. Differences among treatment means were analyzed using Fischer's least significant differences (LSD). All analyses were performed at the α=0.05 level.

Field Shading Experiment

A 10 m^2 plot free of trees and dominated primarily by forbs and graminoids was selected at the interior of Juniper Bay. The plot had vegetation and soil similar to the surrounding interior of the bay and was located in the approximate center of the bay, south of the main horizontal ditch (Fig. 2.3).

Nine 1.5 m^2 plots were assigned a shade treatment in Latin squares design (Fig. 2.4). Shade treatments were bare soil with full sun ('B' or bare), bare soil with 70% light reduction ('S' or shaded), and natural vegetation ('V' or vegetated). Shade cast by natural vegetation and shade cloth were expected to be similar at some point during the experiment. The 70% shade treatment simplified soil CO_2 efflux by eliminating the root respiration component, similar to the unshaded treatments. The vegetation treatment was useful for estimating shade effects with the root respiration component still present.

Full sun and 70% treatment squares were cleared of all vegetation and debris and kept devoid of plant growth via mechanical removal for the duration of the experiment. Shading was achieved with 1.5 m^2 shade tents constructed of 5x5 cm lumber and covered with 70% light reducing shade cloth. Tents were 45 cm high to allow adequate air flow. Plants in vegetated treatments were allowed to grow uninhibited. To characterize light reduction under shade treatments, a pyranometer was placed within a wire frame wrapped with 70% shade cloth from March 13 to August 9. Thereafter, the pyranometer was moved to ground level under treatment square V3 for 14 d, treatment square V2 for 10 d, and back to V3 for the remainder of the experiment. TSI was recorded in a manner identical to the greenhouse mesocosm experiment.

Monitoring equipment was installed to record hourly soil temperature at three depths within each square. PVC thermocouple installation devices were constructed to precisely install thermocouples to the desired depths: 2.5, 7.5, and 17.5 cm. Nine 25 cm lengths of 1.9 cm schedule 80 PVC pipe were drilled at the aforementioned depths. Type T thermocouple wire was fed through the holes and adhered with two part marine epoxy. The pipe was then filled with insulating spray foam to minimize thermal conductivity of the pipe. One thermocouple installation device was driven into each of the treatment squares. Data acquisition was similar to the method used in the greenhouse.

Soil matric potential was monitored with custom made tensiometers of similar construction to those detailed by Cassel and Klute (1986). The tensiometer body was 1.75 cm schedule 80 PVC with a 1 bar porous ceramic cup epoxied to the bottom. A 5 cm clear acrylic sight tube epoxied to the top allowed the viewer to gage the height of water column within the tensiometer. Rubber septae were used to seal the tops of the tensiometers. Tensiometers were installed at 10 and 22.5 cm depths in each treatment square. Matric potential was measured with a tensimeter (Soil Measurement Systems, Tuscon, AZ) during each visit. Water table depth was collected from a pre-existing data-logging monitoring well (Remote Data Systems, Navassa, NC) directly adjacent to the site (Environmental Services Staff, 2007). A soil water retention curve for the top 7.6 cm of the topsoil was developed using a method similar to the low pressure system described in Klute (1986).

To monitor soil respiration response to shade effects, CO_2 efflux was measured weekly to biweekly between the hours of 1230 and 1530. We attempted to measure efflux during a three hour window in the afternoon to minimize daily temporal variation. Measurements were conducted in the afternoon when temperature differences between treatments would manifest. There were 16 sampling events between 31 Mar. 2009 and 9 Sept. 2009. Two PVC soil collars, identical to those used for greenhouse mesocosms, were inserted 2 cm into the ground within each treatment square. Soil respiration was measured at each collar during every sampling event. Respiration was not measured when the water table was above the soil surface, which was infrequent. Measurement interval and procedure was similar to that used in the greenhouse.

Diurnal efflux rates were characterized on July 1 and September 9. Attempts were made to conduct six measurements over a 24 h period for both days, but a thunderstorm interfered with one measurement on July 1.

Relationships between efflux and shade treatment, temperature, and water potential were analyzed in SAS. A mixed model was used to test fixed effects significance on CO_2 efflux. Fixed effects were shade, temperature, soil water potential, day, and shade*day. Temperature and soil water potential were treated as covariates. Analysis of variance was used to analyze treatment and covariance effects for all days combined. A $\log_{10}$ transform guaranteed normality and equality of variance. Data from May 15, June 26, July 1, and August 28 were missing water potential values and excluded from this analysis.

Greenhouse Mesocosm Study Results and Discussion

Total Solar Irradiance

Ambient total solar irradiance in the greenhouse was consistently less than TSI in full sun. The greenhouse roof was treated with whitewash to mitigate extreme temperatures during the North Carolina summer. Nevertheless, TSI was still intense during daylight hours so TSI reduction from the whitewash was not limiting to treatment comparisons within the experiment.

Shade tents were effective for reducing sunlight reaching the mesocosms for the experiment duration. Shade cloth used to achieve 70% and 90% TSI reduction successfully reduced TSI to approximately 30% and 10% of ambient, respectively (Fig. 2.5). The 70% shade cloth was slightly more effective at achieving the desired percent light reduction than the 90% treatment. Actual TSI reaching mesocosms under 90% shade treatments was about 88%, which was sufficiently close to the target of 90%.

Soil Temperature

Temperature data among the mesocosms verified that the shade treatment had an effect on soil temperature. For both water table conditions and soil layers, the unshaded mesocosms were

consistently warmer than both shaded treatments. A 5 d period representative of conditions when water tables were present is shown in Fig. 2.6. However, soil temperature did not respond as predicted under shaded treatments, as the 90% treatments were warmer than 70% treatments in both topsoil and subsoil mesocosms. We believe the tightly knit 90% shade cloth restricted air flow through the tents despite attempts to increase air flow while minimizing unwanted light inputs. Consequently, the mesocosms under 90% shade experienced higher air temperatures than those under 70% shade and higher soil temperatures resulted.

Differences in maximum daily temperatures are useful for comparing shade effects because the maximum daily temperature is typically reached after peak daily TSI. At the inception of the experiment, when the water tables were present, there was little temperature difference between unshaded and shaded mesocosms (Fig. 2.7). Shade tents were completely covered with cloth and hot air stagnation raised soil temperatures of shaded mesocosms. The ends of the tents were rolled up on June 16 to increase air flow. After June 16, shaded mesocosms experienced lower daily maximum temperatures relative to unshaded mesocosms. Daily maximum temperature differences between unshaded and 70% shaded mesocosms ranged from 0.7° to 3.3°C. Daily maximum temperature differences between unshaded and 90% shaded mesocosms was lower, ranging from -0.3° to 2.7°C.

Soil temperature within mesocosm profiles deviated from typical diurnal variation with depth. Soil temperatures within the mesocosms should resemble the idealized daily fluctuation, where sinusoidal waves dampen and shift horizontally with increasing depth (Hillel, 2004). While there was a horizontal phase shift of the sinusoidal temperature wave with increasing depth in the mesocosms, temperatures did not decrease as expected (Fig. 2.8). The magnitude of deviation from expected soil temperature behavior seemed to be influenced by shade treatment.

In unshaded treatments (Fig. 2.8ad), soil temperatures at 14 cm were often similar to those at 2.5 cm. At times, conditions were warmest at 14 cm, which was more common in subsoil mesocosms. Mesocosms under 70% shade (Fig. 2.8be) deviated more from convention. Temperatures at 14 cm often exceeded those at 2.5 cm, though more consistently in subsoil material. In 90% shaded mesocosms (Fig. 2.8cf), the 14 cm depth almost always saw the highest daily temperature, followed by 7.6 cm and 2.5 cm; a complete reversal of what is typically expected.

The temperature data in Fig. 2.8 suggest a secondary source of heat input, aside from solar radiation reaching the mesocosm surface. A likely explanation for warmer subsurface temperatures is conductive heat flow from the bench upward through the mesocosms. The differing sine waves among treatments seem to reinforce this explanation. A similar amount of heat was likely moving upward from the bench, but the effect was dampened in unshaded mesocosms where solar radiation contributed a significant amount of surface heat. In shaded mesocosms, where very little sunlight reached the mesocosm surface, the heat contribution from the bench was a higher proportion of total heat input to the system.

While unwanted, we do not believe the possible heat transfer from the benches largely affected efflux differences between the shade treatments. The bottom portion of the mesocosms experienced the greatest influence due to unwanted heat flux, but the majority of C mineralization likely occurred in the top few cm of the cores (Fang and Moncrieff, 2004). When the water table was present, the bottom 5 cm of the cores were completely saturated, not including the capillary fringe. It is probable that the bottom portion of the mesocosms was responsible for only a fraction of the total efflux, so temperatures deviating from typical in-situ conditions would not significantly affect differences among shade treatments.

Soil Moisture

Volumetric soil moisture water content (θ) was calculated each day mesocosms were weighed, for a total of 16 water contents from June 20 to September 12. Soil water content for replicates was averaged to represent soil moisture conditions for the respective shade treatments. Volumetric water content was measured on three days before water tables were removed: June 20, July 14, and August 1. The water tables were removed on August 1 and the remaining θ values, from August 4 to September 12, reflect conditions during the dry-down period. Data loss prevented calculation of θ for subsoil mesocosms.

Volumetric water content in topsoil mesocosms was static from June 20 to August 1 (Fig. 2.9), suggesting the imposed water tables performed well for maintaining constant water content. During this period, θ in unshaded mesocosms was approximately 0.63 m^3 m^{-3} while θ in 70% and 90% shaded mesocosms was 0.54 and 0.55 m^3 m^{-3}, respectively. Immediately following water table removal, there was a rapid loss of water from August 1 to 4, especially in the unshaded mesocosms. More rapid water loss from unshaded mesocosms was observed until August 25. Thereafter, all mesocosms lost water at similar rates. On August 15, θ in unshaded mesocosms dropped below θ observed in both shaded mesocosms and remained lower for the duration.

The volumetric water contents suggest the unshaded mesocosms were much wetter than their shaded counterparts. However, the soil water retention curve for the soil indicates that soil water potential was similar (Fig. 2.10). At 0.63 m^3 m^{-3}, the matric potential of the unshaded cores was slightly less than 0 kPa. Matric potential in the shaded cores was about -3 kPa at 0.54 m^3 m^{-3}. So, while θ in unshaded cores was higher, actual soil water availability was comparable among all shade treatments when water tables were present.

Redox Potential

Redox potential was first measured 1 d after water table removal. Initial redox values were considered indicative of conditions prior to water table removal because water was slow to drain from the cores. The soil was considered reduced at a measured depth if the corrected redox potential was lower than the $Fe(OH)_3/Fe^{2+}$ boundary of 575 mV. This boundary was determined using an Eh-pH phase diagram (Vepraskas and Faulkner, 2001) with soil pH of 4.5. See appendix A for mesocosm redox potentials. Reduction was observed in all but two mesocosms: replicate 2 of topsoil under 90% shade and replicate 1 of subsoil under 70% shade. Reduction was observed at 2.5, 15, and 19 cm in 3, 9, and 6 mesocosms, respectively. The duration of reduction varied, from 2 to 16 d. By August 16, all but one mesocosm had become aerobic, and remained so for the duration of the experiment.

Carbon Dioxide Efflux

From June 18 to September 12, CO_2 efflux from each mesocosm was measured on 41 occasions. Twenty-one measurements were taken when water tables were imposed and the remaining 20 were conducted during the water table dry-down period. Efflux rates measured on June 13 to June 17 were discarded because mesocosms under 70% and 90% shade treatments were affected by air stagnation and higher than expected temperatures. Four fixed effects were significant at the α=0.05 level. Two were main effects (shade and soil layer) and two were interactions (shade*layer and water*layer). Fig. 2.11 shows a summary of efflux rate by shade treatment and soil type.

Individual data points for topsoil and subsoil mesocosms during the wet and dry-down periods were summarized graphically (Fig. 2.12). The data have high temporal variability, likely due to temperature and cloud cover variability accompanying daily and seasonal weather patterns. Some variability was also introduced once water tables were removed. The data did show some

trends, in spite of the high variability. One trend, day to day temperature effects on CO_2 respiration, is shown in Fig. 2.13. A temperature spike from June 20 to July 1 corresponded with an increase in efflux during the same period. The same correlation between mesocosm temperature and measured efflux was observed in all mesocosms.

Layer (depth from which cores were extracted in the profile) was highly significant in affecting efflux (p=0.0005). Mean (estimated) respiration rate from topsoil mesocosms was 3.2082 μmol CO_2 m^{-2} s^{-1} while subsoil mesocosms respired only 1.4535 μmol CO_2 m^{-2} s^{-1} on average. Differences in respiration rates may be explained via physical or microbiological processes, or both. The topsoil cores, with their granular structure, probably had more interconnected pores and macropores than the structureless, massive subsoil. Less tortuosity would permit high diffusion rates in the topsoil, resulting in higher observed efflux. The materials also differed in their quality of organic matter. Personal observation showed topsoil had a much larger quantity of plant roots than the subsoil. The higher concentration of labile organic matter in the topsoil may have stimulated higher rates of microbial decomposition and CO_2 respiration.

While the water main effect was not significant (p=0.4088) the water*layer interaction was (p=0.0135). The 'water' effect was the presence or absence of water tables. Surprisingly, efflux from topsoil and subsoil did not respond similarly to removal of the water tables. Table 2.3 shows estimated efflux means for topsoil and subsoil layers for both water table conditions. When the water tables were present, topsoil mesocosms had a mean efflux of 3.0779 μmol CO_2 m^{-2} s^{-1} that increased to 3.3385 μmol CO_2 m^{-2} s^{-1} after the water tables were removed. Efflux from subsoil mesocosms decreased after water table removal, from 1.6739 μmol CO_2 m^{-2} s^{-1} to 1.2331 μmol CO_2 m^{-2} s^{-1}.

The dissimilar response to changes in water status may be due to differences in topsoil and subsoil microbial communities. Redox potential data (appendix A) indicate topsoil and subsoil

mesocosms reached aerobic conditions at similar rates, suggesting differences in redox potential were not the cause of the dissimilar response. Kechavarzi et al. (2010) evidenced differing CO_2 efflux sensitivity to temperature and moisture between horizons within the same soil profile. They postulated that microbes in the cooler, permanently saturated deeper horizons reacted more strongly to environmental stresses than those in surfaces layers. Microbes in the topsoil mesocosms, possibly better adapted to aerobic conditions, would more efficiently decompose organic matter once water tables were removed, pores dewatered, and atmospheric gas exchange increased. On the other hand, subsoil microbial communities, better adapted to organic matter decomposition in reduced, anaerobic soil, may have suffered greater shock during air re-entry. The result would have been the observed reduction in efflux from the subsoil mesocosms following water table removal.

Shade treatment also had a significant effect on efflux ($p=0.0430$). Estimated mean efflux for unshaded, 70% shade, and 90% shade treatments was 2.5578, 2.6474, and 1.7873 μmol CO_2 m^{-2} s^{-1}, respectively. There was also a strong interaction between shade and soil layer (shade*layer) ($p=0.0119$). The shade*layer interaction is almost certainly attributable to efflux from the unshaded, subsoil mesocosms. Subsoil mesocosms did not respond as expected to shade effects (Fig. 2.14b). While the unshaded, subsoil mesocosms were consistently warmer than the shaded mesocosms (Fig. 2.6b), their efflux rates were lowest of the three shade treatments. Conversely, topsoil mesocosms responded as predicted to shade effects (Fig. 2.14a). Hotter, unshaded mesocosms (Fig. 2.5a) respired the most CO_2.

A couple of mechanisms could be responsible for the unexpected efflux response to shade observed in unshaded, subsoil mesocosms. Temperatures in unshaded mesocosms may have been too high for the subsoil microbial communities. Rapid decreases in microbial metabolism are common once temperatures rise above optimum (Madigan and Martinko, 2006). If temperatures

were high enough, microbial production of CO_2 may have been significantly reduced. A less likely explanation is restricted or preferential gas diffusion. The area within the PVC soil collars, from which efflux was measured, may have been less permeable than the same area on shaded mesocosms. The less permeable unshaded cores would consistently have lower efflux. Macropores present outside the PVC collar may also have caused preferential gas diffusion in unshaded cores, which would also result in low efflux rates. Reduction was not a likely influence because redox potentials were relatively similar among shade treatments of subsoil mesocosms.

Shade treatment effects on CO_2 efflux are likely attributable to temperature differences among mesocosms, especially in the topsoil. There was a strong positive relationship between mesocosm temperature and CO_2 efflux from topsoil mesocosms (Fig. 2.15a). The figure shows the highest temperature and efflux rates were often from unshaded mesocosms. The lowest temperatures and efflux rates were from mesocosms under 90% shade. Mesocosms holding subsoil did not show such a strong relationship between temperature and efflux rate (Fig. 2.15b). While the unshaded subsoil mesocosms were often the warmest, they also respired the least CO_2. The 70% and 90% shaded subsoil mesocosms behaved in a slightly more predictable manner, with higher efflux coming from the 70% shaded mesocosms.

Soil CO_2 respiration was influenced not only by temperature, but also by soil water content. Peak efflux was reached at approximately the same water content for all shade treatments, 0.50 m^3 m^{-3} or -4.5 kPa (Fig. 2.16). Peak efflux for unshaded mesocosms was reached at slightly higher θ than shaded treatments, 0.54 m^3 m^{-3}, but the matric potential was essentially the same. Because the matric potentials of the cores were so similar, we can conclude that efflux differences between shade treatments were most likely due to shade induced temperature effects.

Field Experiment Results and Discussion

Total Solar Irradiance

Total light reduction within the shade cloth wrapped frame was consistently higher than expected, blocking 79% of daily TSI (Fig. 2.17a). TSI reduction of the shade cloth was likely overestimated in the cloth wrapped frame due to overlapped fabric. Actual TSI percent reduction is probably somewhere between 70% as observed in the greenhouse (Fig. 2.17b) and 79%. TSI under vegetated treatments was comparable to TSI under the shade cloth wrapped frame (Fig. 2.18). TSI was reduced by approximately 80% in both V2 and V3 treatment squares. TSI was not measured in the V1 treatment square, although visual comparison of vegetative cover between plots suggests TSI reduction would be similar to that seen in V2 and V3. Appendix B shows vegetative growth.

Soil Temperature

Daily soil temperature fluctuation in all treatments squares followed a sinusoidal wave function as described by Hillel (2004). Wave amplitude was greatest nearest the surface at 2.5 cm and dampened with depth (Fig. 2.19) in both the spring and late summer. Additionally, time at which daily maximum temperature was achieved was highly dependent on depth, with shallowest thermocouples reading their daily maximum temperature sooner than the deepest thermocouples. Correct thermocouple placement was verified with these data.

The daily soil temperature wave shifted to a higher temperature in August compared to May, correspondent with warmer summer air temperatures (Fig. 2.20a) The 2.5 cm soil temperature amplitude was greater in August (Fig. 2.19bdf) than May (Fig. 2.19ace) for 70% shaded (Fig. 2.19cd) and unshaded (Fig. 2.19ab) treatments. Amplitude at 2.5 cm in vegetated (Fig. 2.19ef) treatments decreased from May to August, possibly due to lower TSI later in the season.

Initially, soil temperatures in 70% shaded treatments were cooler than or equal to those in vegetated treatments. From March 31 to July 1, vegetated soil was warmer than shaded soil in 5 of

10 d. Shaded and vegetated soil temperatures were nearly equal in all other instances before July 1. After July 1, vegetated soil temperatures decreased and were cooler than shaded soil during 4 of 5 sampling events. Fig. 2.21 shows additional days before and after the vegetated treatments temperature decrease. From May 7 to May 14 (Fig. 2.21a), maximum daily soil temperature at 2.5 cm is greater in vegetated than shaded treatments for 5 of 7 days. From Aug 10 to Aug 17 (Fig. 2.21b) the converse is true; maximum daily soil temperature is consistently greater in shaded treatments than in vegetated treatments.

There are two possible explanations for decreased soil temperatures in vegetated treatments following July 1. First, it is possible that shading due to vegetative cover surpassed shading supplied by the greenhouse shade cloth. TSI was not measured under vegetative treatments during this time, but Fig. 2.2 indicates TSI reduction in vegetated treatments was greater than the 70% supplied by the greenhouse shade cloth. Secondly, increasing plant biomass within vegetated treatments after July 1 resulted in higher evapotranspiration, which led to lower temperatures via latent heat loss. In all likelihood, the correct explanation was probably a combination of both.

Fig. 2.22 shows 2.5 cm soil temperatures during each afternoon CO_2 sampling event. During every sampling event, soil temperatures were warmest in the bare treatments where all litter and vegetation had been removed. Bare soil treatments were between 2.2° to 10.1°C warmer than vegetated treatments and 3.8° to 7.4°C warmer than shaded treatments. Temperature differences became more pronounced after the month of May.

Shade effects on soil temperature, while most pronounced at the 2.5 cm depth, were apparent even at 17.5 cm. In May, 70% shade treatments were 3°C cooler than unshaded soil and in August vegetated treatments were 4°C cooler than unshaded soil treatments (Fig 2.21ef). It is noteworthy that shade effects were apparent at the lowest depth of observation.

Soil Moisture

Soil water potential was measured on twelve visits to the field site (Fig. 2.23a). To better understand temporal soil moisture trends, refer to Fig. 2.24 for water table depth and precipitation data. Within all treatment squares, soil water potential followed a seasonal pattern of wetness. Tensiometers at 10 cm were saturated from late March to mid-June. During this time, matric potential (Ψ_m) ranged from 1.62 kPa in shaded treatments to -0.30 kPa in bare treatments. After June 19, Ψ_m in all treatments dropped below 0 kPa and remained negative for the remainder of the experiment. Bare treatments remained slightly dryer (1 to 4.5 kPa) than vegetated and 70% shade treatments after June 19.

From March 31 to June 19, soil water potential at 10 cm was similar among shade treatments. Plant biomass was relatively low during this time, which may have minimized treatment differences attributable to transpiration in vegetated squares. Before July 23, the water table was within centimeters of the 10 cm tensiometer cup (Fig. 2.24), fluctuating between 11 and -17 cm. The capillary fringe probably eliminated any Ψ_m difference between treatments at this depth. The data show some deviation among treatments as early as July 23 (Fig 23a).

Based on the water retention curve (Fig. 2.10) volumetric soil water content at 10 cm depth was quite high for the entire measurement period. For all positive Ψ_m values, the soil was completely saturated at 0.63 $m^3\ m^{-3}$. θ remained above 0.53-0.58 $m^3\ m^{-3}$ in all treatments until after August 15. Soil water content decreased thereafter and reached a low of 0.42 $m^3\ m^{-3}$ in unshaded treatments and 0.49 $m^3\ m^{-3}$ in 70% shaded treatments.

Significant differences in soil moisture at 10 cm due to shading effects did not occur until August 18. Unshaded treatments were dryer than both 70% shaded and vegetated treatments on August 18 and September 9. Lower matric potential at 10 cm in unshaded treatments was probably

a result of higher TSI and soil temperatures found in full sun. High TSI raised soil temperatures, which led to greater rates of evaporation compared to other treatments.

Matric potential at 22.5 cm (Fig. 2.23b) followed the same temporal pattern, but remained positive in all treatments until July 23 when Ψ_m in unshaded treatments reached -0.15 kPa. From March 31 to June 19, Ψ_m ranged from 3.31 kPa in vegetated treatments to 0.38 kPa in unshaded treatments. Thereafter, Ψ_m became more negative in all treatments, until August 4 when Ψ_m plateaued for 14 d in vegetated and bare treatments. No plateau was observed in shaded treatments during this time. After August 18, Ψ_m continued to drop in all treatments until the last measurement date, September 9. Throughout the experiment, vegetated treatments were wetter at 22.5 cm than shaded and bare treatments with one exception; bare treatments were wetter on May 27. Total potential at 22.5 cm did not differ between shaded and bare soil treatments.

The data show that soil water potential at 10 cm did not vary widely among shade treatments for the majority of the experiment. The potential for unequal water loss between treatments, due to higher evaporation in unshaded treatments and transpiration from vegetation, seemed to be mitigated by the presence of a relatively high water table.

Soil Respiration and CO_2 Efflux

Diurnal efflux was measured at the hours of 11:30, 15:30, 19:30, 5:30, and 8:00 on July 1-2 and 13:00, 16:00, 20:00, 0:00, 8:00, and 10:30 on September 9-10. On both days, soil chamber humidity was too high during early morning measurements to collect viable efflux data. Peak daily efflux was observed at 15:30 on July 1 and 16:00 on September 9, corresponding approximately to the period used for daily measurements.

CO_2 efflux rates at Juniper Bay ranged from 0.755 – 10.888 μmol CO_2 m^{-2} s^{-1} during the 5 mo measurement period. Efflux rates across treatments were lowest in March and April and increased throughout the growing season, reaching peak in August. CO_2 respiration rates at Juniper

Bay were comparable to those observed in sphagnum derived peats in West Virginia (Yavitt et al., 1987) and other swamps and marsh ecosystems (Schlesinger, 1977).

Efflux from shade treatments followed a clear trend throughout the experiment. Unshaded soil treatments respired the most CO_2 on every day of measurements (Fig. 2.25b). Higher rates of efflux from unshaded soil were almost certainly due to temperature differences among the treatments. Soil temperature in unshaded treatments was higher than vegetated and 70% shaded treatments. On no day during times of CO_2 measurement did soil temperature in either of the shaded treatments approach within 2.5°C of the unshaded soil.

Vegetated and 70% shaded treatments respired comparable amounts of CO_2 on most days. Efflux from vegetated treatments was higher on all but two days, May 27 and June 19. The difference in efflux between shaded treatments was likely a combination between total TSI reduction and the root respiration component where vegetation was present, which complicated efflux comparison. While TSI reduction under 70% shade treatments remained constant, TSI under vegetation decreased throughout the season as the plants grew. As TSI decreased in vegetated treatments, so did soil temperature relative to unshaded and 70% shade treatments, likely decreasing CO_2 efflux. At the same time, root respiration was presumably increasing as plant biomass increased in vegetated treatments, resulting in an increase in CO_2 efflux.

The combined influence of decreasing TSI and increasing root respiration is difficult to quantify, primarily due to the root respiration component. Hanson et al. (2000) summarized a variety of studies designed to determine the percentage of total soil CO_2 respiration attributable to the vegetative root component. Estimates of the root respiration component varied from 10-90% for all soils and vegetation types. Unfortunately, peat soils and non-forest plant communities were underrepresented in this analysis. Root respiration from one peat soil was estimated to contribute

between 35-45%, but the vegetation type was not indicated. The actual root respiration component within the vegetated treatments remains unquantified in the present study.

Though specific quantification of the root respiration component in this experiment may be somewhat limited, by referring to efflux from 70% shaded treatments, where root respiration is eliminated and shade is constant, we see no large change in efflux compared to vegetated treatments. It seems the net temporal effect due to decreasing TSI and increasing root respiration accompanying plant canopy development may be close to zero.

The shade effect on soil temperature and CO_2 respiration is further supported by Fig. 2.26. The figure shows the highest observations of temperatures and CO_2 respiration were from unshaded soil. Efflux from vegetated treatments fell between unshaded and 70% shaded treatments. Vegetated and 70% shaded soil temperatures were similar, but efflux in vegetated treatments was higher due to the added root respiration component.

Tensiometry showed small differences in Ψ_m between shade treatments after August 18 (Fig. 2.23a). These differences were not large enough to cause significant CO_2 efflux differences between shade treatments (Fig. 2.29). We can conclude with some certainty that temperature, rather than moisture, was responsible for the observed soil respiration differences between treatments.

There was also a strong temporal relationship between efflux and water table depth seen across treatments. The water table remained close to the soil surface from March 31 to June 19, dropping no lower than 13 cm on May 8 (Fig. 2.27a). After June 19, the water table dropped to 19 cm, increased slightly on July 23, then continued to drop to a low of 42 cm on August 28. Respiration across treatments followed roughly the same trend as the water table (Fig. 2.27b) and could be broken into two distinct periods.

During the wet period when the water table was close to the surface, efflux was relatively low. Mean respiration rates from March 31 to June 19 for unshaded, vegetated, and 70% shade

treatments were 3.464, 2.470, and 1.775 μmol m^{-2} s^{-1}, respectively. Efflux rates were much higher during the dry-down period after June 19 (Fig. 2.28). Mean efflux for unshaded, vegetated, and 70% shade treatments were 8.173, 6.472, and 5.604 μmol m^{-2} s^{-1}, respectively.

The substantial increase in CO_2 respiration is probably not entirely attributable to water table fluctuation and changes in soil moisture, but a combination of changing soil water content and soil temperature. There was a seasonal increase in soil temperature that corresponded with the receding water table. Fig. 2.26 showed a strong positive correlation to increases in soil temperature and efflux rate, suggesting a part of the increase in efflux was due to increasing soil temperature.

There were no significant differences among shade treatments (p=0.1783) for all days combined (Table 2.4). The lack of significant difference among shade treatments may be credited to (1) seasonal variations in water table depth, (2) seasonal variation in soil temperature and TSI, and (3) high variability of efflux measurements. The water table had two distinct phases (Fig. 2.27a) which may have complicated the shade effect. There was also seasonal variation in soil temperature (Fig. 2.22). Shade effects, presumably controlling soil temperature differences among treatments, would have no influence on efflux when there was no difference in soil temperature among treatments. Fig. 2.22 shows temperature differences among unshaded and shaded treatments were greater after June 2, before which shade treatments may have not had enough effect on temperature to influence efflux. In such a case, the shade effect for the entire experiment duration would probably not be significant. Estimated efflux was also highly variable. Fig. 2.29 shows 95% confidence intervals for treatments. The magnitude of the confidence interval for some treatments exceeded the estimated mean value. In this experiment, it seems high efflux variability essentially masked all but the most extreme shade effects.

In spite of the high variability, the shade*day effect was significant (p=0.0419). Shade was significant on two days; May 8 (p=0.0087) and June 19 (p=0.0212). On May 8, efflux from

unshaded treatments was higher than efflux from 70% shaded treatments (Fig. 2.29). On June 19, efflux from 70% shaded treatments was non-estimable, but unshaded treatments respired more CO_2 than vegetated treatments.

CO_2 respiration shows temporal variability. So many environmental factors, both chemical and physical, can affect C mineralization and soil respiration that choosing two or three for statistical analysis is dubious at best. Despite the lack of significant shade effects at the α=0.05 level, the observed data paint a relatively clear picture. Reducing total solar irradiance will decrease soil temperatures. In response to lower soil temperature, CO_2 respiration will decrease due to lower C mineralization rates.

Greenhouse and Field Experiments Summary

The critical point at which TSI reduction decreases soil temperature enough to slow C mineralization is still unknown. In the greenhouse, efflux from mesocosms under 90% shade was significantly less than efflux from full sun and 70% shade treatments. Because there was very little difference in soil water content between the shade treatments, we can be almost certain that observed differences in C mineralization rates were due to shade induced temperature differences. In both the field and greenhouse, 70% was not significant at α=0.05 but was consistently lower than efflux from full sun. The inherent variability of efflux measurements tended to mask statistical significance of efflux difference between the unshaded and 70% shaded treatments. Regardless of statistical significance, there appeared to be a difference between the unshaded and 70% shaded treatments. It is safe to say more data are needed to determine the critical amount of light reduction required to decrease C mineralization rates.

In the meantime, we can conclude that simple establishment of herbaceous vegetation, similar to that seen at Juniper Bay, will be effective for reducing soil temperature and C mineralization

compared to totally bare soil. One drawback of using herbaceous plants for light reduction is the temporal variability in canopy thickness and soil temperature reduction. The lowest soil temperatures under the herbaceous vegetation were observed late in the growing season when plants had reached full height and sunlight reduction was highest. The litter layer from previous years caused some light reduction during the spring, but the effect on soil temperature reduction was dampened.

Probably the best solution for consistent light and soil temperature reduction, in terms of vegetative establishment, would be to bypass herbaceous plant communities by promoting rapid establishment of evergreen vegetation. Evergreen vegetation can provide the benefit of constant light reduction throughout the year. Additionally, canopy thickness will continue to increase, decreasing soil level TSI each year.

REFERENCES:

Barton, D.B., D.M. Andrews, and R.K. Kolka. 2008. Evaluating hydroperiod response in restored Carolina bay wetlands using soil physiochemical properties. Restor. Ecol. 16:668-677.

Bridgham, S.D., C. Ping, J.L. Richardson, and K. Updegraff. 2001. Soil of northern peatlands: Histosols and gelisols. *In* J.L. Richardson and M.J. Vepraskas (ed.) Wetland soils: genesis, hydrology, landscapes, and classification. CRC Press, New York.

Cassel, D.K. and A. Klute. 1986. Water potential: tensiometry. p. 563-596. *In* A. Klute (ed.) Methods of soil analysis. Part 1. 2nd ed. Agron. Monogr. 9. ASA and SSSA, Madison, WI.

Environmental Services, Inc. Staff. 2008. Juniper bay wetland mitigation site: 2007 annual monitoring report. NCDENR Ecosystem Enhancement Program. Raleigh, NC.

Ewing, J.M. 2003. Characterization of soils in a drained Carolina bay wetland prior to restoration. Ph.D. diss. NC State Univ., Raleigh, NC.

Ewing, J.M. and M.J. Vepraskas. 2006. Estimating primary and secondary subsidence in an organic soil 15, 20, and 30 years after drainage. Wetlands 26:119-130.

Fang, C. and J.B. Moncrieff. 2004. Then variation of soil microbial respiration with depth in relation to soil carbon composition. Plant and Soil 268: 243-253.

Hanson, P.J., N.T. Edwards, C.T. Garten, and J.A. Andrews. 2000. Separating root respiration and soil microbial contributions to soil respiration: A review of methods and observations. Biogeochem. 48: 115-146.

Havens, A.V. 1998. Climate and microclimate of the New Jersey pine barrens. *In* R.T.T. Forman (ed.) Pine Barrens: Ecosystem and Landscape.Rutgers University Press, NJ.

Hillel, D. 2004. Introduction to environmental soil physics. Elsevier Academic Press, New York.

Kechavarzi, C., Q. Dawson, M. Bartlett, and P.B. Leeds-Harrison. 2010. The role of soil moisture, temperature, and nutrient amendment on CO_2 efflux from agricultural peat soil microcosms. Geoderma 154: 203-210.

Klute, A. 1986. Water retention laboratory results. p. 635-662. *In* Klute (ed.) Methods of soil analysis. Part 1. 2nd ed. Agron. Monogr. 9. ASA and SSSA, Madison, WI.

Lilly, J.P. 1981. The blackland soils of North Carolina: their characteristics and management for agriculture. North Carolina Agricultural Experiment Station. Bulletin 270. North Carolina State Univ. Raleigh, NC.

Madigan, M.T. and J.M. Martinko. 2006. Biology of Microorganisms. p. 151. Prentice Hall, NJ.

National Oceanic and Atmospheric Administration. 2002. Climatography of the United States No. 81. National Climatic Data Center/NESDIS/NOAA. Asheville, NC.

Norman, J.M., C.J. Kucharik, S.T. Gower, D.D. Baldocchi, P.M. Crill, M. Rayment, K. Savage, and R.G. Striegl. 1997. A comparison of six methods for measuring soil-surface carbon dioxide fluxes. J. Geophys. Res. 102: 771-777.

Schlesinger, W.H. 1977. Carbon balance in terrestrial detritus. Ann. Rev. Ecol. Syst. 8:51-81.

Soil Survey Staff. 2008. Soil Series Classification Database. Available at http://soils.usda.gov/technical/classification/scfile/index.html, (accessed on 30 Sep. 2009) USDA-NRCS. Lincoln, NE.

Vepraskas, M.J. and S.P. Faulkner. 2001. Redox chemistry of hydric soils. p. 91. *In* J.L. Richardson and M.J. Vepraskas (ed.) Wetland Soils: genesis, hydrology, landscapes, and classification. CRC Press, New York.

Yavitt, J.B., G.E. Lang, and R.K. Wieder. 1987. Control of carbon mineralization to CH_4 and CO_2 in anaerobic, Sphagnum derived peat from Big Run Bog, West Virginia. Biogeochem. 4:141-157.

Table 2.1. Comparison of a warm-climate (Pamlico) and cool-climate (Waskish) Histosols.

Property	Pamlico Series	Waskish Series
Location	NC, AL, FL, MS, SC, VA	MN, ME, NH
Taxonomic description	Sandy or sandy-skeletal, siliceous, dysic, thermic Terric Haplosaprists	Dysic, frigid Typic Sphagnofibrists
Parent Material	various plant matter	sphagnum moss
Structure	coarse granular or massive	weak platy or massive
Mean annual temperature, °C	17	1 – 7
Mean annual precipitation, mm	1219	457 – 1168
Vegetation	pond pine, tupelo, sweetbay, cypress, greenbrier	sphagnum peat, labrador tea, leather leaf, black spruce
Geographic setting	level to depressional surfaces, floodplains	bogs in glaciated terrain

† Source: Soil Survey Staff. 2008. Soil Series Classification Database. Available at http://soils.usda.gov/technical/classification/scfile/index.html, (accessed on 30 Sep. 2009) USDA-NRCS. Lincoln, NE.

Table 2.2. Horizon depth, organic C, bulk density, and particle size of a typical profile from Juniper Bay. Adapted from Ewing and Vepraskas (2006).

Horizon	Depth	Organic C	Bulk Density	Sand	Clay
	(cm)	%	g cm^{-3}	----------%----------	
Oap	0-10	44.58	0.57	13.5	42.7
Oa1	10-41	46.45	0.35	6.7	21.3
Oa2	41-51	30.32	0.35	4.9	30.0
A	51-58	8.02	0.35	5.9	43.3
Bw	58-97	3.56	0.65	8.4	37.4
C	97-110	1.43	1.18	35.7	29.1

Table 2.3. CO_2 efflux means from surface and subsurface mesocosms during wet and dry-down phases. Letters signify difference of efflux means between layers within the same phase at the α=0.05 level.

Layer	Phase	Efflux
		$\mu mol\ m^{-2}\ s^{-1}$
topsoil	wet	3.0779 a
subsoil	wet	1.6739 b
topsoil	dry-down	3.3385 a
subsoil	dry-down	1.2331 b

Table 2.4. Mixed model ANOVA type 3 tests for fixed effects from field experiment.

Effect	Degrees of Freedom	F-Value	Pr > F
shade	2	2.53	0.1783
temperature	1	2.46	0.1226
matric potential	1	0.01	0.9158
day	11	18.18	<0.0001
shade*day	21	1.68	0.0419

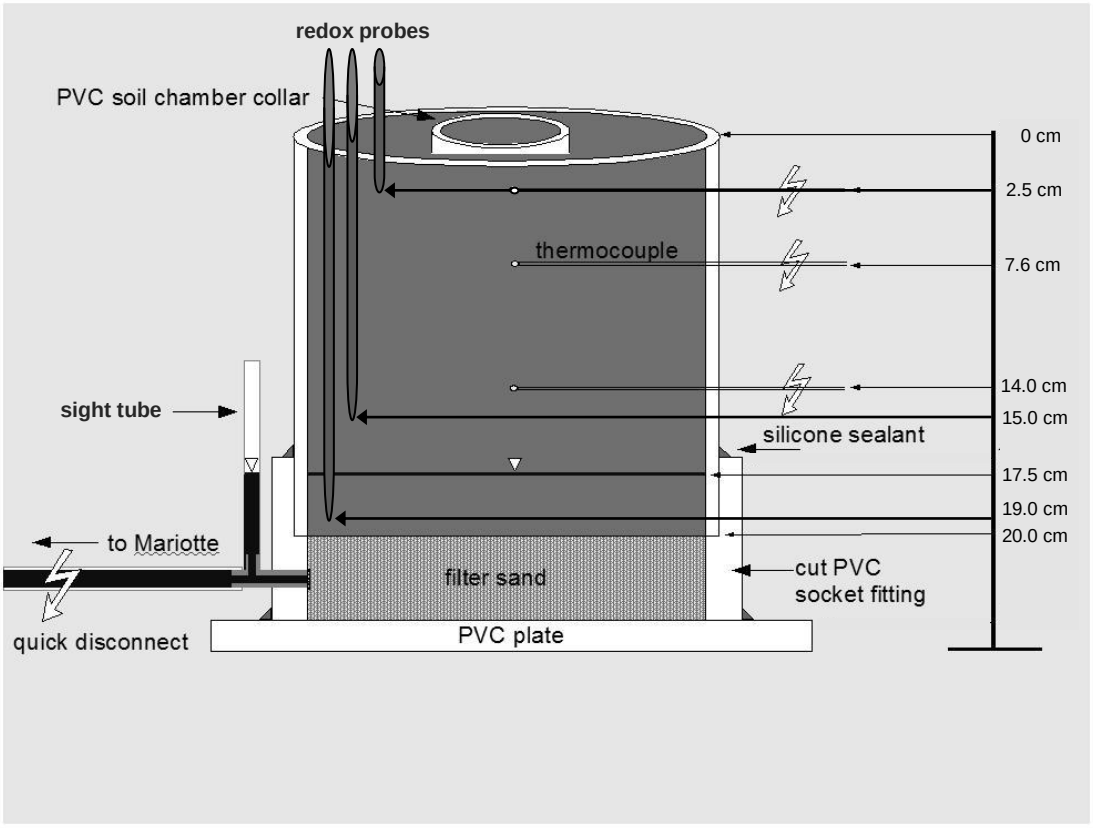

Figure 2.1. Cross section of core holding apparatus used in greenhouse experiment.

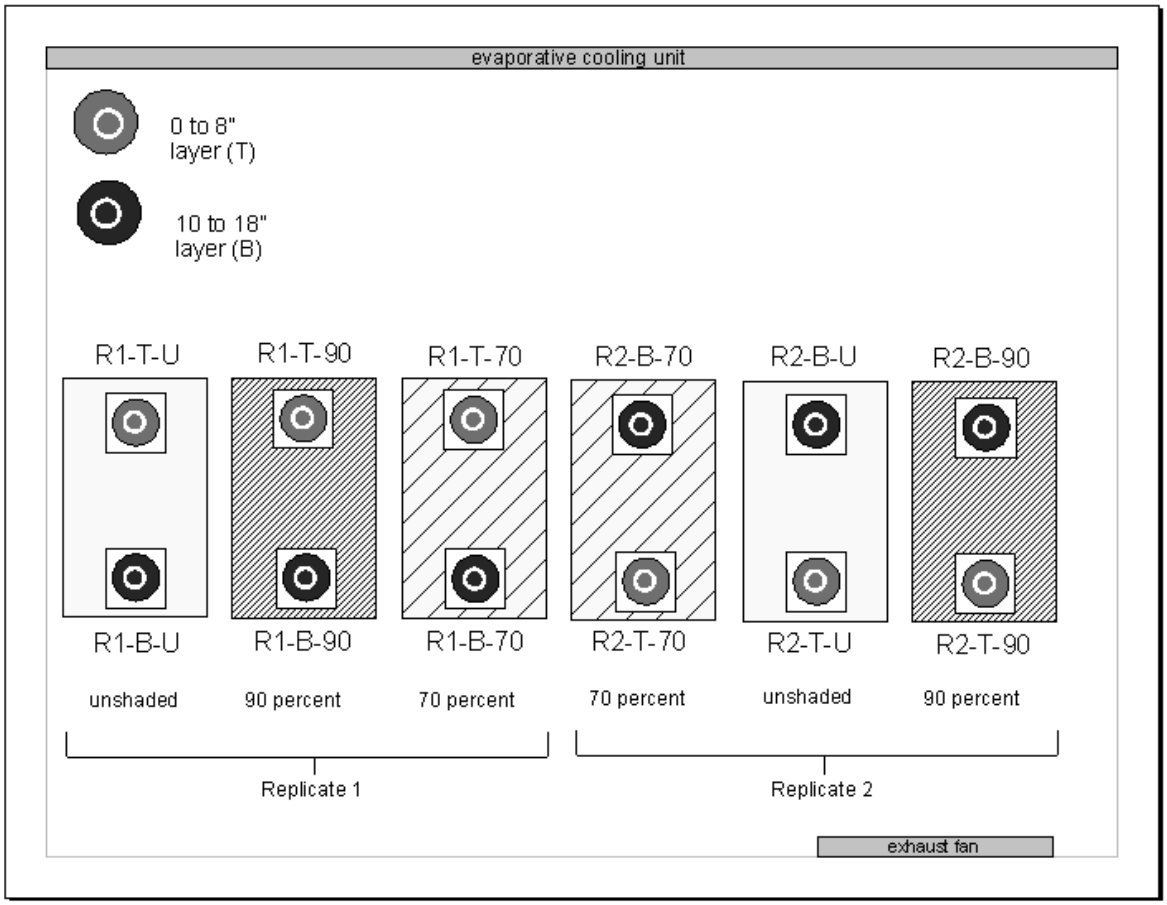

Figure 2.2. Split-plot randomized complete block design used in the greenhouse experiment. R# indicates replicate. T and B indicate topsoil and subsoil, respectively. U, 70, and 90 denote shade treatment: unshaded, 70% shade, and 90% shade, respectively.

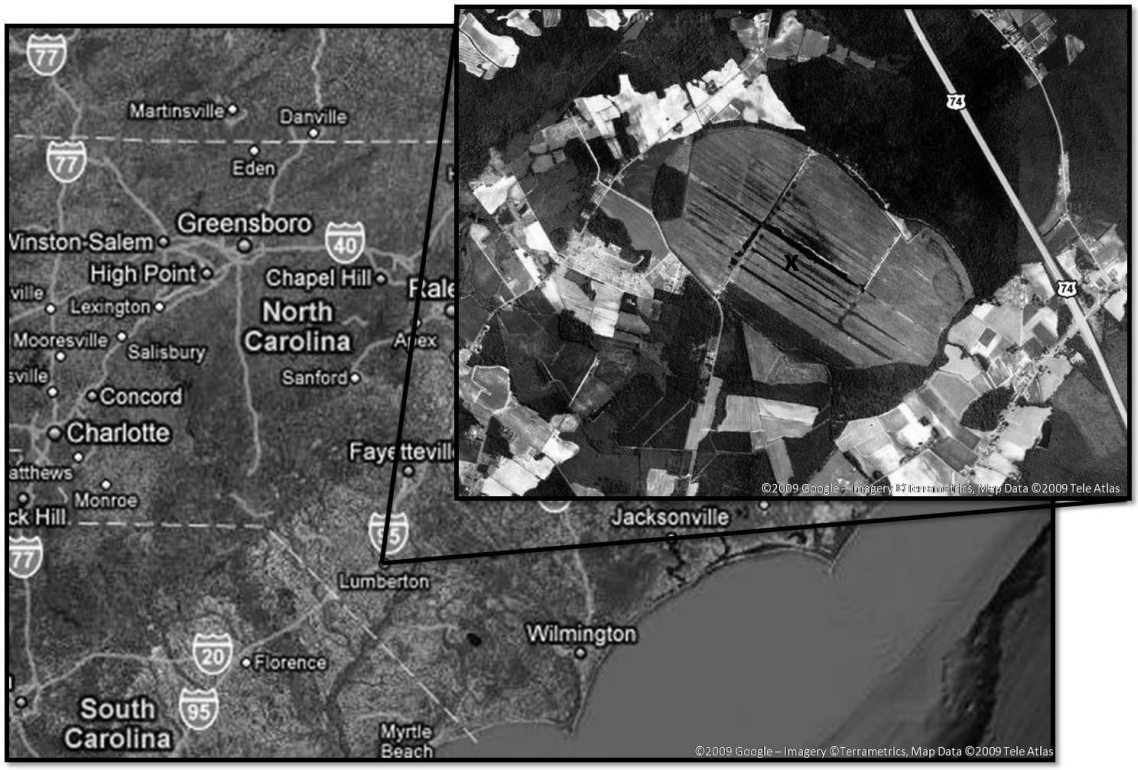

Figure 2.3. Study Location. An aerial photograph of Juniper Bay is shown in the upper right inset. Approximate site location is indicated by the 'x'.

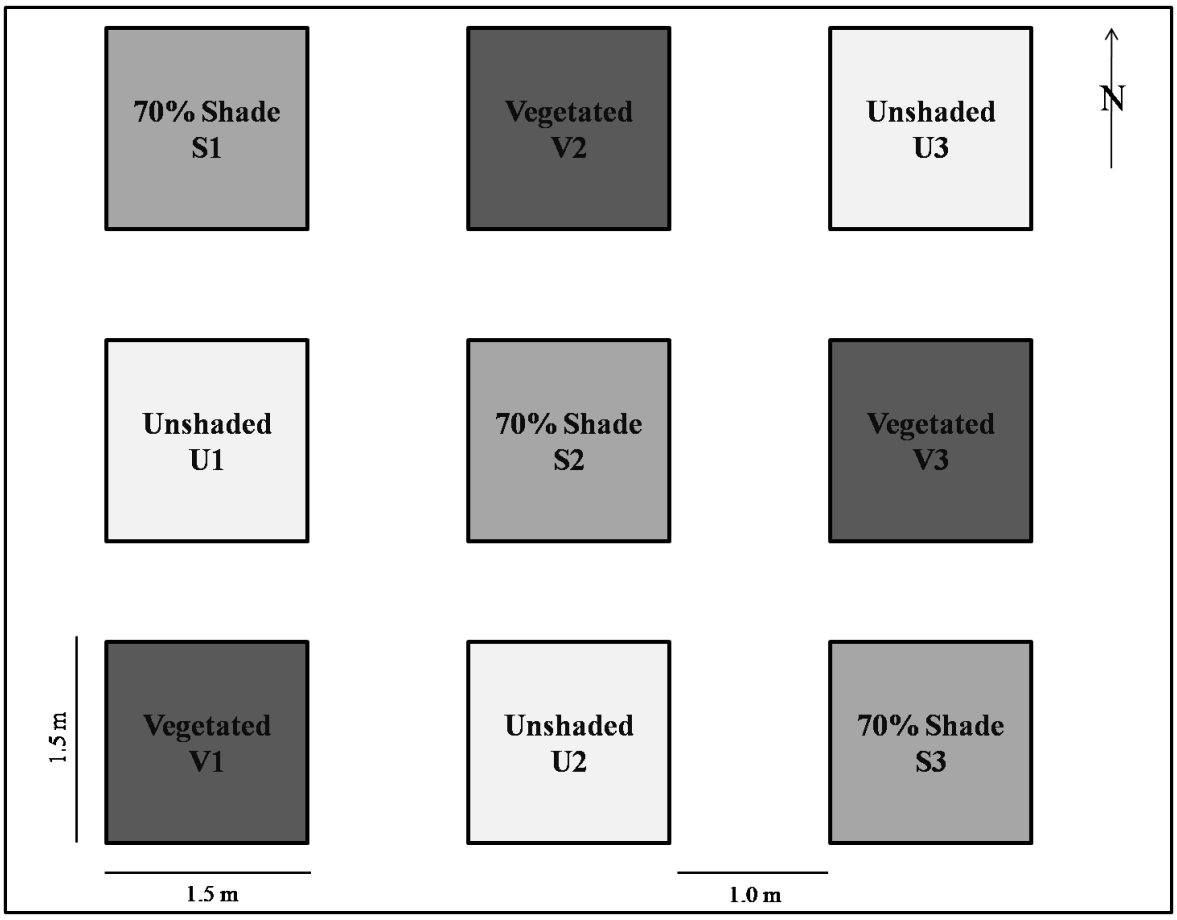

Figure 2.4. Latin squares design used for field shading experiment at Juniper Bay. Dimensions are not to scale.

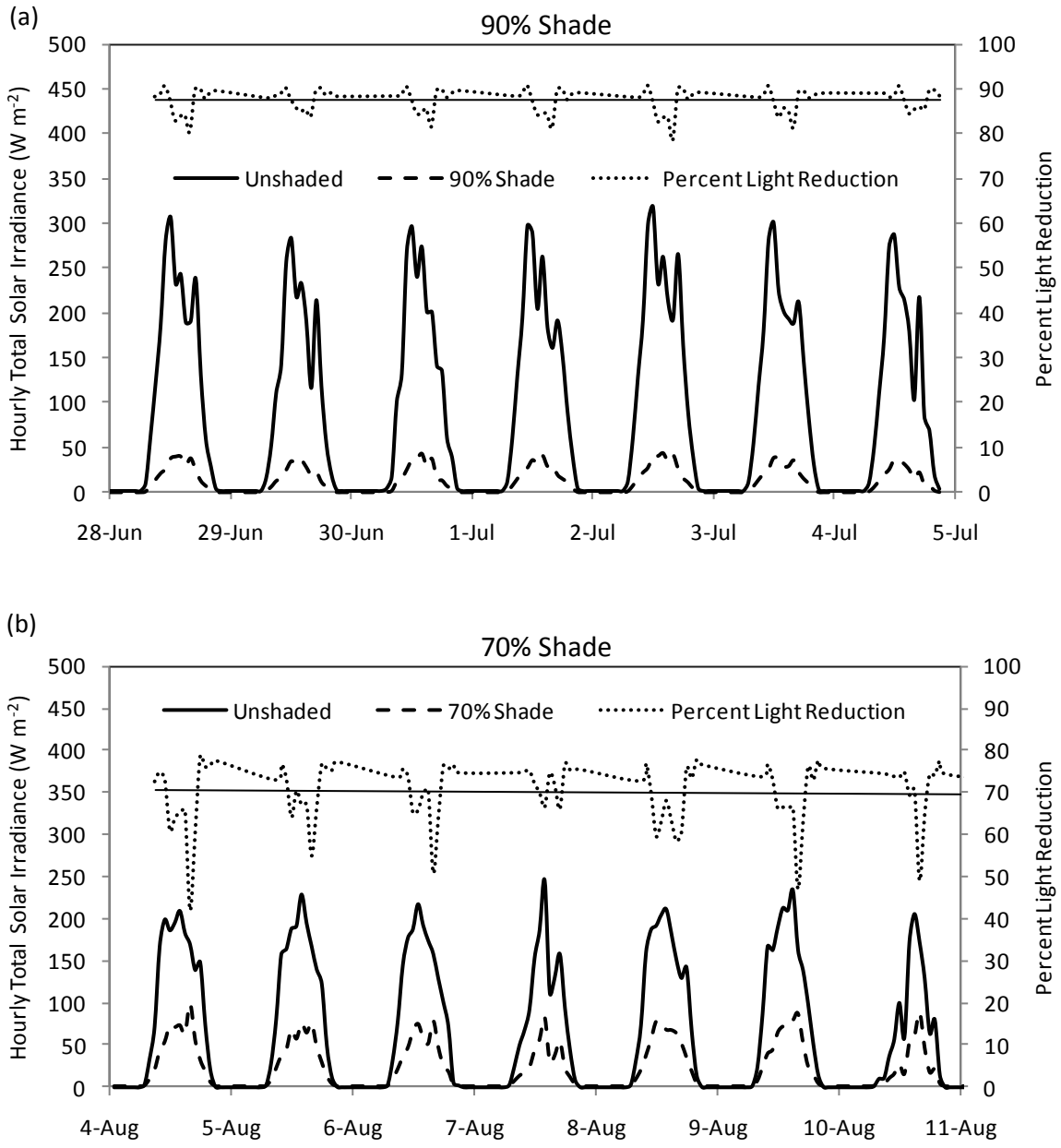

Figure 2.5. Total solar irradiance under 90% (a) and 70% (b) shade treatments in greenhouse, with percent light reduction relative to full sun.

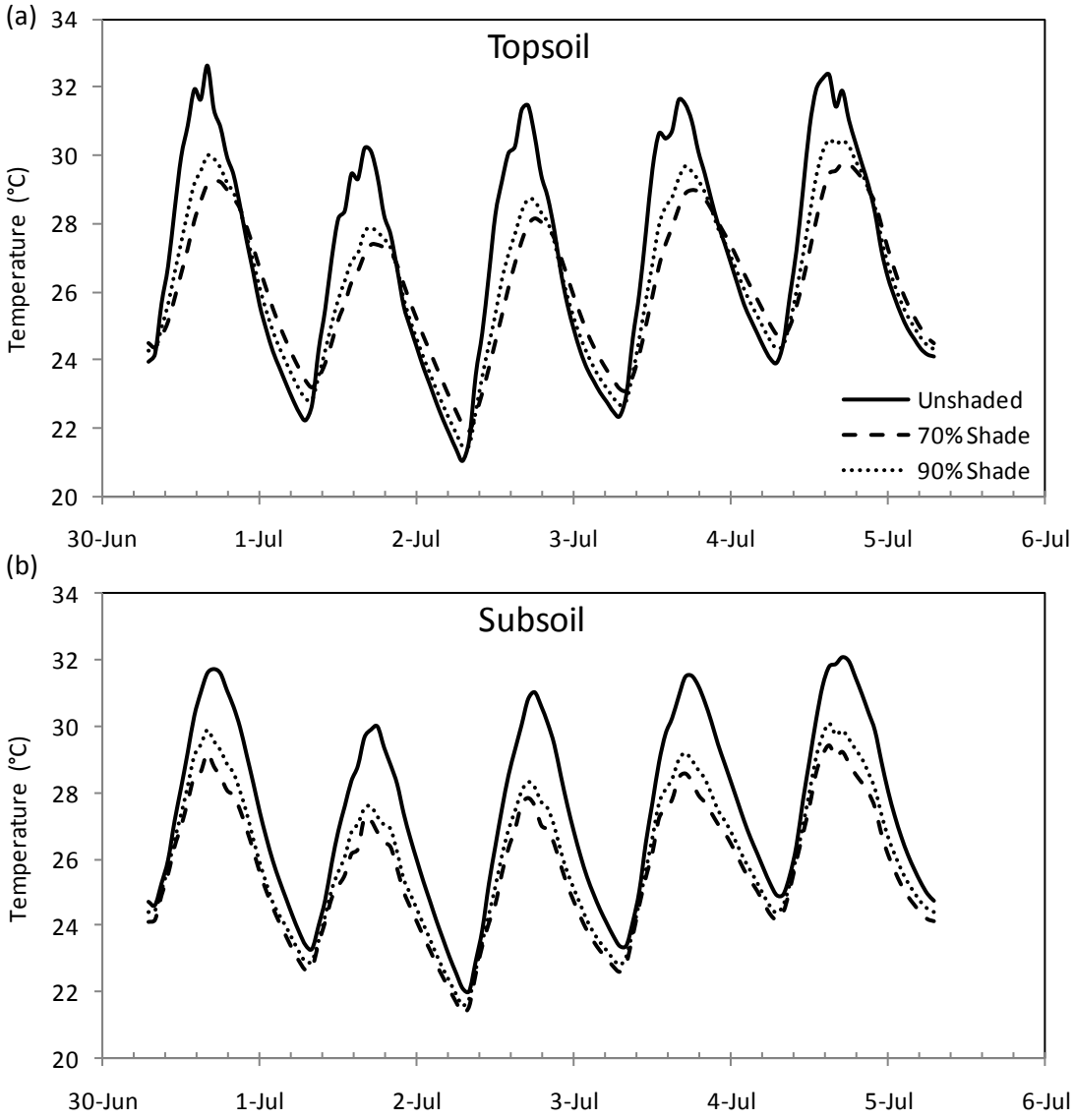

Figure 2.6. Comparison of soil temperatures at 2.5 cm among mesocosms under full sun, 70%, and 90% shade in surface (a) and subsurface (b) material.

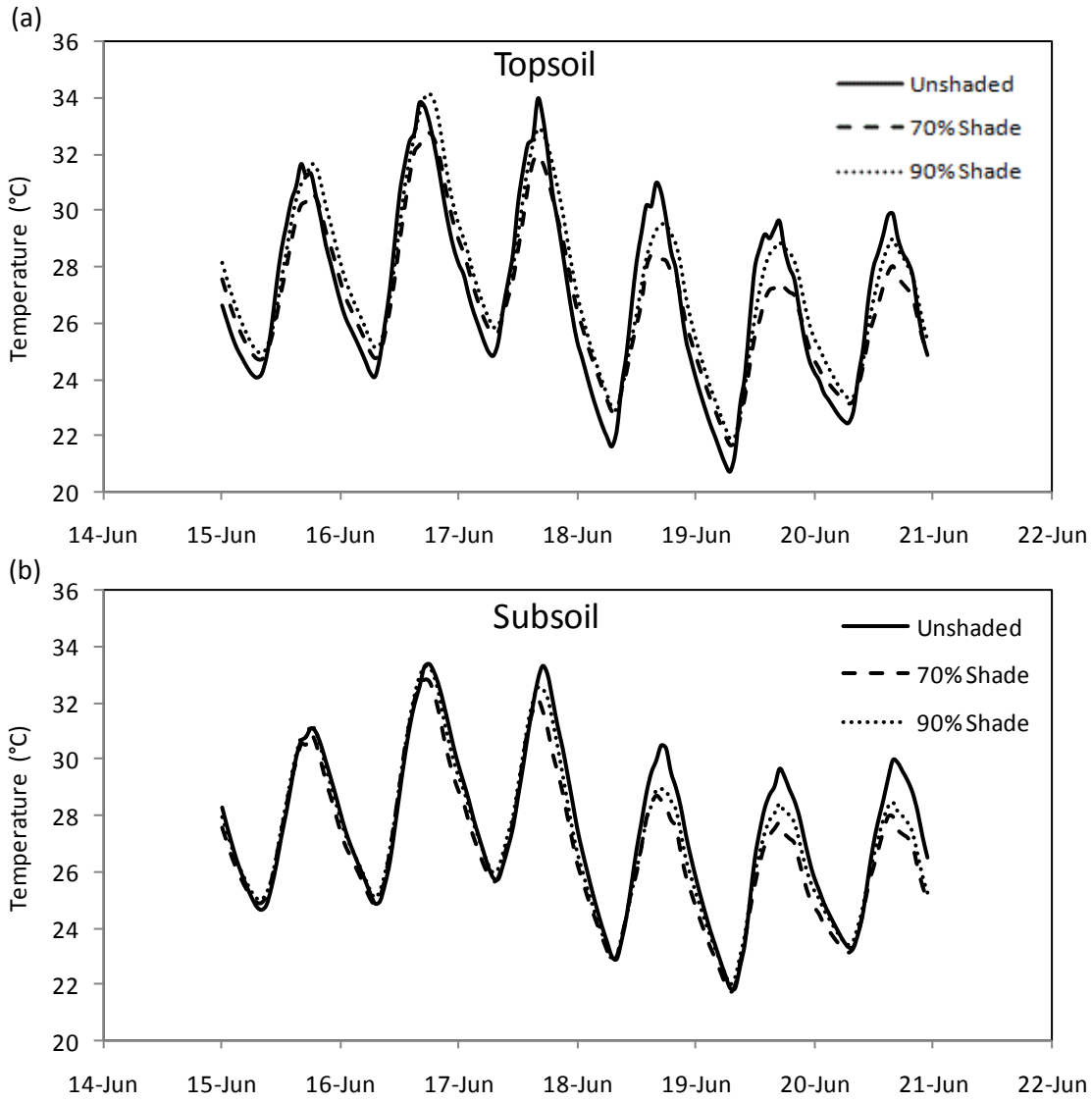

Figure 2.7. Topsoil (a) and subsoil (b) mesocosm soil temperatures at 2.5 cm before and after shade cloth was adjusted on June 16 to increase airflow.

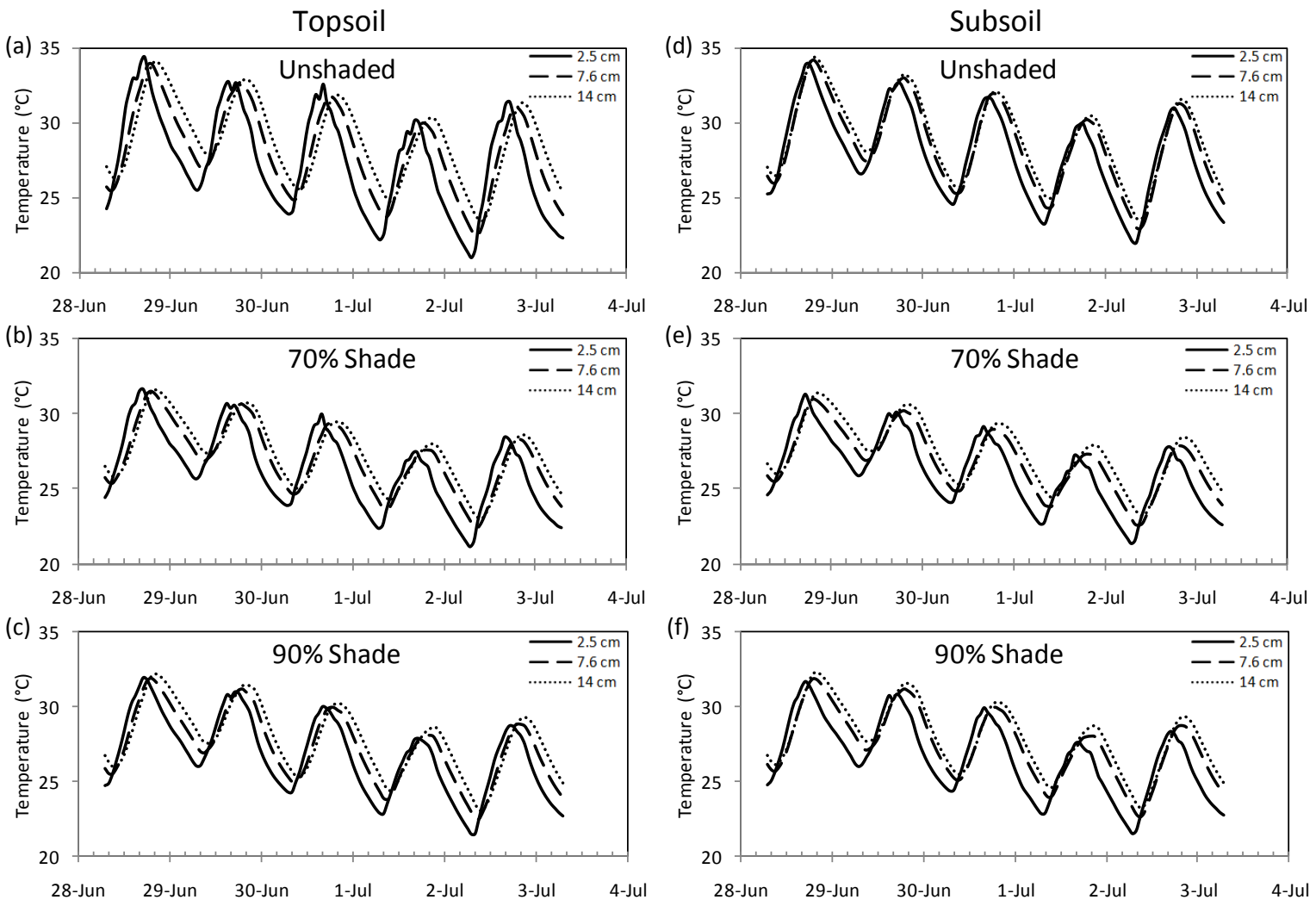

Figure 2.8. Temperature profile for topsoil (a-c) and subsoil (d-f) mesocosms.

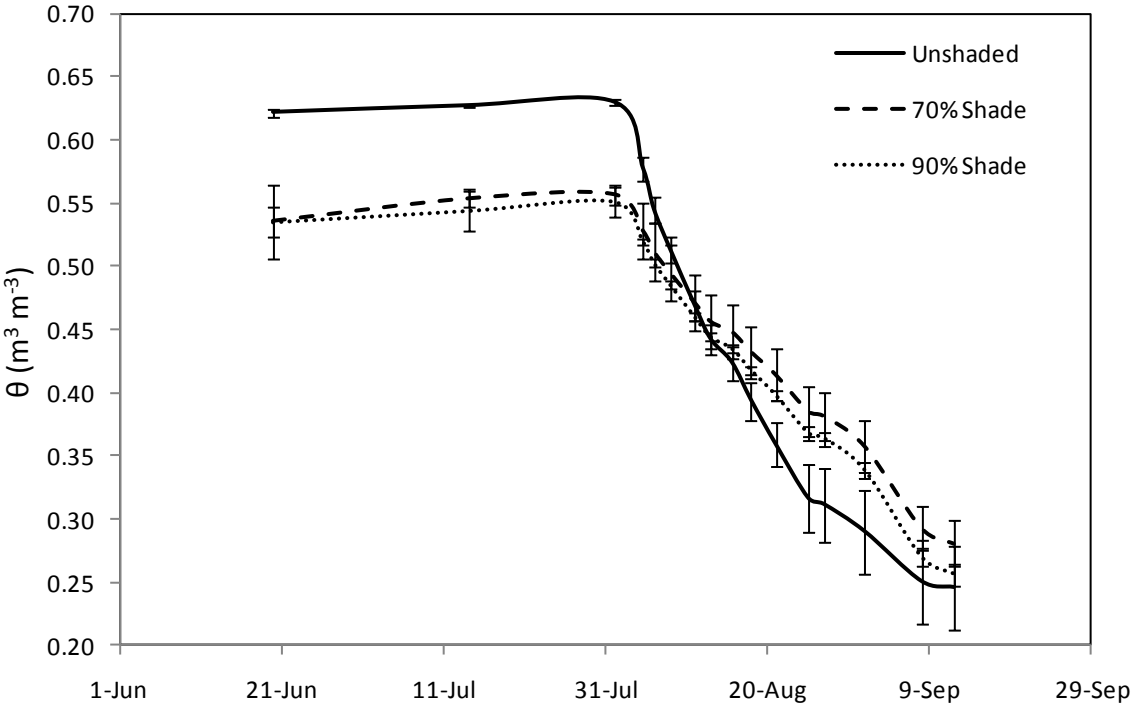

Figure 2.9. Volumetric water content (θ) of topsoil mesocosms before and after August 1 water table removal. Error bars indicate one standard deviation.

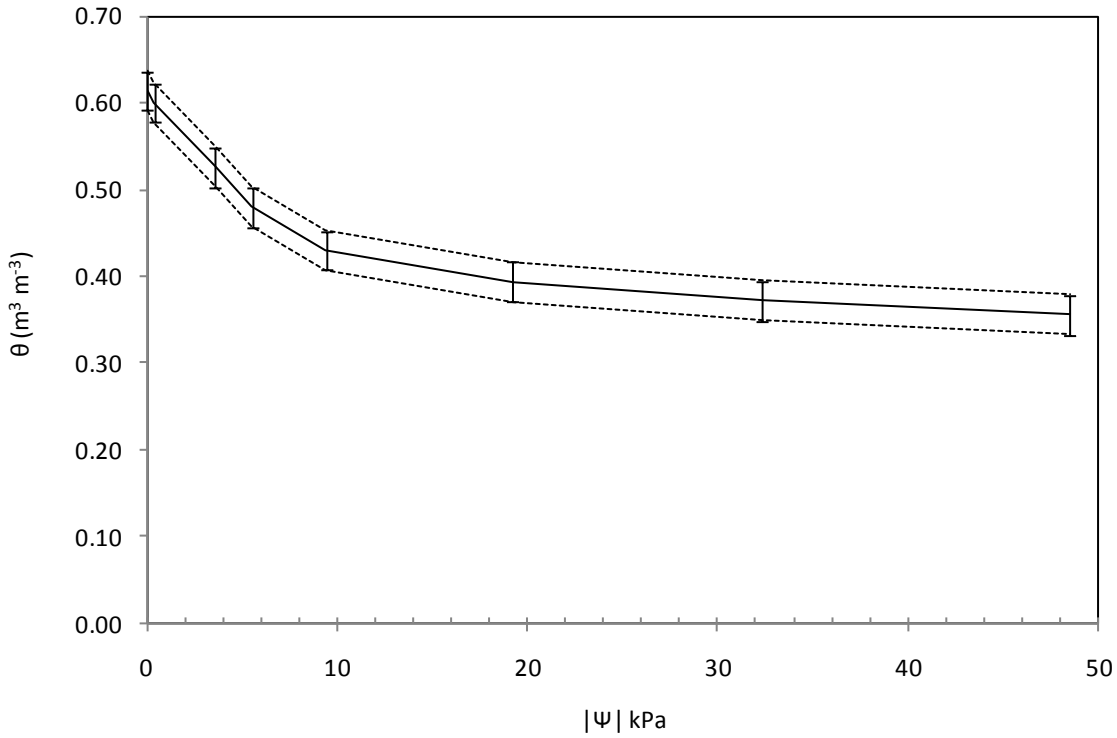

Figure 2.10. Soil water retention curve for topsoil collected from soil mapped as Ponzer series. 95% CI is shown. Volumetric water content and matric potential are indicated as θ and ψ, respectively.

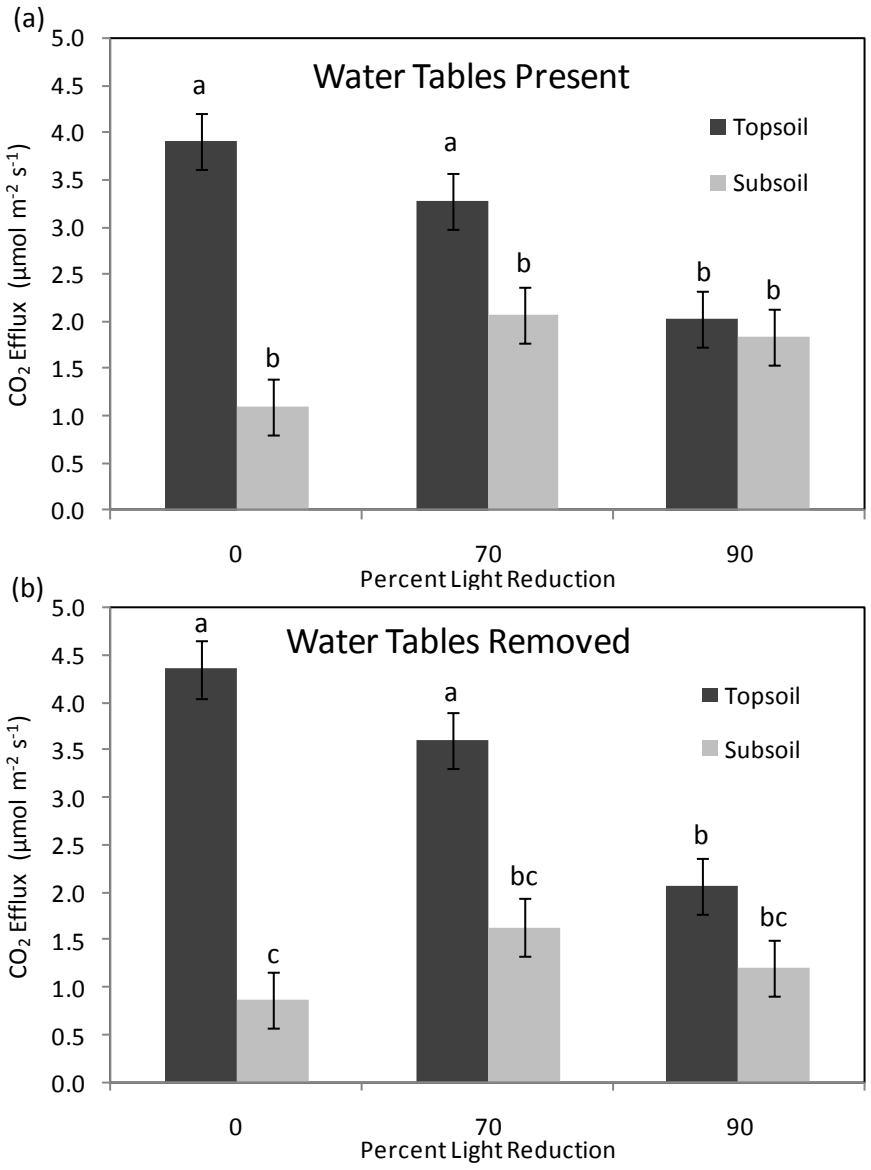

Figure 2.11. Estimated CO_2 efflux rates among shade treatments before (a) and after (b) removal of water tables from mesocosms. Means with similar letters do not differ at $\alpha=0.05$. Comparisons apply to all means within a figure. Error bars indicated standard error of the mean.

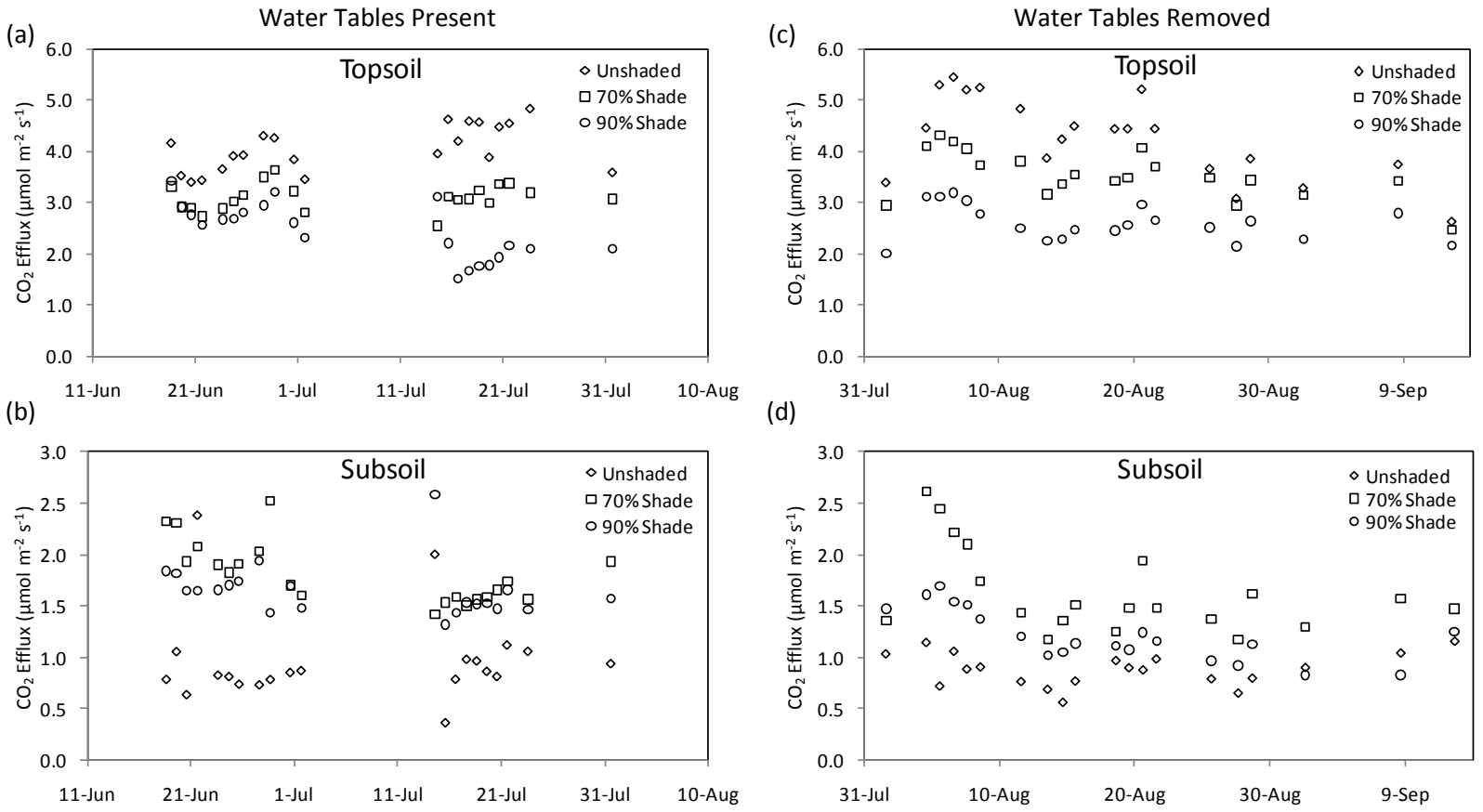

Figure 2.12. Mesocosm CO_2 efflux for topsoil (ac) and subsoil (bd) material with water tables present (a and b) and after removal (c and d).

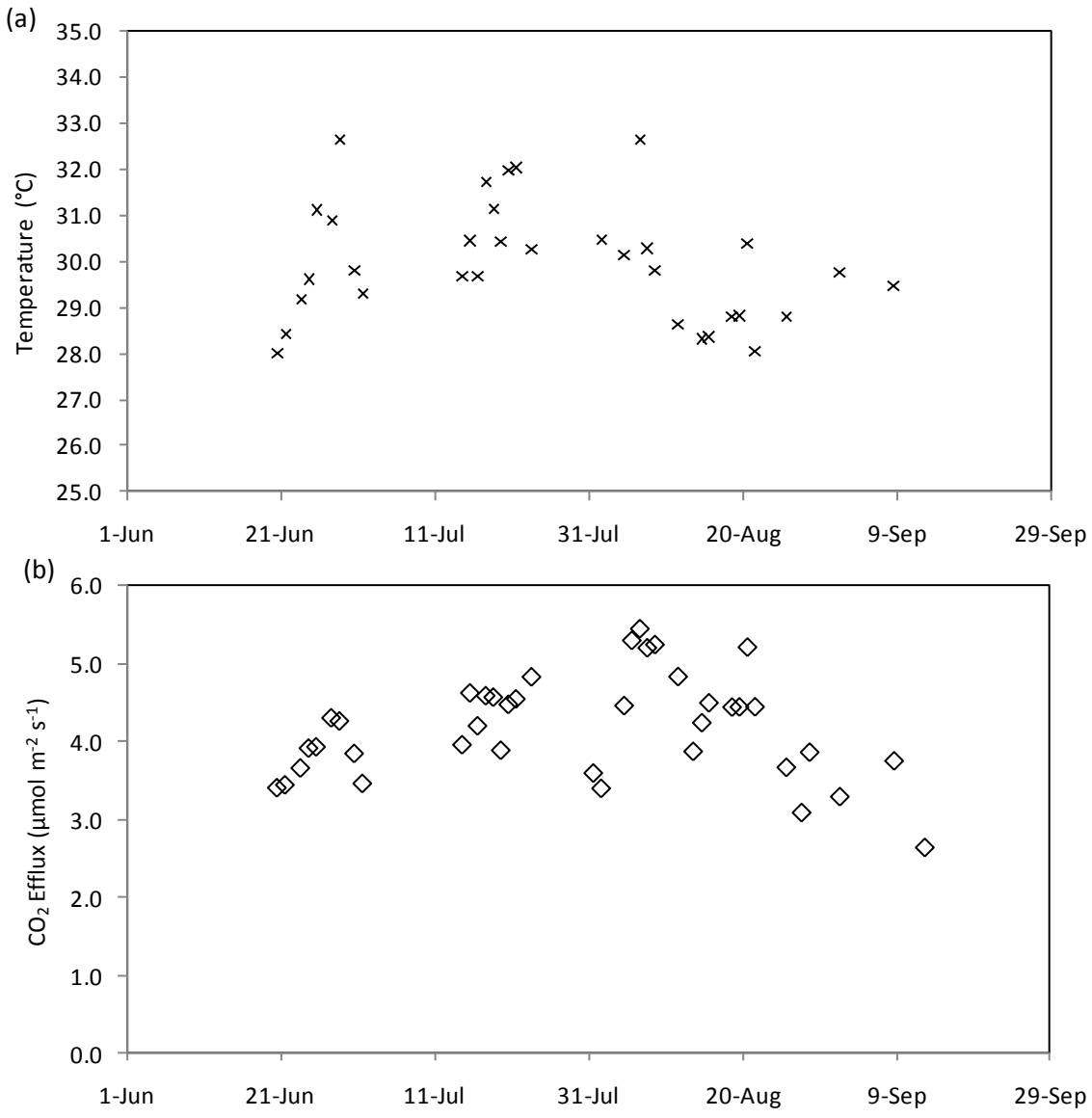

Figure 2.13. Soil temperature at the 2.5 cm depth (a) and corresponding CO_2 efflux (b) for unshaded topsoil mesocosms.

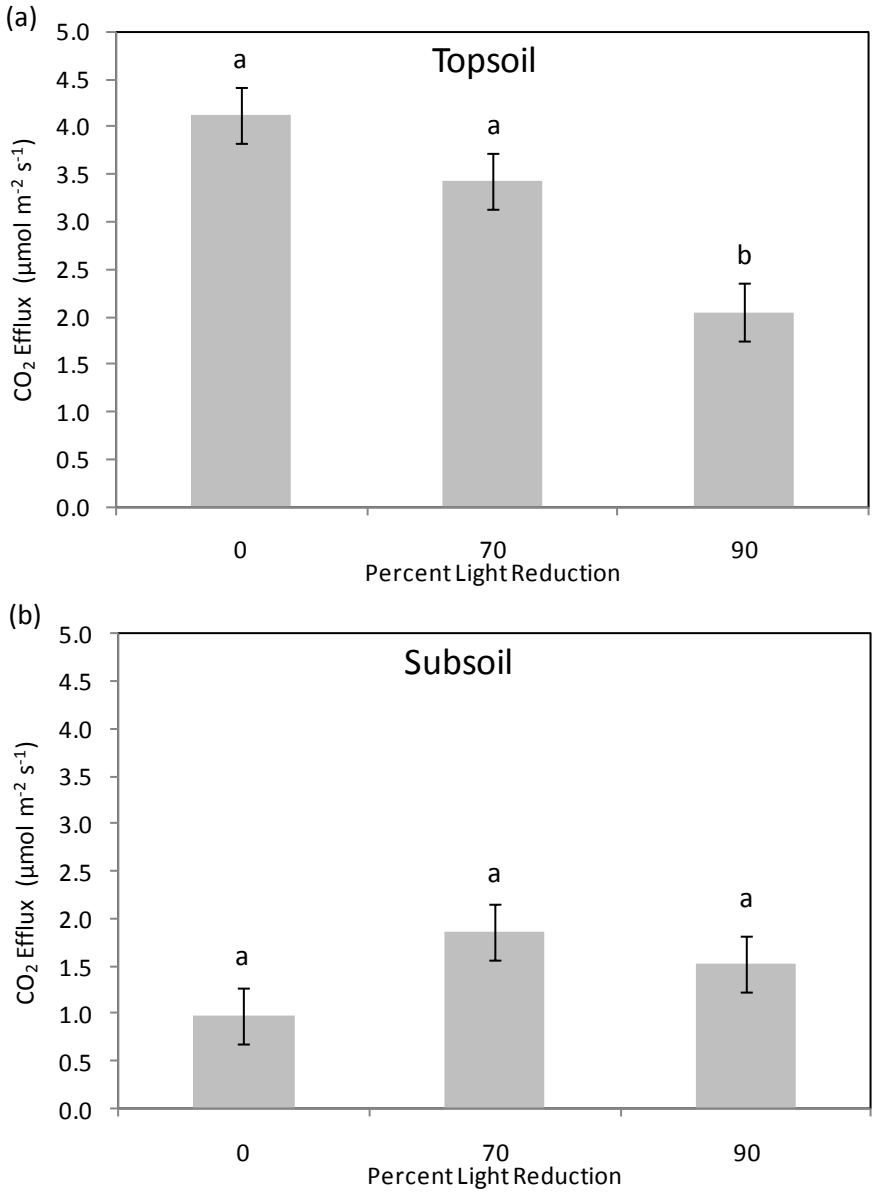

Figure 2.14. Shade*soil type effect on CO_2 efflux for topsoil (a) and subsoil (b) mesocosms for entire experiment duration. Letters indicate significant difference at $\alpha=0.05$. Error bars show standard error of the mean.

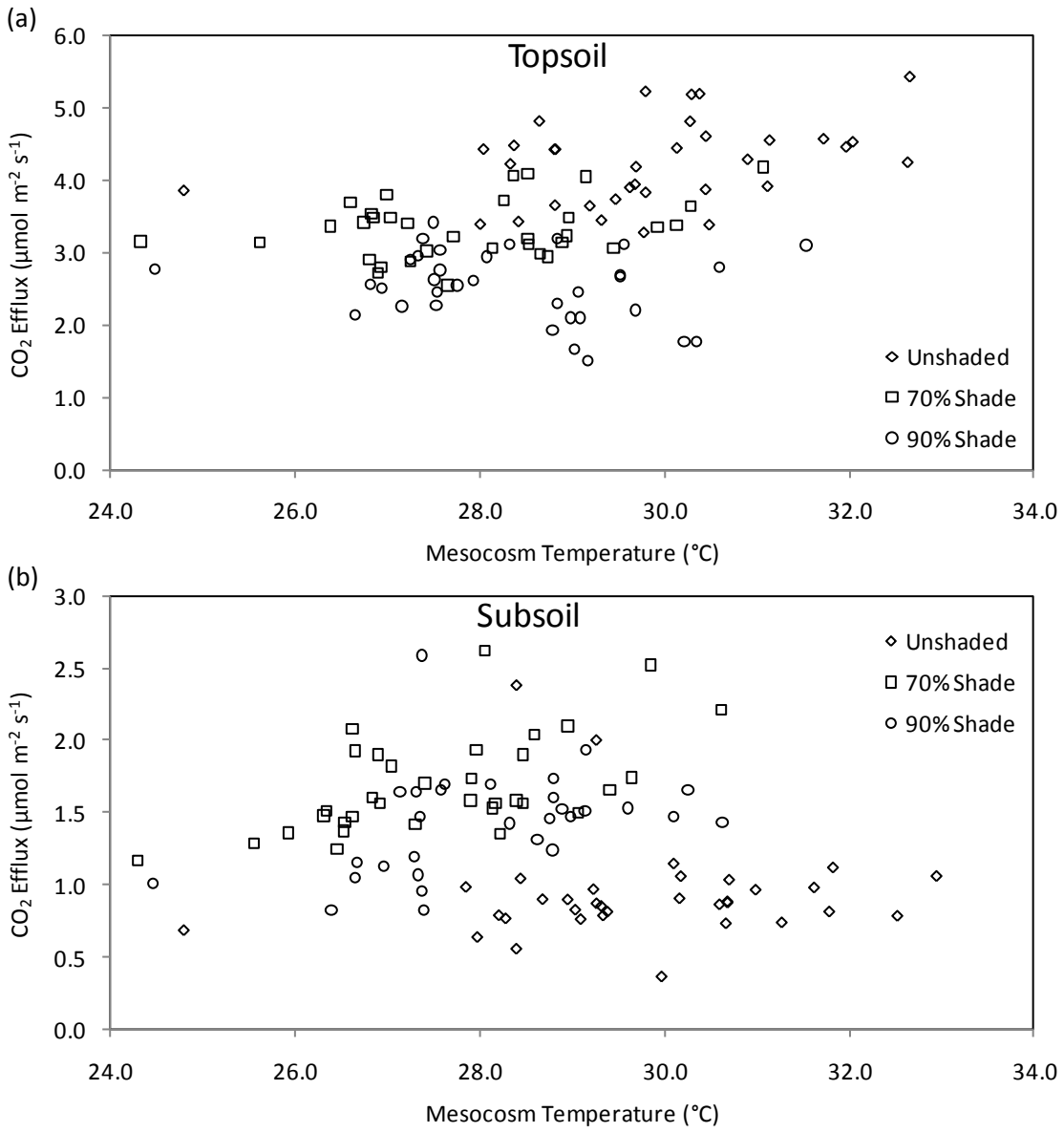

Figure 2.15. CO_2 efflux relationship to soil temperature (2.5 cm depth) for topsoil (a) and subsoil (b) mesocosms.

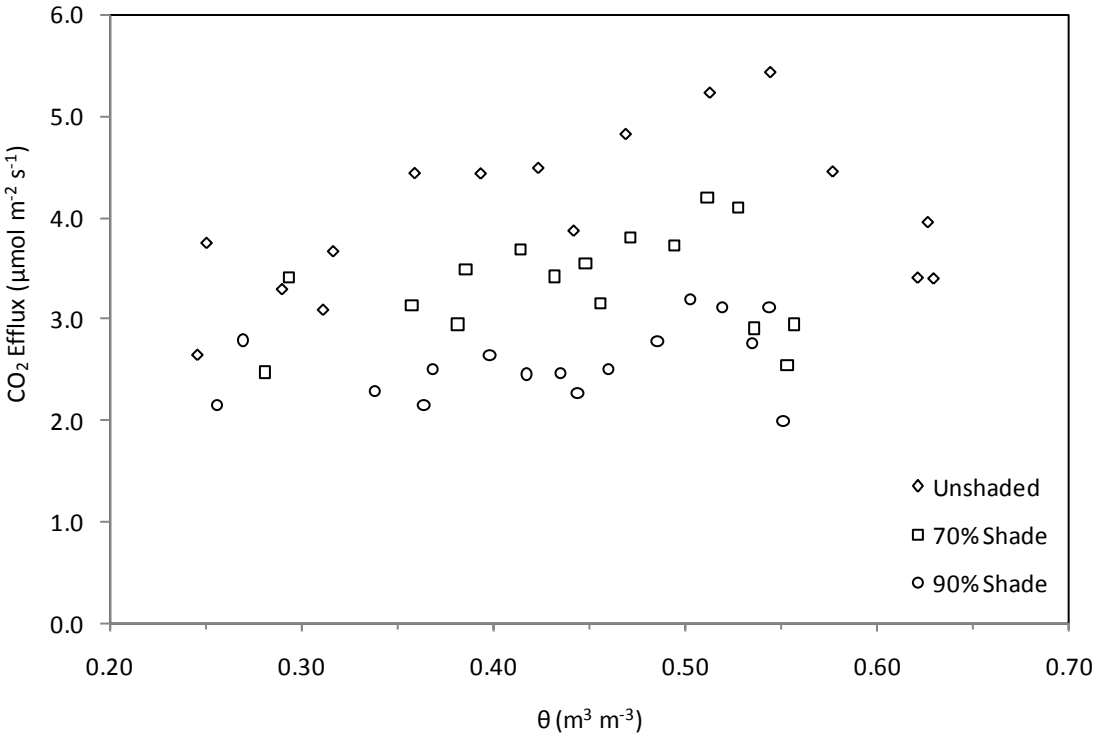

Figure 2.16. Relationship between volumetric soil water content (θ) and CO_2 efflux from topsoil mesocosms.

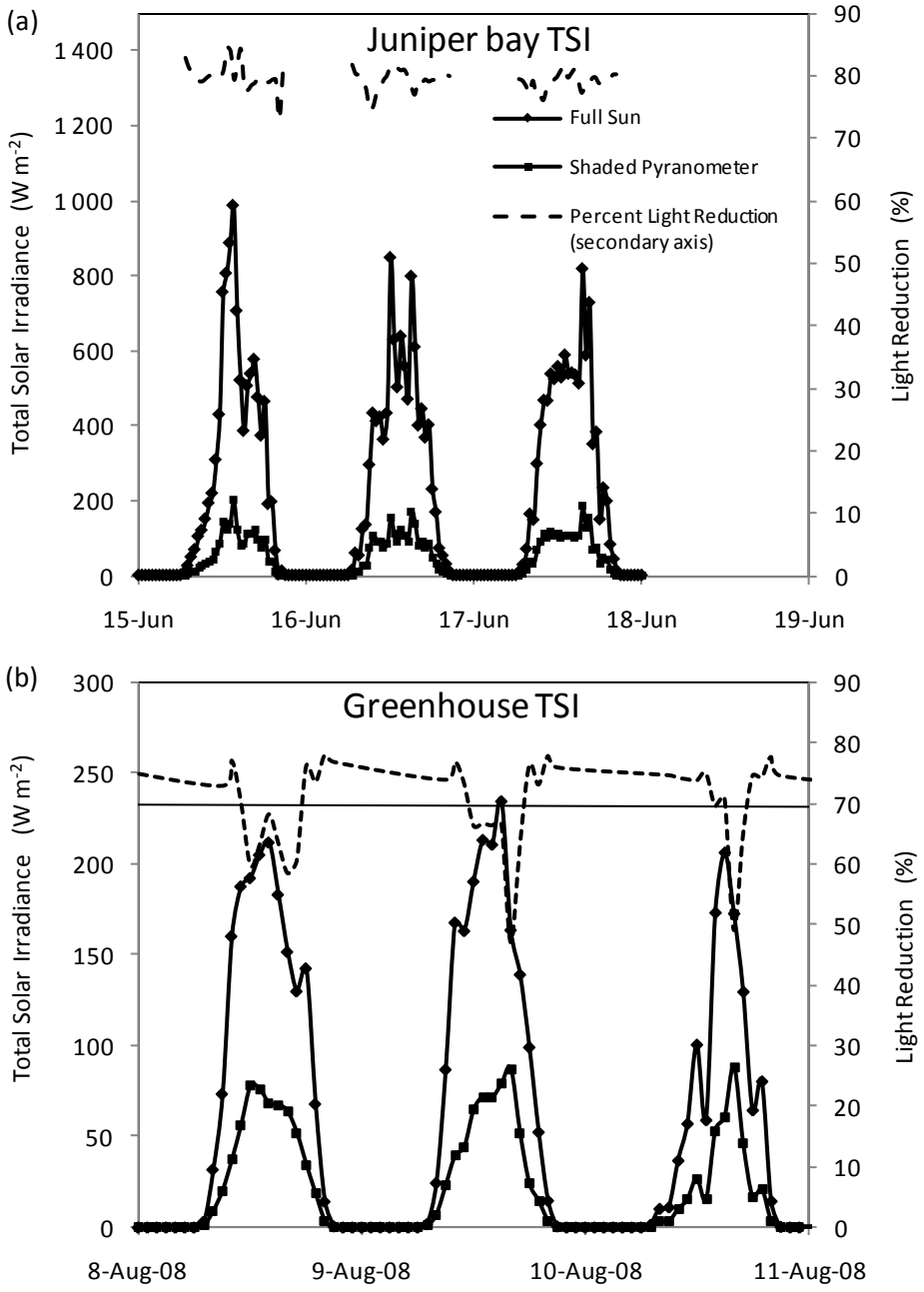

Figure 2.17. Total solar irradiance values observed at Juniper Bay (a) and the greenhouse (b).

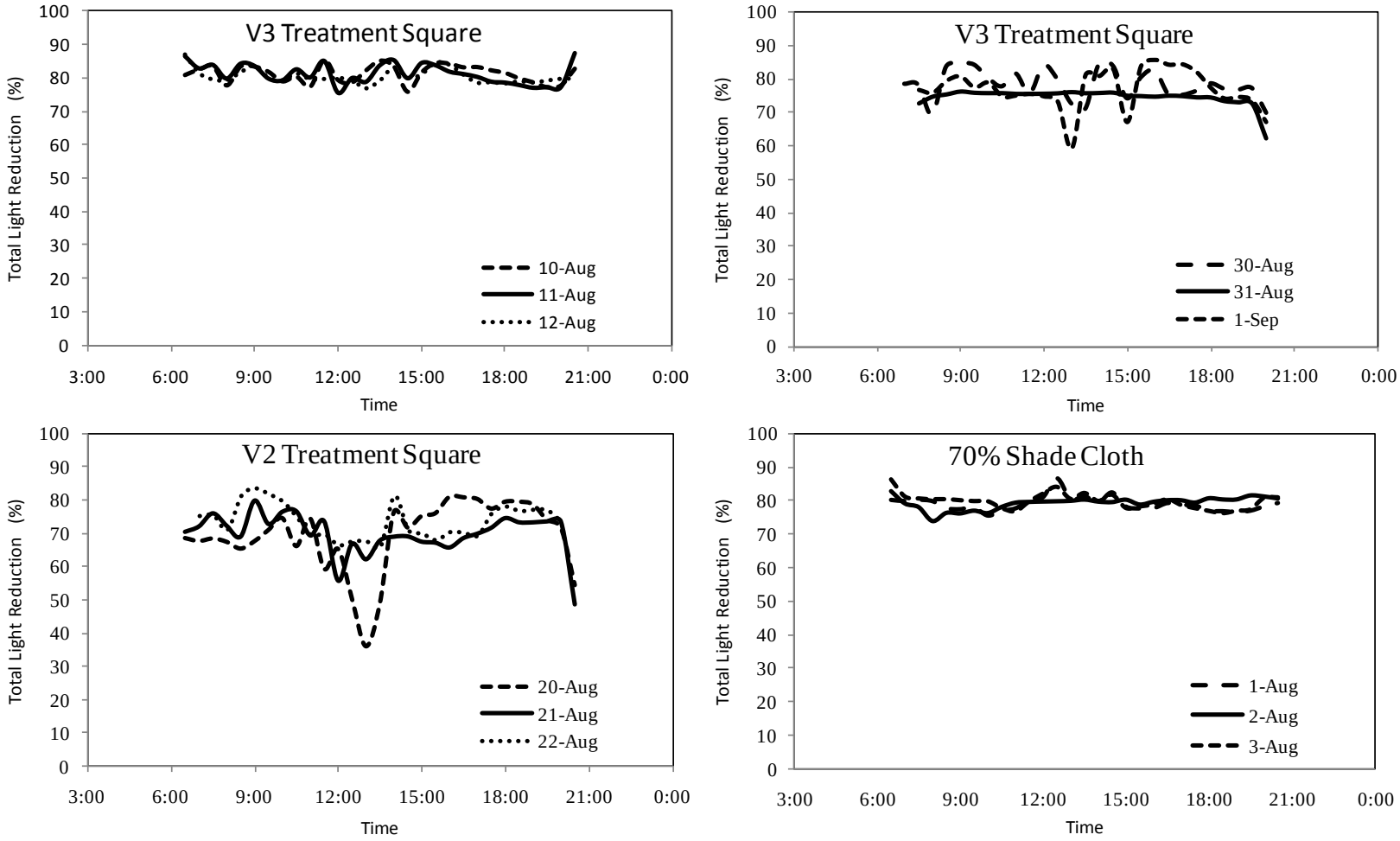

Figure 2.18. Ground level total solar irradiance reduction under vegetated treatment squares compared to that under the shaded pyranometer in the field experiment.

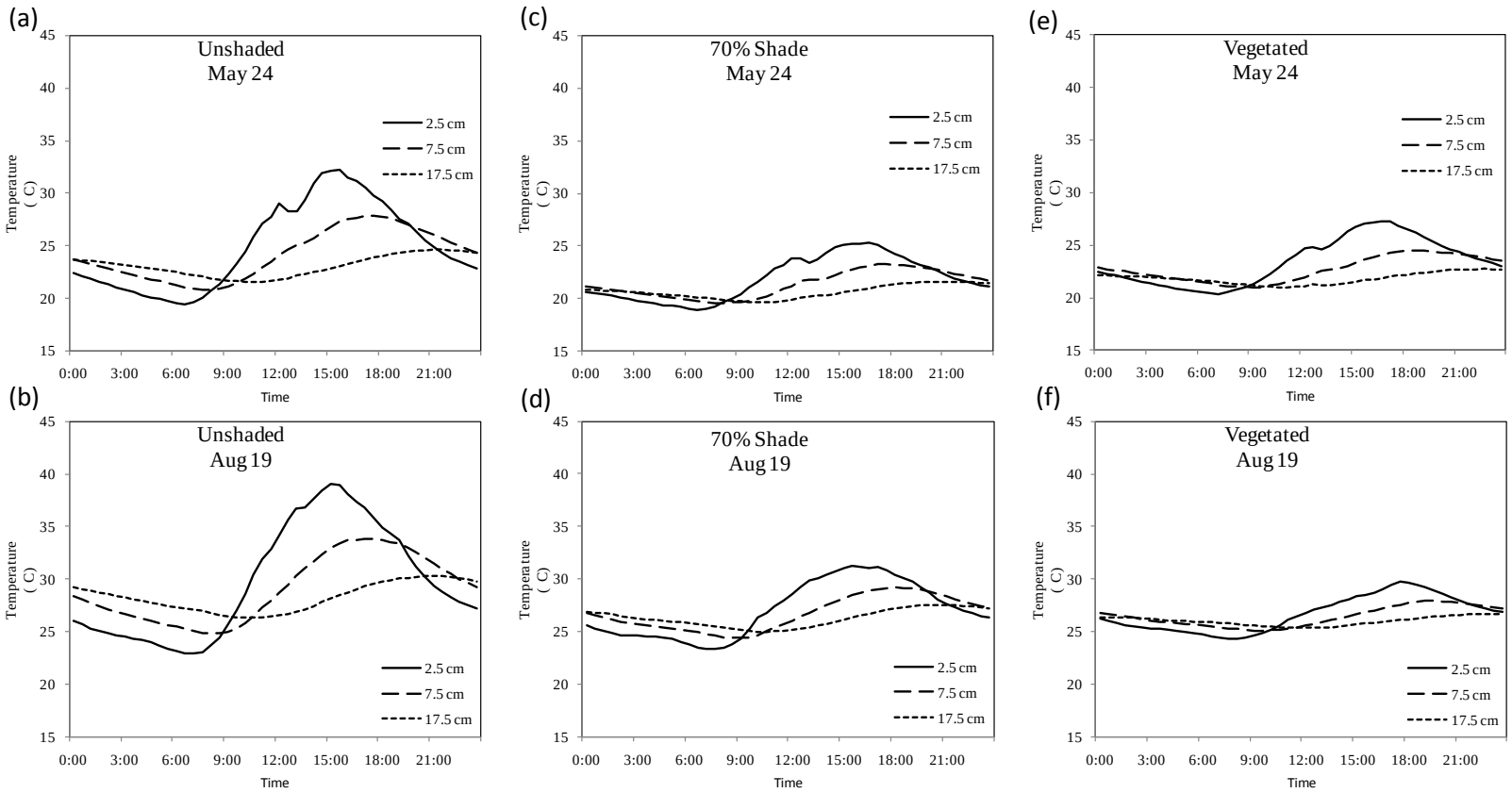

Figure 2.19. Field soil temperatures at 2.5, 7.5, and 17.5 cm on May 24 and August 19. Data are from replicate 1 but well characterize the diurnal trend seen in all replicates.

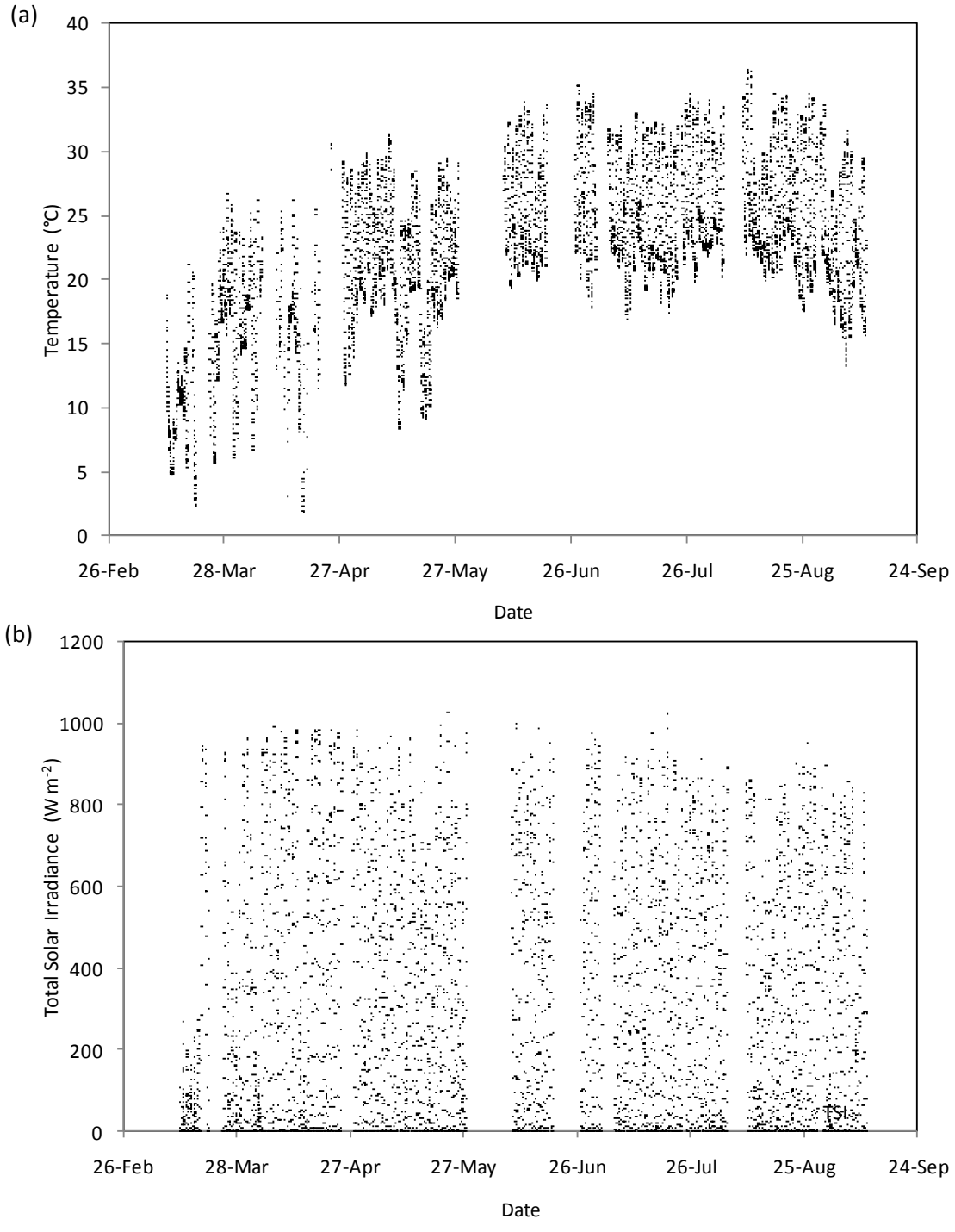

Figure 2.20. Air temperature (a) and total solar irradiance (b) summary for the field experiment duration. Blanks indicate data loss due to logger failure.

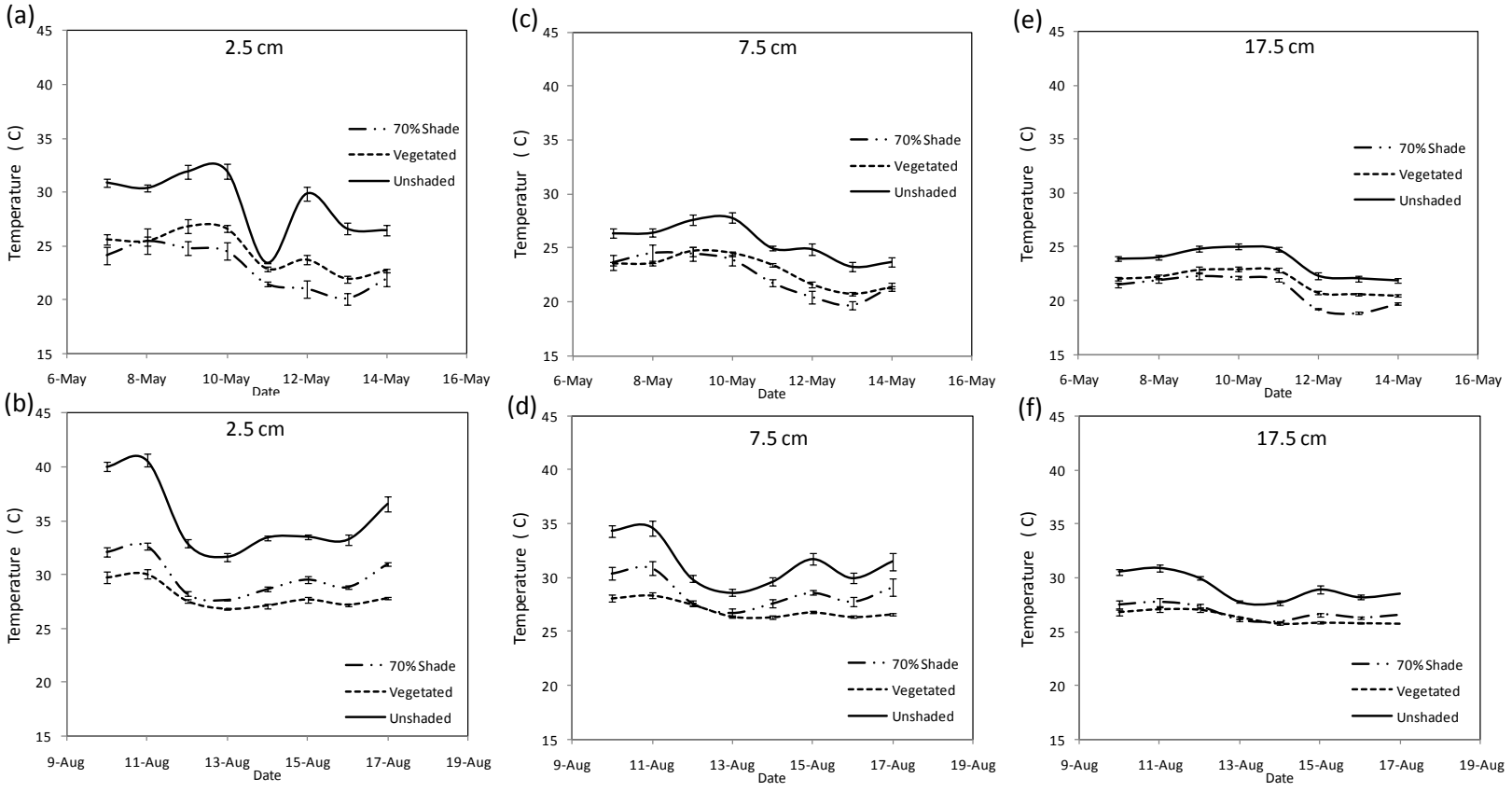

Figure 2.21. Maximum daily soil temperature at three depths through the soil profile at Juniper Bay. Two seven-day periods were chosen to illustrate conditions before (a,c, and e) and after (b, d, and f) vegetation establishment. Error bars indicate standard error of the mean.

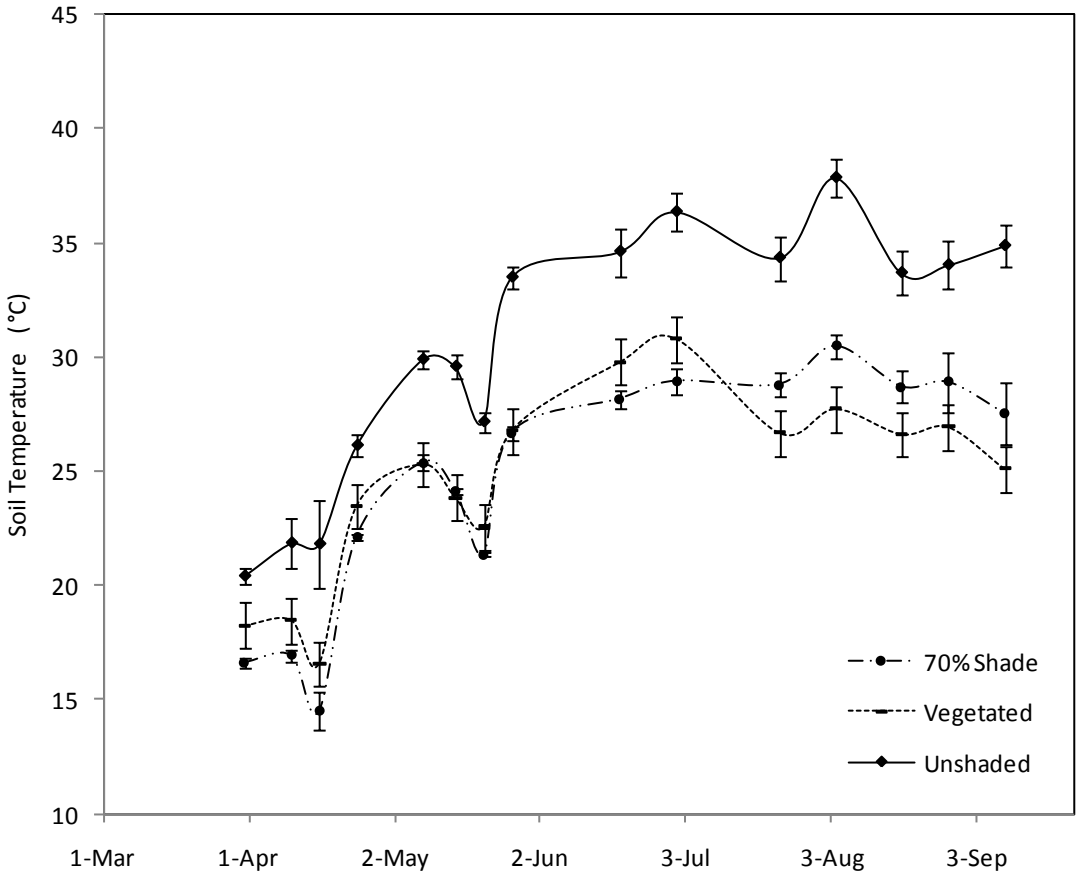

Figure 2.22. Observed near surface (2.5 cm) soil temperature under shade treatments at Juniper Bay on days when CO_2 efflux was measured. Error bars indicate standard error of the mean.

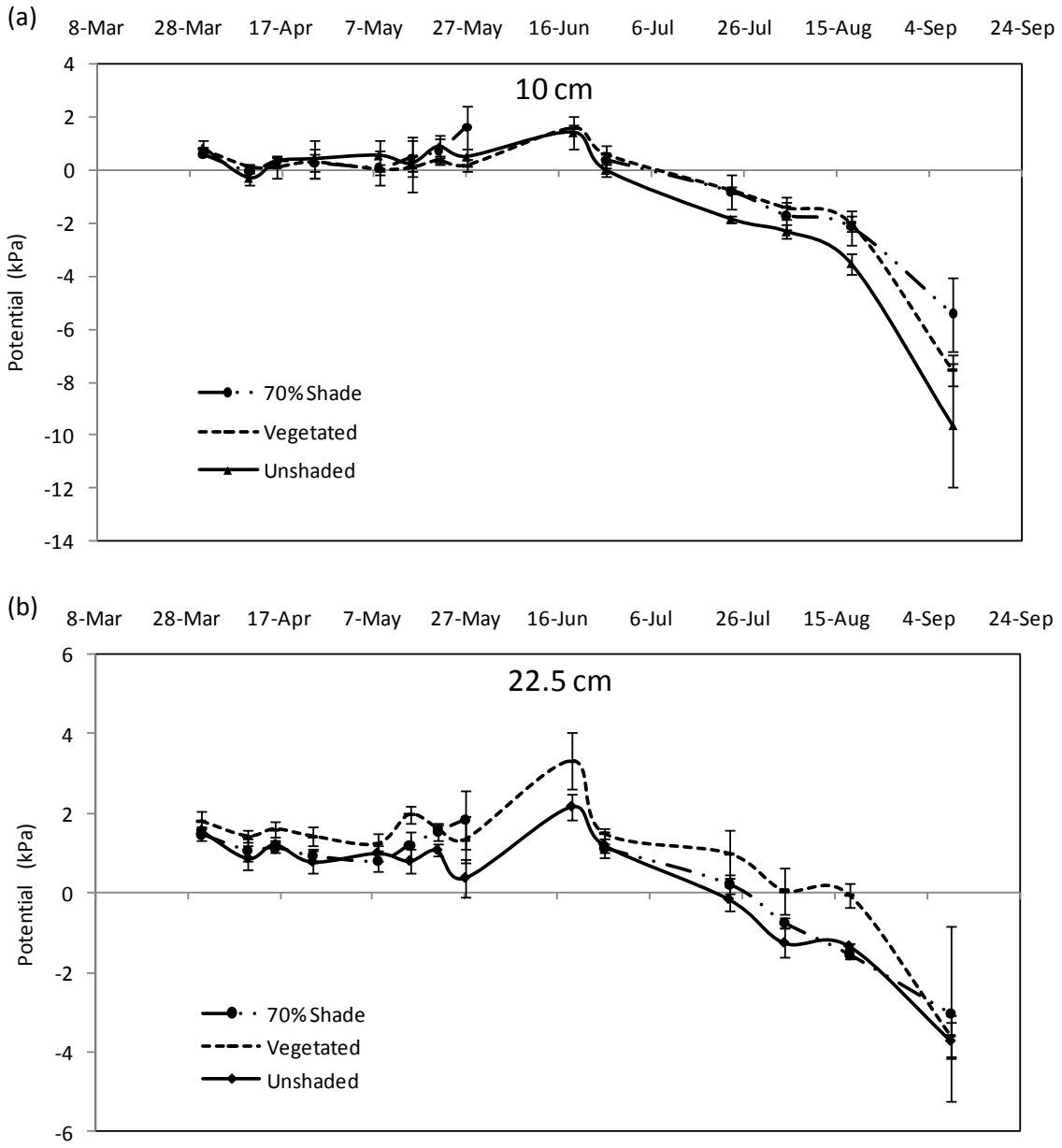

Figure 2.23. Field soil water potential under shade treatments at 10 (a) and 22.5 (b) cm. Error bars indicate standard error of the mean.

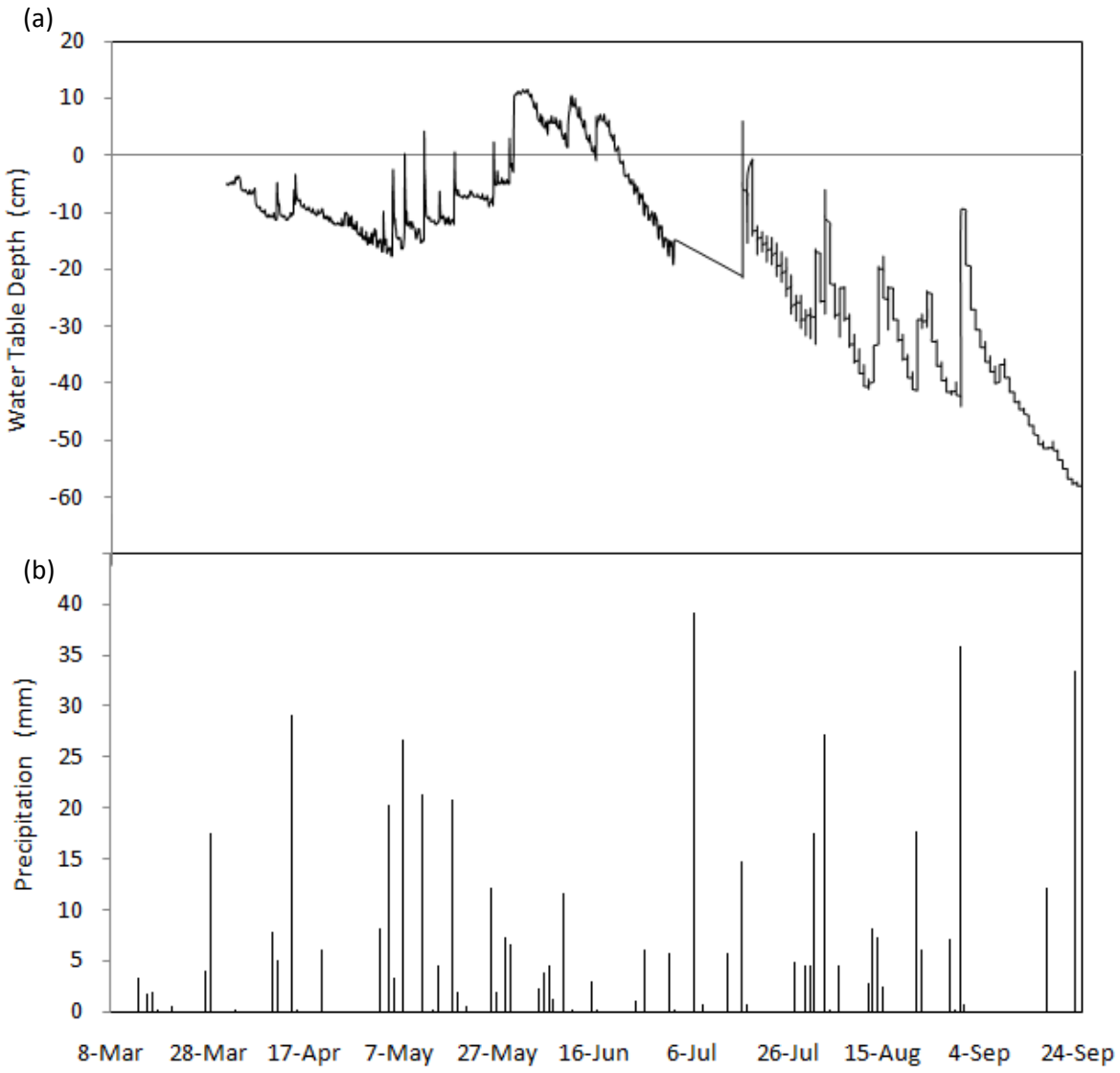

Figure 2.24. Precipitation (a) recorded at Lumberton County Airport and water table depth (b) recorded at the Juniper Bay field site.

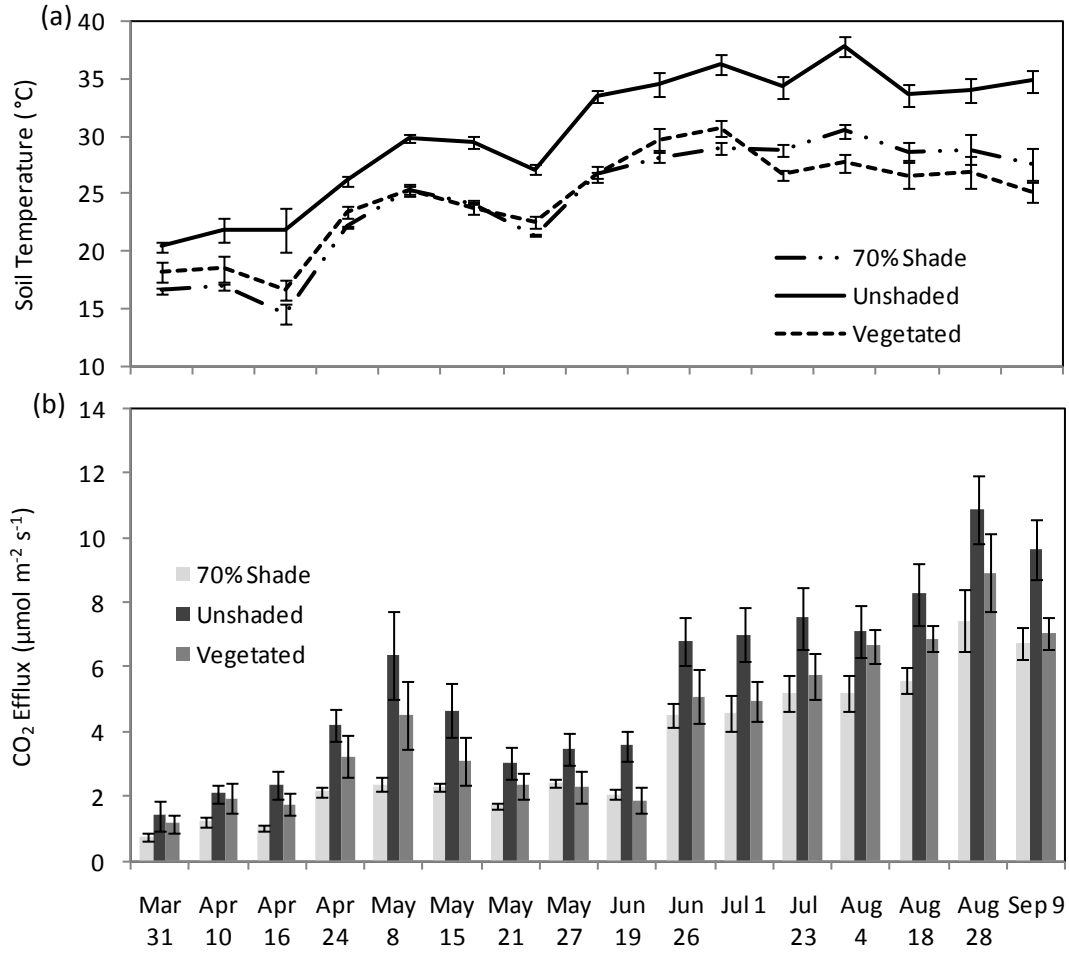

Figure 2.25. Observed field CO_2 efflux (b) and corresponding soil temperature (a) at 2.5 cm during time of measurement. Error bars indicate standard error of the mean.

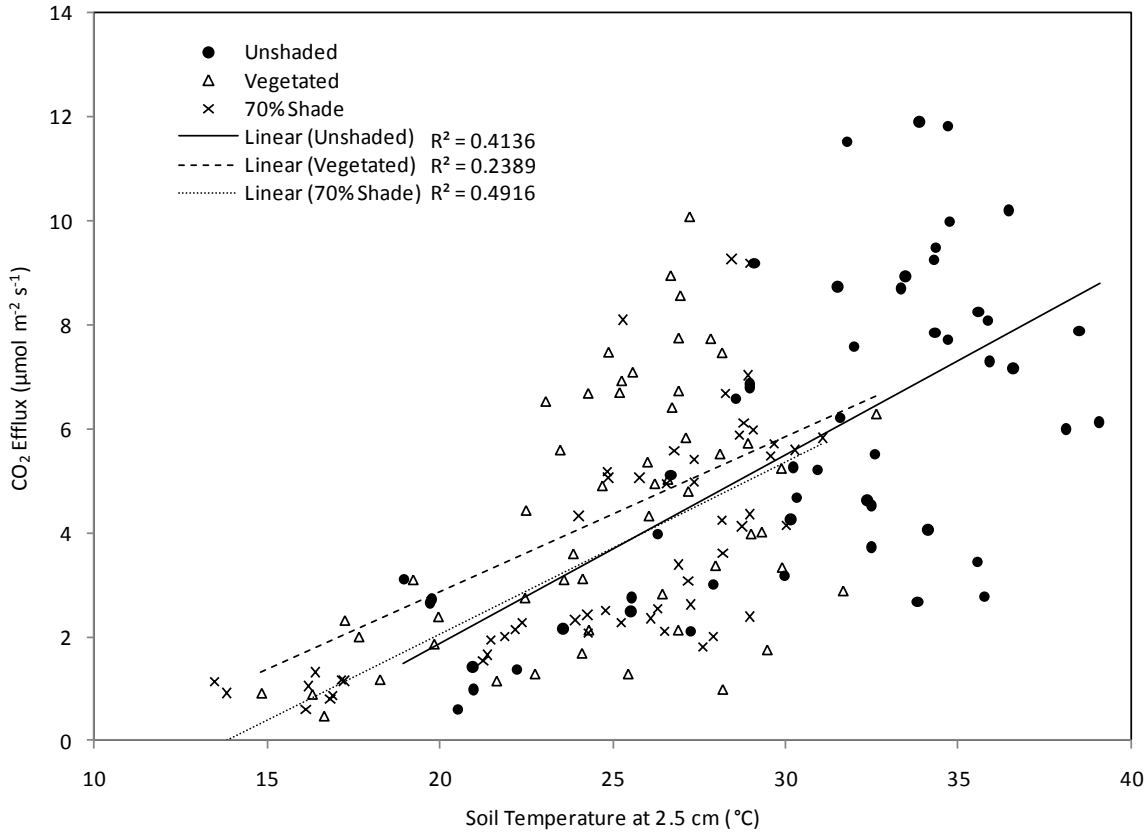

Figure 2.26. Scatter plot of field soil temperature (2.5 cm depth) and observed CO_2 efflux from shade treatments for all days of measurement.

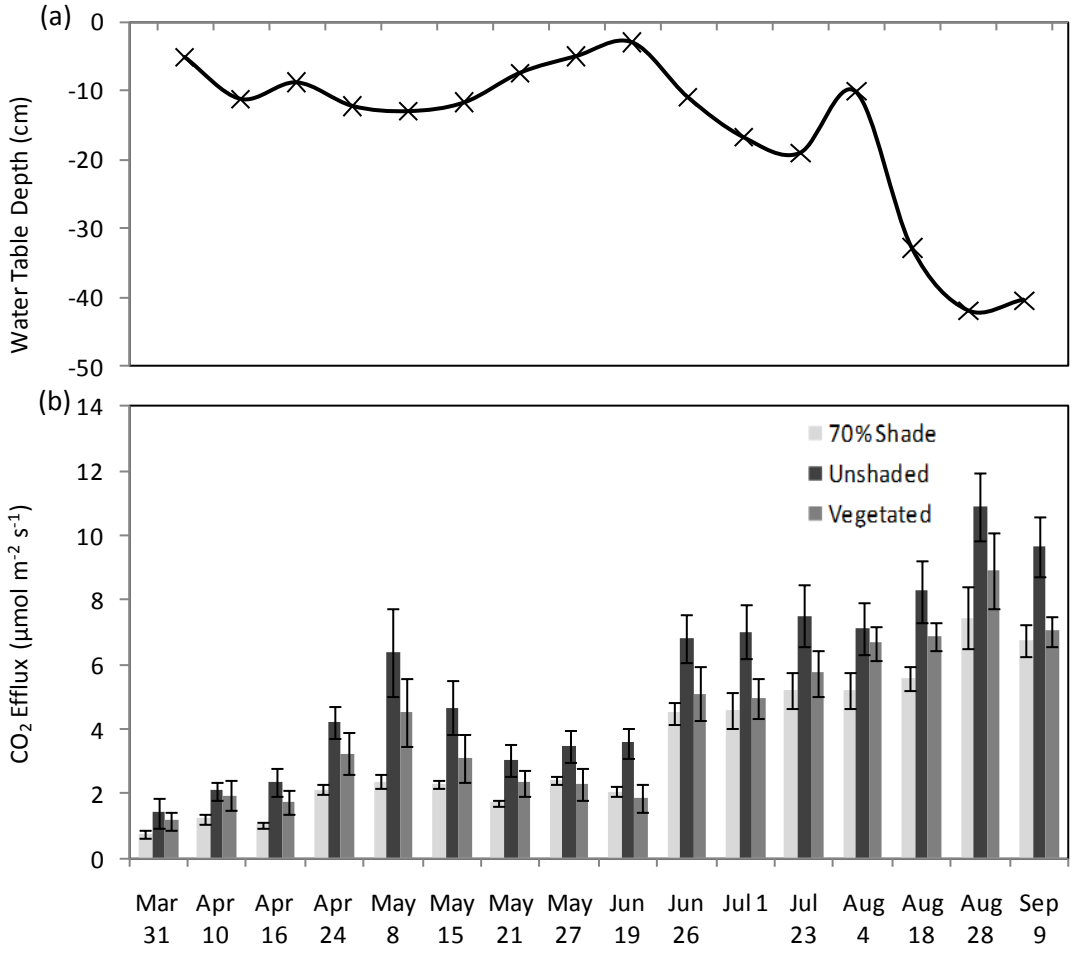

Figure 2.27. Observed field CO_2 efflux (b) and corresponding water table depth (a) during time of measurement. Error bars indicate standard error of the mean.

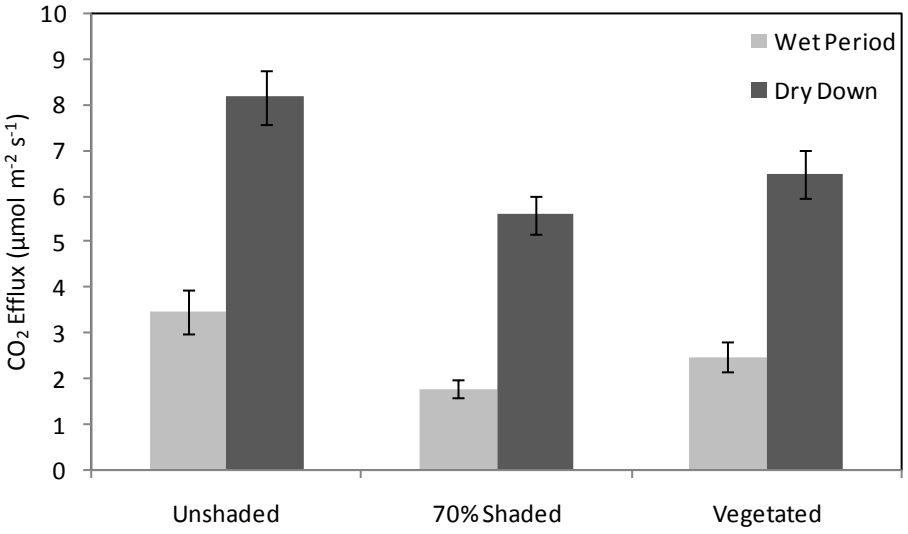

Figure 2.28. Mean observed field CO_2 efflux for shade treatments from March 31 to June 19 (wet period) and June 26 to September 9 (dry period). Error bars indicate standard error of the mean.

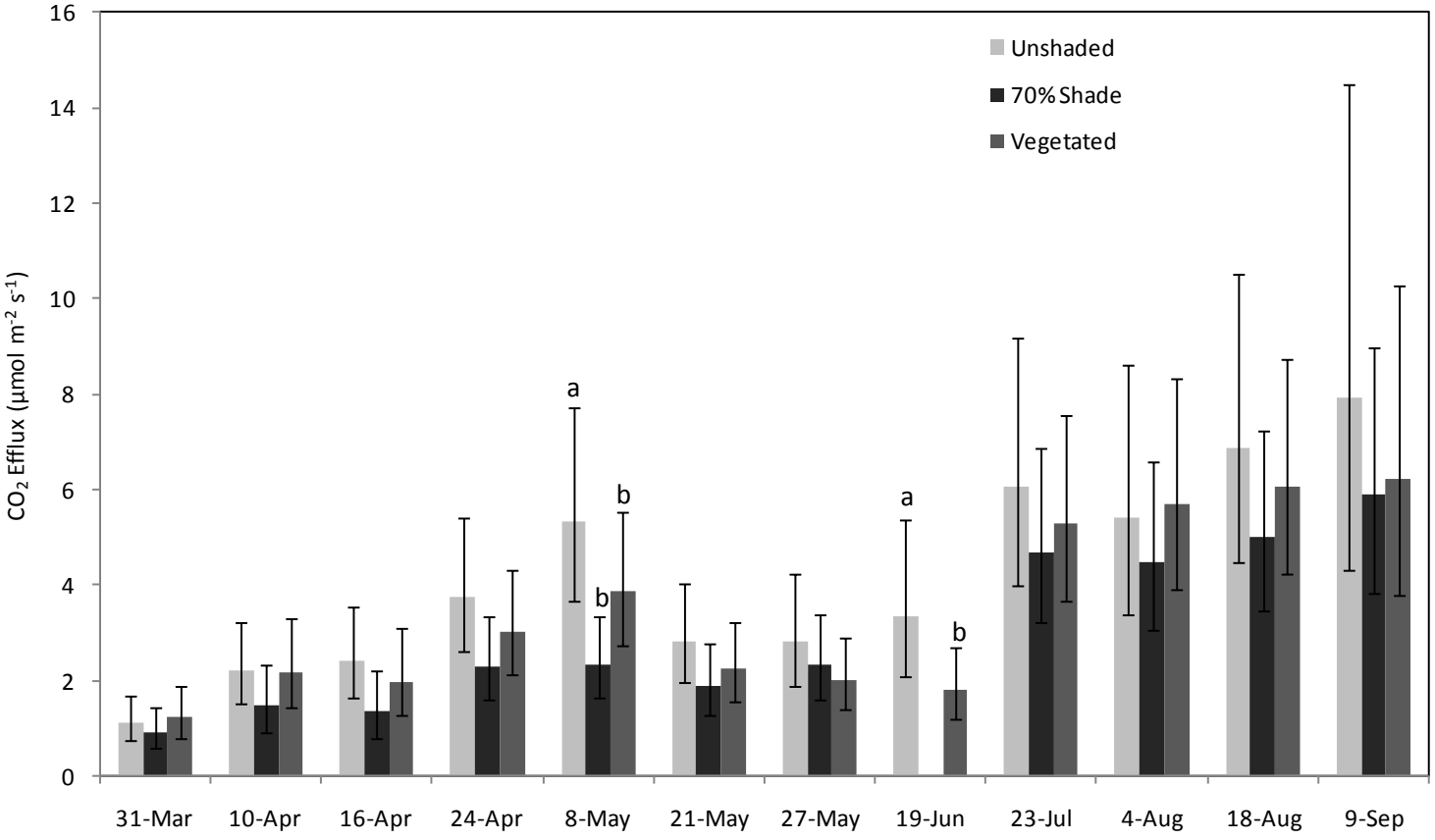

Figure 2.29. Least squares means and 95% confidence intervals of field CO_2 efflux for shade treatments. Letters show means differ at α=0.05.

Chapter 3: Sapric Soil Material Incubation

Introduction

Incubations have been a useful tool for researchers since the early days of soil science (Fulmer, 1917; McBeth, 1917; Waksman and Cook, 1916). Techniques have advanced since the days of Marbut, Winogradsky, and others, but the purpose of most soil incubations remains the same. They provide a simple means for measuring microbially mediated transformations, especially nutrient cycling. Incubations have been used to quantify nitrification (Davidson et al., 2006), denitrification (Burford and Bremner, 1975), methanogenesis (Sugimoto and Wada, 1993), sorption kinetics (Mervosh et al., 1995), and C mineralization (Agarwal et al., 1971) to name a few.

Possibly thousands of incubation experiments have been conducted to measure soil organic matter decomposition and C mineralization. Researchers have concentrated on numerous factors controlling C mineralization, including but not limited to: substrate quality (Nadelhoffer et al., 1991), temperature (Leirós et al, 1999), soil water content (Miller and Johnson, 1964), soil texture (Hasink, 1992), pH (Curtin et al., 1998), and redox potential (Reddy et al., 1986). In spite of the voluminous literature investigating Histosols in alpine and high northern latitude soils, there are far fewer incubations of Histosols found in thermic and warmer soil temperature regimes (Qualls and Richardson, 2008). The low global abundance of these Histosols is a likely explanation for their limited use as an incubation medium. Still, they can be quite common in more localized regions like the Florida Everglades, Carolina bays, and coastal freshwater marshes. Information garnered from incubating these soils can be useful for understanding how the soil C dynamic may respond to changing environmental conditions.

Rather than relying on results already present in the literature, we conducted a soil incubation to test temperature and moisture effects on our particular soil of interest, a Histosol

common to Carolina bays and the southeastern US. Performing our own incubation presented a number of benefits.

First, incubating the soil used for the experiments detailed in Chapter 2 allowed us to bolster the argument that temperature differences created by varying shade treatments were responsible for differences in observed C mineralization rates. Similar responses of C mineralization decreases in the lab and field would provide a link between shade reducing soil temperatures and lower soil temperature decreasing soil C loss via mineralization reductions.

Second, we were able to calculate a Q_{10} value to quantify the rate at which C mineralization increases at temperatures similar to those observed in the field in the absence of additional environmental complications. Q_{10} is affected by a number of factors and can vary greatly with temperature, ranging from near 8 at 0° to 5°C to less than 2 at 30° to 35°C (Kirschbaum, 1995). Not only does Q_{10} change with temperature, but few researchers incubate above approximately 33°C (Kirschbaum, 1995). We observed field temperatures above 33°C and saw a need to gather information underrepresented by the literature.

Furthermore, the literature tends to favor incubations of the Fibrists and Hemists more commonly found northern latitudes rather than the Saprists common to Carolina bays. The characteristics of these suborders can vary widely. For example, comparing soil water effects on C mineralization between the suborders is especially difficult because soil water retention can vary so widely between suborders (Fig. 3.1). The limitations of using results from peat incubations currently present in the literature for describing soil water effects in Carolina bay Saprists was another reason for conducting our own incubations.

The objectives of this incubation experiment were to: (1) observe temperature effects on SOM decomposition in the same soil used in the greenhouse and field study, (2) calculate a

temperature coefficient (Q_{10}) to quantify the expected rate of change for C mineralization at temperatures observed in the greenhouse and field, and (3) determine the optimum soil water content for C mineralization and create a model to predict C mineralization when water content is known.

Materials and Methods

Incubation Procedure

Soil material from Juniper Bay in Robeson County, North Carolina, was collected from the Oap horizon of a soil mapped as the Ponzer series. A thorough description of the soil and field site can be found in Chapter 2. Soil was air dried, ground, and passed through 2 mm sieve. Organic carbon and total nitrogen were determined by the NC State University analytical services laboratory via a dry combustion CHN analyzer (PerkinElmer, San Jose, CA). Soil pH 4 was measured in 1:1 soil water solution by glass electrode pH meter (Fisher Scientific, Pittsburgh, PA).

Soil material was brought to one of three water contents, θ = 0.15, 0.30, or 0.45 m^3 m^{-3}. Volumetric soil water contents 0.15, 0.30, and 0.45 m^3 m^{-3} corresponded to degrees of saturation 25, 50, and 75%, respectively, when bulk density (ρ_b) was 0.6 Mg m^{-3} and particle density (ρ_s) was 1.51 Mg m^{-3}. Particle density was determined using an air pycnometer technique (Flint and Flint, 2002.) Sources report peak C mineralization occurs between 50% (Luo and Zhou, 2006) and 60% (Linn and Doran, 1984) water-filled pore space. Water contents were chosen to capture approximately the optimum water filled pore space for peak C mineralization in addition to mineralization values at water contents commensurate with field θ caused by natural fluctuation of the water table.

After wetting to the desired water content, soil was kept in cold storage at 1°C until needed. Twenty-four hours prior to incubation, approximately 48 g of soil solids was packed to 0.6

Mg m^{-3} bulk density in 100 mL vessels. Vessels were placed into 1 L Ball canning jars (Ball, Daleville, IN) and sealed to minimize water loss. Eighteen jars were prepared in this manner, six for each water content. Jars were placed in an incubation chamber for 24 h to reach incubation temperature. Following acclimation, lids were removed for 300 s to allow total air replacement. Sodium hydroxide CO_2 traps were placed in each jar prior to replacing the lids. Jars were incubated for 48 h following lid replacement. Six jars containing traps only were incubated as controls. Two 48 h incubations were run for each temperature (Fig. 3.2).

Incubation temperatures 25°C and 37°C were chosen for a few reasons. We estimated growing season soil temperatures near the surface at Juniper Bay would likely fall somewhere within this range and wished to measure mineralization under conditions reflective of a Carolina bay during the growing season. As previously discussed, relatively few incubations are conducted above 33°C. Secondly, the warmer and cooler incubation temperatures could represent soil temperature conditions in full sun and extreme shade or even daily high and low temperatures. C mineralization data from these temperatures would be useful for predicting whether temperature differences induced by shade would significantly affect SOM decomposition rate and how C mineralization fluctuates diurnally. Finally, two temperatures provided sufficient data to calculate Q_{10} for the soil material.

To measure CO_2 respiration, we used aqueous alkali CO_2 traps and titrimetric analysis (Anderson, 1982). CO_2 respired from the soil reacted with the alkali solution to ultimately yield sodium carbonate.

$$CO_2(g) + NaOH(l) \rightarrow NaHCO_3(l) \quad (1)$$

$$NaHCO_3(l) + NaOH(l) \rightarrow Na_2CO_3(l) + H_2O(l) \quad (2)$$

Alkali traps were made by placing 7 mL of 0.27N NaOH into 25 mL vials. Vials were immediately capped after incubation to cease atmospheric CO_2 adsorption. Prior to titration, 5 mL of 1M $BaCl_2$ were added to each vial to precipitate trapped CO_2 as insoluble $BaCO_3$ precipitate.

$$BaCl_2 + Na_2CO_3 \rightarrow 2NaCl(l) + BaCO_3(s) \quad (3)$$

Vials were titrated with 0.1N HCl to a phenolphthalein indicated endpoint of pH 8.2.Total CO_2 evolved in each jar was calculated by subtracting the titrant required to titrate the respective alkali trap from the mean titrant required for the controls and dividing by two to correct for the stoichiometric ratio of 2 NaOH molecules required to trap each CO_2. Because the total amount of soil in each jar varied, mmol CO_2 evolved was normalized by soil mass to mg C kg^{-1} soil d^{-1} for unbiased comparison between temperature and water treatments.

Soil mass, ρ_b, and gravimetric water content (W) for each sample were measured after incubation. Gravimetric water content was determined by oven drying at 105°C until no further mass loss was observed. Mass of soil water was the difference of wet soil minus oven dry soil. Bulk density was the mass of solids divided by the soil volume within the 100 mL vessel. From W, soil volume, and ρ_b we calculated volumetric soil water content, porosity, and degree of saturation.

SAS version 9.1 (Cary, NC) was used to analyze the observed mineralization data. Using the mixed model procedure, we constructed two models, one for each temperature, to predict CO_2 mineralization with water content. Temperature was treated as a class variable. Q_{10} was calculated as

$$Q_{10} = (R_1/R_2)^{[10/(T2-T1)]} \quad (4)$$

where R_1 and R_2 are mineralization rates at temperatures T_1 and T_2, respectively.

Soil Water Retention Curve

A soil water retention curve was developed to represent the incubated soil. The retention

curve was developed to determine the corresponding matric potential for each volumetric water content. Five intact cores were collected from the surface of the Oap horizon, 0 to 7.6 cm. Cores were placed in Buchner funnels with good contact between the core base and underlying 1 bar ceramic plate. Cores were fully saturated from the bottom. Water was removed from the excess air space in the Buchner funnels. Funnels were sealed at the top, with the exception of a single port connected to a central pressurized air reservoir. Free water drained through the ceramic plate and was collected in a 100 mL graduated cylinder.

Pressure was applied to the cores in six steps: 3.91, 5.87, 9.78, 19.56, 32.57, and 48.9 kPa. A correction was applied to the absolute pressure to compensate for the height of the cores, 7.6 cm, by assuming the pressure at all heights in the core was equal to the pressure at the core center. Corrected pressures were 3.54, 5.5, 9.41, 19.19, 32.32, and 48.53 kPa. Pressures were applied until water loss from cores ceased. Volume of water drained at each pressure was recorded, and the next pressure was applied.

Following the final pressure step, cores were removed from the funnels, weighed, and dried at 105°C until no further mass loss was observed. Gravimetric water content and bulk density were determined as described previously. Total porosity was calculated by adding the cumulative volume of drained water to the volumetric water content at the final pressure step. Volumetric water content at each pressure step was the volumetric water content at saturation minus the cumulative volume of water lost at the respective pressure. Soil water retention data were analyzed with StatCrunch (Integrated Analytics).

Results and Discussion

Incubation and Soil Parameters

Soil mass and bulk density of the incubated samples were consistent for all incubations. The average mass of soil incubated was 47.7 g with standard deviation 0.423g. There was one outlier in a 37°C incubation weighing 43.2 g. Like mass, ρ_b was consistent among soil samples with the exception of the same outlier. Average ρ_b was 0.60 Mg m^{-3} with standard deviation 0.009 Mg m^{-3}. Low variability of ρ_b was a good indication that differences in mineralization were not attributable to bulk density.

Soil water content of samples with similar desired θ did not vary widely within incubations (Table 3.1). Soil water content was initially considered a class variable. This approach was later abandoned after θ differences between incubations manifested. Samples within replicate 1 of the 37°C incubation were consistently drier than the other three incubations. The soil showed some hydrophobicity upon wetting and it is possible that the soil had not yet wetted to the desired θ. Instead, θ was treated quantitatively and there were still three distinct conditions of soil moisture for each period of incubation: dry, moist, and wet. Among all incubations, dry treatments fell between 0.12-0.17 m^3 m^{-3}, moist were 0.19-0.32 m^3 m^{-3}, and wet were 0.24-0.48 m^3 m^{-3}. If replicate 1 of the 37°C incubation is omitted, the range of water contents narrows to: 0.15-0.17 m^3 m^{-3}, 0.23-0.32 m^3 m^{-3}, and 0.38-0.48 m^3 m^{-3}.

Temperature Effects

Mineralization rate respective to soil mass, rather than absolute mineralization, was reported to eliminate differences due to varying soil sample mass. The magnitude of observed mineralization rates appeared reasonable for all incubation temperatures and water contents. Total C mineralized per kg soil was generally higher than values reported for mineral soils (Lomander et

al., 1998; Zak et al., 1999), which was consistent with the larger pool of C in our incubated soil. C mineralization showed a strong positive response to incubation temperature for all water contents. Q_{10} across all water contents was 2.00. Kirschbaum (1995) synthesized Q_{10} results from numerous incubations and fitted a curve to describe the Q_{10} relationship with temperature (Fig. 3.3). The Q_{10} from our incubation falls squarely on the line at 25°C. While not all synthesized incubations were performed under similar conditions, our Q_{10} does seem to agree with results from the 20 experiments used to create the curve.

Soil Moisture Effects

The rate of C mineralization at 25° and 37°C was highest under moist soil water conditions, 46.65 and 96.51 mg C kg^{-1} soil d^{-1}, respectively, especially when θ fell between 0.29 and 0.32 m^3 m^{-3} (Fig. 3.4). Soil pores were 49-54% water filled at these water contents, respectively. For the 25°C incubation, mineralization was lowest in the wettest soil samples, 26.53 mg C kg^{-1} soil d^{-1}. At 37°C the driest soil samples respired the least CO_2, 52.91 mg C kg^{-1} soil d^{-1}. The variety of methods used to report soil water content creates some difficulty when comparing water contents for optimum microbial decomposition. Ilstedt et al (2000) achieved maximum C mineralization rate at 45% water filled porosity while Curiel Yuste et al. (2007) observed optimum respiration at 0.26 m^3 m^{-3}. Still others observed 70% and 50% water holding capacity for incubated litter layer and mineral soil (Bowden et al., 1998), respectively and 60% water filled pore space (Linn and Doran, 1984) in mineral soil. Unfortunately, while θ and other methods of reporting water content are often used, parameters like bulk density and soil texture complicate comparisons of optimum water content for C mineralization. Complicating factors are avoided when soil water potential is used to report soil water availability.

Soil Water Retention Curve

Results from the soil water retention curve were summarized graphically (Fig. 3.5). Total porosity of the cores ranged from 0.58 to 0.64 m^3 m^{-3}. Soil water decreased to a minimum of 0.33 to 0.38 m^3 m^{-3} at -496.2 kPa. The soil water retention curve shows qualities expected for highly organic soil. Total porosity was high, approximately 61.5%. Some published retention curves show porosity as high as 85-90% (Fig. 3.1), but those soils may have contained a higher percentage of organic matter. Analysis revealed the incubated soil contained 34.28 to 36.85% total organic carbon. The soil also showed an initial large pore dewatering from 0 to -10 kPa where θ decreased from 0.62 to 0.43 m^3 m^{-3}. The soil stayed relatively wet from -10 to -49 kPa, decreasing from 0.43 to 0.36 m^3 m^{-3}.

Due to equipment restrictions, the soil water retention curve did not extend into the optimum zone (moist) of soil water content, though it still remained useful. Incubation data show C mineralization rate corresponded with initial pore dewatering. Mineralization decreased when soil water content was greater than 0.42 m^3 m^{-3} or approximately -8 kPa. Optimum mineralization rates were observed after initial dewatering when soil water contents corresponded with the flat portion of the curve, from -10 to less than -50 kPa. Using the retention curve, we can predict that microbial decomposition will begin to increase after initial pore dewatering, below -10 kPa.

Temperature Moisture Interaction

Interestingly, soil moisture content appeared to affect the mineralization response to increasing temperature. Mineralization response to temperature tended to increase with soil water content. The driest incubated soil tended to exhibit the lowest temperature response. Q_{10} of the driest samples, 1.64, was the lowest observed (Table 3.2). Temperature response increased to 1.83 in the moist soil samples and peaked at 2.51 for the wettest samples. Similar interaction between

temperature and water content has been observed by others. Reichstein et al. (2002) saw a linear two-fold increase in Q_{10}, 1.0 to >2.0, as water content increased from 35% of field capacity to 100% field capacity. Wen et al. (2006) observed a non-linear response to increasing water content unlike Reichstein's and our own. Where Reichstein's data and our data show Q_{10} increasing with water content, Wen et al. (2006) observed a decrease when water content exceeded the optimum for C mineralization. Q_{10} was 1.3 at 0.12 m^3 m^{-3}, increased to 2.3 at 0.2 m^3 m^{-3}, and decreased to 1.6 at 0.31 m^3 m^{-3}. Optimum C mineralization occurred slightly below 0.2 m^3 m^{-3}. The absence of decreasing Q_{10} for water contents wetter than optimum in Reichstein's and our own data does not necessarily imply disagreement. Reichstein et al. (2002) did not show Q_{10} data for conditions wetter than optimum, possibly omitting the water content range where Q_{10} decreases. We calculated Q_{10} for only three ranges of water contents, the highest of which may have been too low to cause a decrease in Q_{10}.

Several mechanisms have been proposed to explain the water content effect on Q_{10}. Anderson (1991) suggested the labile organic matter fraction, the majority of which is surface plant litter, is the first to dry out, becoming unavailable to microbial decomposition. Consequently, the total mineralizable C pool is effectively decreased in size. Boone et al. (1998) hypothesized partial inactivation of the rhizosphere during drying led to lower Q_{10}. While these explanations may apply to in-situ soil responses, our soil contained no litter layer or plant roots. The most likely explanation for decreased Q_{10} under dryer conditions was probably limitation diffusion of soluble substrate supply (Linn and Doran, 1984). Once microbial growth and organic matter decomposition became limited by moisture, a temperature increase would have less impact. For water contents above optimum, atmospheric gas exchange is limited and oxygen becomes depleted, reducing the microbial capacity for organic matter decomposition (Linn and Doran, 1984; Wen et al., 2006).

Predicting C Mineralization

Two models were produced to predict soil C mineralization rate, R_s, at both 25° (eq 2) and 37°C (eq 3). Goodness of fit statistics show the models describe the dependence of C mineralization on water content at each temperature quite well (Table 3.3).

$$R_{s,25} = -52.843 + 419.98 * \theta - 430.96 * \theta^2 \qquad R^2 = 0.9085 \qquad (5)$$

$$R_{s,37} = -102.62 + 836.25 * \theta - 823.86 * \theta^2 \qquad R^2 = 0.8571 \qquad (6)$$

The 25°C incubation was well represented at a wide range of water contents and the points did not deviate widely from the curve (Fig. 3.6). Observed values were not as well centered around the 37° C model. There was one low outlier on the dry side and several low values on the opposite, wet side of the curve. There was some mineralization variability around the optimum (~0.3 m^3 m^{-3}) water content on both curves. Values here tended to be slightly higher than the model predicted. Also familiar to both models was an overestimation of C mineralization at the wettest water contents. Four of six observed values at 25° and 37°C fall below the predicted value. Despite the variability, the models appear to be a simple, useful tool for predicting C mineralization at the respective temperatures of incubation.

Incubation Summary

The dependence of C mineralization rate on temperature and water content in a C rich soil was clearly demonstrated by the preceding incubations. While the magnitude of C mineralization per kg soil was much higher than mineral soils, we were still able to make useful comparisons between the two. The incubated soil had a two-fold increase in C mineralization when ambient temperature was increased by 10°C from 25°C, a Q_{10} similar to most mineral soils incubated at the same temperature. The high porosity of the incubated soil caused the optimum volumetric water

content for peak C mineralization to be greater than many other mineral soils, approximately 0.31 m^3 m^{-3}. Although, C mineralization was not greatly reduced until θ reached almost 0.45 m^3 m^{-3}. A noteworthy soil water and temperature interaction was observed, as temperature response increased with water content. The data do not show Q_{10} decreasing for water contents wetter than optimum for peak mineralization, suggesting that additional incubations of saturated soil are required to capture the water content at which temperature response decreases.

The temperature and water content interaction is especially important to note with respect to the soil's position on the landscape, Carolina bays. A lowering of the water table during the growing season in Carolina bays can produce near surface matric potentials that closely correspond to the optimum volumetric water content for both C mineralization and temperature response (Q_{10}). Such conditions were detailed in Chapter 2. Consequently, the time when C mineralization is highest is concurrent with the optimum period for reducing C mineralization via temperature reduction. The results of this incubation further suggest that temperature reduction during the growing season, when the water table is low, could be critical to decreasing annual soil C loss via C mineralization.

REFERENCES:

Anderson, J.P.E. 1982. Soil Respiration. p. 831-871. *In* A.L. Page, R.H. Miller and D.R. Keeney (eds.) Methods of soil analysis. Part 2. 2nd ed. Agron. Monogr. 9. ASA and SSSA, Madison, WI.

Anderson, J.M. 1991. The effects of climate change on decomposition processes in grassland and coniferous forests. Ecol. Appl. 1: 326-347.

Agarwal, A.S., B.R. Singh, Y. Kanehiro. 1971. Soil nitrogen and carbon mineralization as affected by drying-rewetting cycles. Soil Sci. Soc. Am. J. 35: 96-100.

Boone, R.D., K. Nadelhoffer, J.D. Canary, and J.P. Kaye. 1998. Roots exert a strong influence on the temperature sensitivity of soil respiration. Nature 396: 570-572.

Bowden, R.D., K.M. Newkirk, and G.M. Rullo. 1998. Carbon dioxide and methane fluxes by a forest soil under laboratory-controlled moisture and temperature conditions. Soil Biol. Biochem. 30: 1591-1597.

Burford, J.R. and J.M. Bremner. 1975. Relationships between the denitrification capacities of soils and total, water-soluble, and readily decomposable soil organic matter. Soil Biol. Biochem. 7: 389-394.

Curiel Yuste, J., D.D. Baldocchi, A. Gershenson, A. Goldstein, L. Mission, and S. Wong. 2007. Microbial soil respiration and its dependency on carbon inputs, soil temperature and moisture. Glob. Change Biol. 13: 2018-2035.

Curtin, D., C.A. Campbell, A. Jalil. 1998. Effects of acidity on mineralization: pH dependence of organic matter mineralization in weakly acidic soils. Soil Biol. Biochem. 30: 57-64.

Davidson, E.A., S.C. Hart, C.A. Shanks, and M.K. Firestone. 2006. Measuring gross nitrogen mineralization and nitrification by N^{15} isotopic pool dilution in intact soil cores. Eur. J. Soil Sci. 42: 335-349.

Fulmer, H.L. 1917. The relation of green manures to nitrogen fixing. Soil Science. 4: 1-18.

Hassink, J. 1992. Effects of soil texture and structure on carbon and nitrogen mineralization in grassland soils. Biol. Fert. Soils 14: 126-134.

Ilstedt, U., A. Nordgren, and A. Malmer. 2000. Optimum soil water for soil respiration before and after amendment with glucose in humid tropical acrisols and a boreal mor layer. Soil Biol. Biochem. 32: 1591-1599.

Kirschbaum, M.U.F. 1995. The temperature dependence of soil organic matter decomposition and the effect of global warming on soil organic C storage. Soil Biol. Biochem. 27: 753-760.

Leirós, M.C., C. Trasar-Cepeda, S. Seoane, and F. Gil-Sotres. 1999. Dependence of mineralization of soil organic matter on temperature and moisture. Soil Biol. Biochem. 31: 327-335.

Linn, D.M. and J.W. Doran. 1984. Effect of water-filled pore space on carbon dioxide and nitrous oxide production in tilled and nontilled soils. Soil Sci. Soc. Am. J. 48: 1267-1272.

Lomander, A., T. Kätterer, and O. Andrèn. 1998. Carbon dioxide evolution from top- and subsoil as affected by moisture and constant and fluctuating temperature. Soil Biol. Biochem. 30: 2017-2022.

Lucas, R.E. 1982. Organic Soils (Histosols) Formation distribution, physical and chemical properties and management for crop production. Michigan State University, Research Report No. 435 (Farm Science).

Luo, Y., and X. Zhou. 2006. Soil Respiration and the Environment. Academic Press, New York.

McBeth, I.G. 1917. Relation of the transformation and distribution of soil nitrogen to the nutrition of citrus plants. J. Agri. Sci. 9: 183-252.

Mervosh, T.L., G.K. Sims, E.W. Stoller, and T.R. Ellsworth. 1995. Clomazone sorption in soil: incubation time, temperature, and soil moisture effects. Agri. Food Chem. 43: 2295-2300.

Miller, R.D. and D.D. Johnson. 1964. The effect of soil moisture tension on carbon dioxide evolution, nitrification, and nitrogen mineralization. Soil Sci. Soc. Am. J. 28: 644-647.

Nadelhoffer, K.J., A.E. Giblin, G.R. Shaver, and J.A. Laundre. 1991. Effects of temperature and substrate quality on element mineralization in six arctic soils. Ecology 72: 242-253.

Qualls, R.G. and C.J. Richardson. 2008. Decomposition of litter and peat in the everglades: the influence of P concentrations. p. 441-460. *In* Everglades Experiments: Lessons for Ecosystem Restoration. Springer, New York.

Reddy, K.R., T.C. Feijtel, and W.H. Patrick Jr. 1986. Effects of soil redox conditions on microbial oxidation of organic matter. p. 117-133. *In* Y. Chen and Y. Avnimelech (ed.) The Role of Organic Matter in Modern Agriculture. Martinus Nijhoff, Netherlands.

Sugimoto, A. and E. Wada. 1993. Carbon isotopic composition of bacterial methane in a soil incubation experiment: contributions of acetate and CO_2/H_2. Geochim. Cosmochim. Ac. 57: 4015-4027.

Waksman, S.A. and R.C. Cook. 1916. Incubation studies with soil fungi. Soil Science 1:275:284.

Wen , Xue-Fa, Gui-Rui Yu, Xiao-Min Sun, Qing-Kang Li, Yun-Fen Liu, Lei-Ming Zhang , Chuan-You Ren, Yu-Ling Fu, and Zheng-Quan Li. 2006. Soil moisture effect on the temperature dependence of ecosystem respiration in a subtropical *Pinus* plantation of southeastern China. Agr. Forest Meteorol. 137: 166-175.

Zak, D.R., W.E. Holmes, N.W. MacDonald, and K.S. Pregitzer. 1999. Soil temperature, matric potential, and the kinetics of microbial respiration and nitrogen mineralization. Soil Sci. Soc. Am. J. 63: 575-584.

Table 3.1. Mean water content (θ) with standard deviation for soil aliquots within each incubation.

		Incubation			
		----------37°C----------		---------25°C----------	
		Rep 1	Rep 2	Rep 1	Rep 2
Condition	Parameter	θ			
		----------$m^3\ m^{-3}$----------			
Dry	Mean	0.128	0.168	0.153	0.167
	StDev	0.004	0.004	0.003	0.000
Moist	Mean	0.209	0.313	0.257	0.314
	StDev	0.014	0.004	0.023	0.001
Wet	Mean	0.281	0.465	0.405	0.455
	StDev	0.038	0.006	0.018	0.002

Table 3.2. Mineralization rate and temperature response (Q_{10}) for each moisture content condition.

Incubation Temperature	Mineralization Rate		
°C	----------mg C kg-^{1} soil d^{-1}----------		
	Dry	Moist	Wet
25	29.23	46.65	26.53
37	52.91	96.51	80.24
Q_{10}	1.64	1.83	2.51

Table 3.3. Fit statistics for the models used to predict mineralization response.

Goodness of Fit Statistic	Value
-2 Res Log Likelihood	254.3
AIC	258.3
AICC	258.5
BIC	257.1

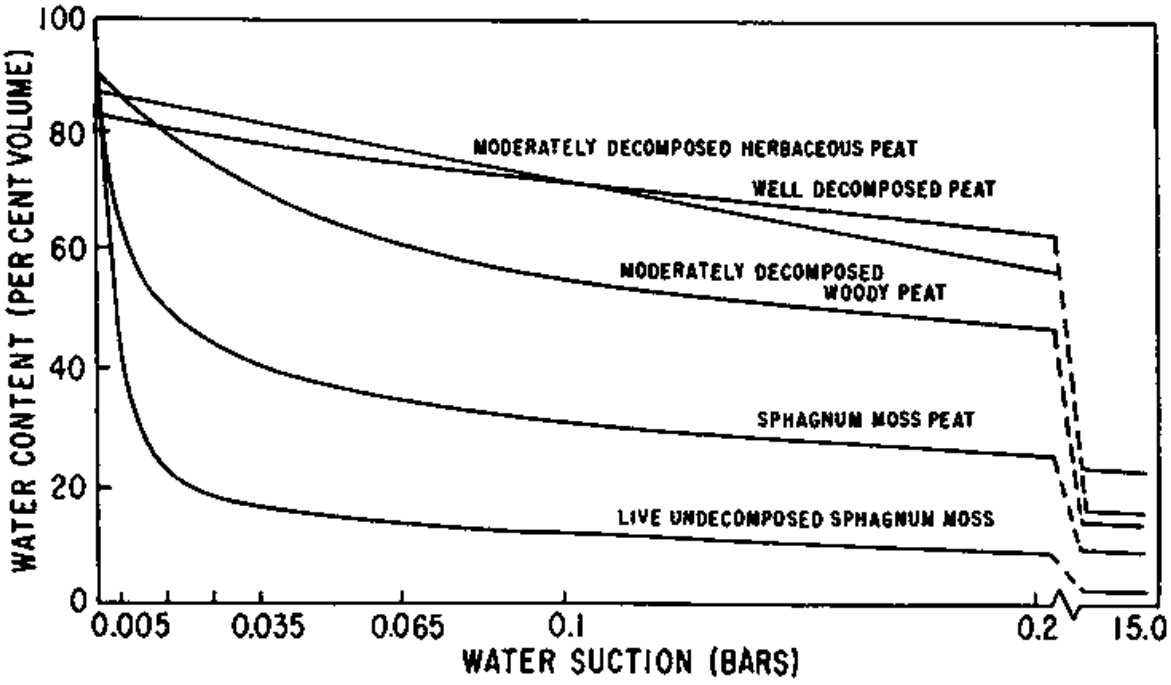

Figure 3.1. Soil water retention curves for peat in varying stages of decomposition (Lucas, 1982).

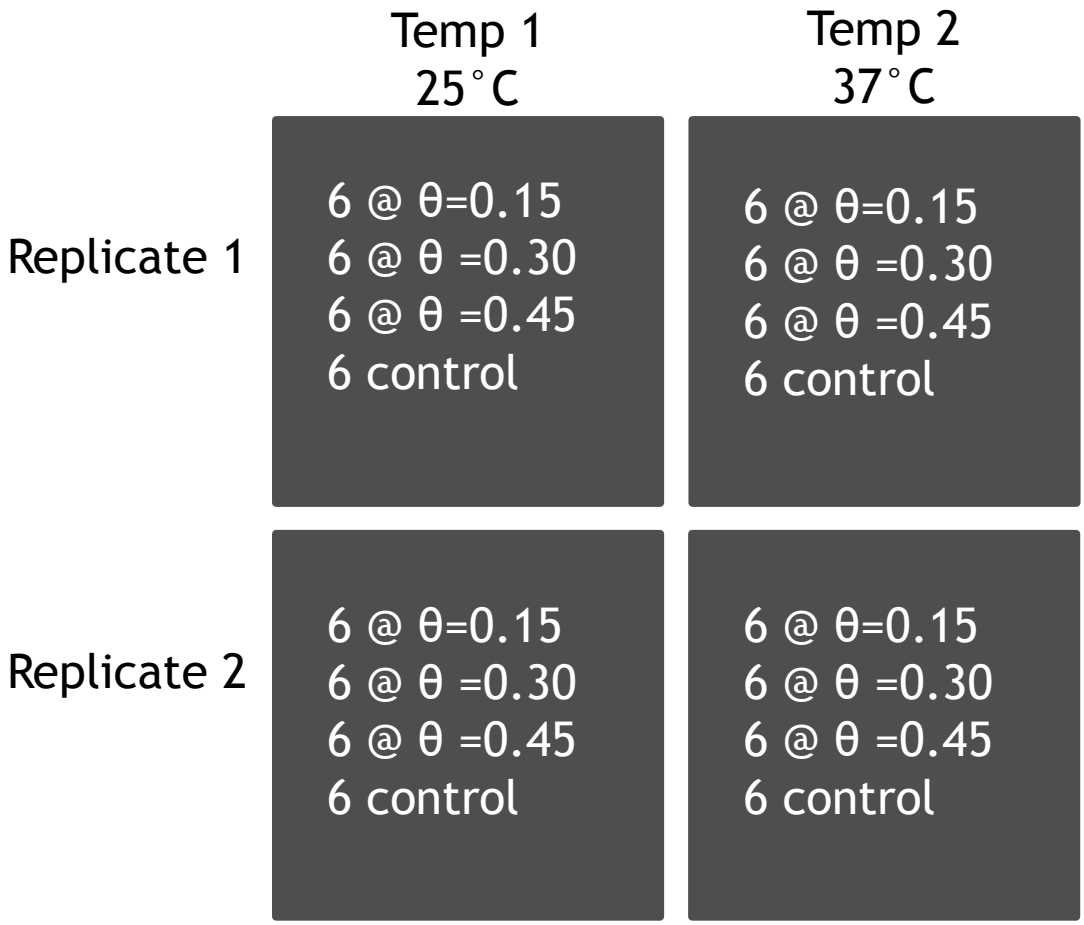

Figure 3.2. Incubation experiment design. Each box represents one 48 h incubation of 18 soil samples.

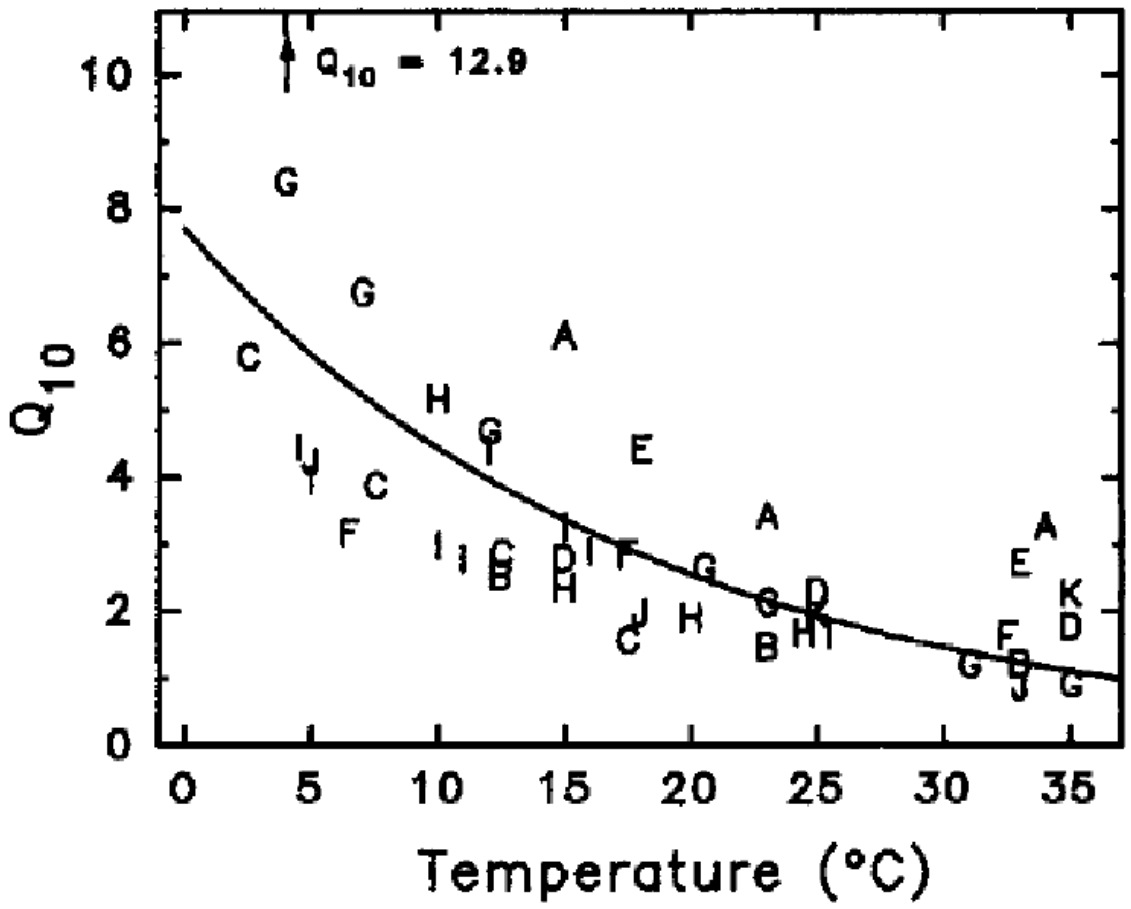

Figure 3.3. Experimental C mineralization Q_{10} values with corresponding temperature (Kirschbaum, 1995).

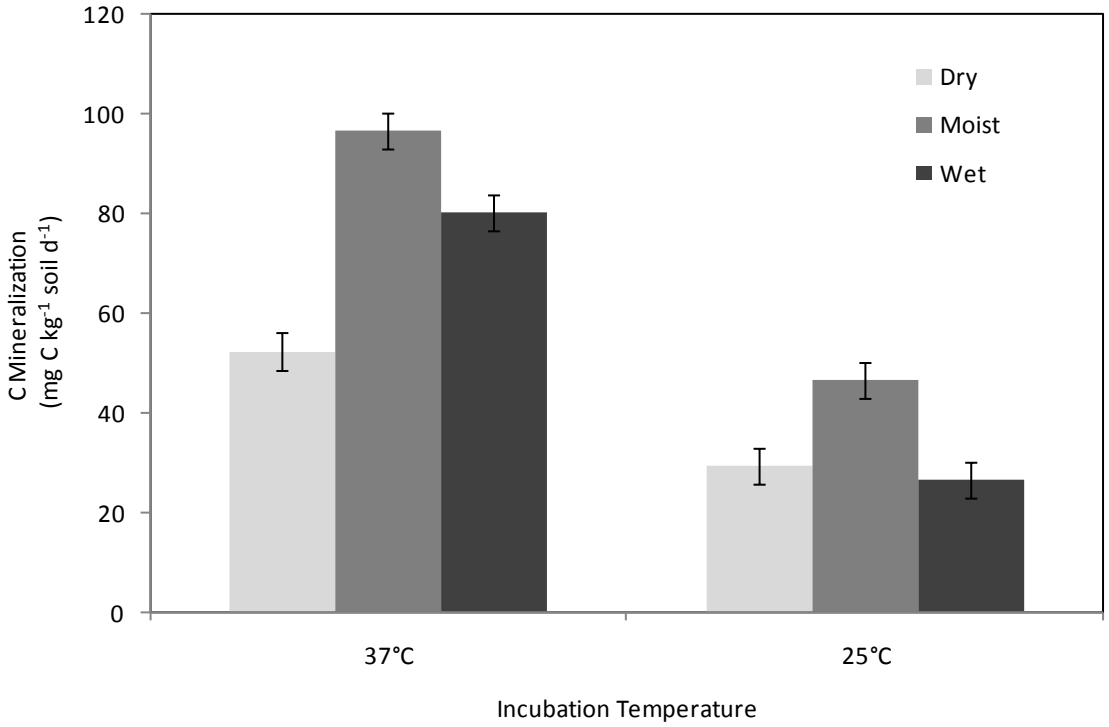

Figure 3.4. Mean C mineralization rate by soil water condition and incubation temperature. Error bars indicate standard error of the mean.

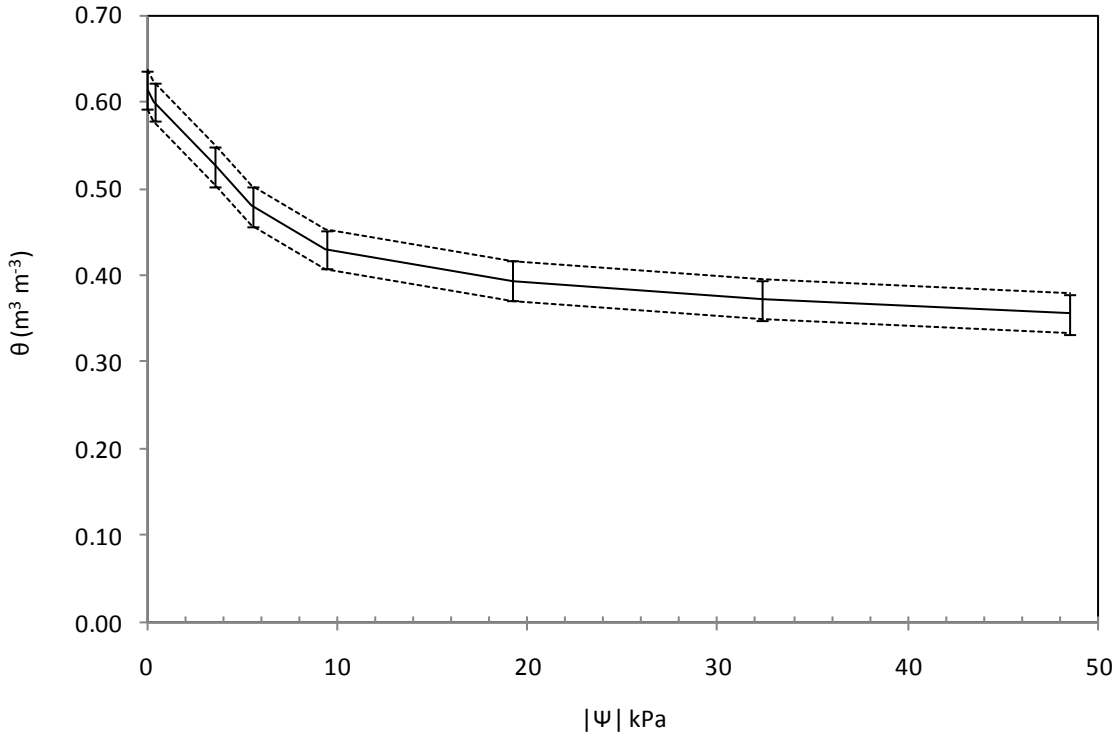

Figure 3.5. Soil water content (θ) versus matric potential (ψ) with 95% CI for intact cores of incubated soil.

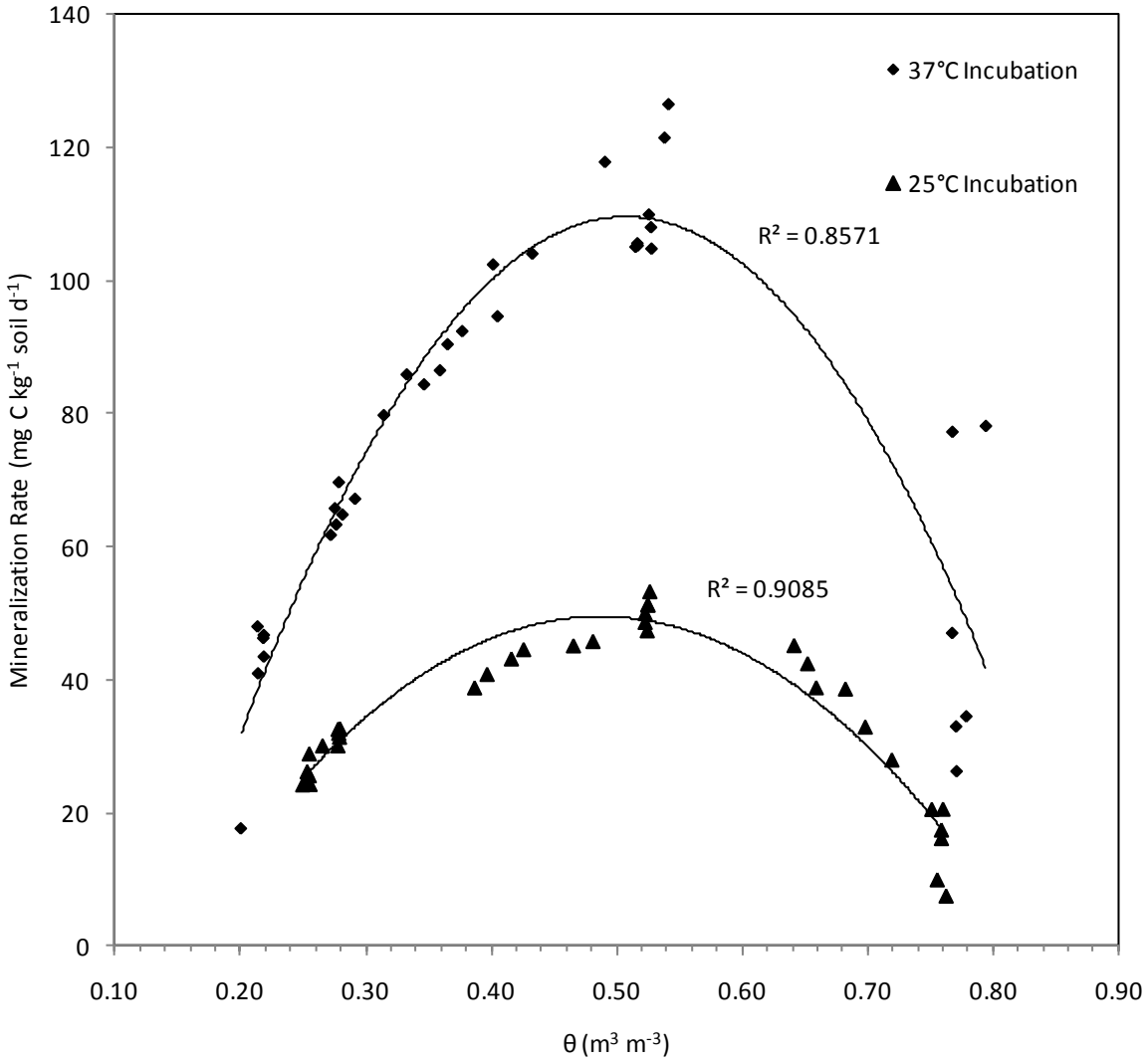

Figure 3.6. Observed C mineralization rates (points) for various water contents (θ) at two incubation temperatures and their respective models (lines). Model equations are given in the text.

Chapter 4: Conclusions and Significance of Results

A series of three experiments conducted to better understand C dynamics in peat soils unique to warm weather regions were performed for a number of reasons. Histosols possess high potential for soil C sequestration, and conversely as CO_2 emitters. Histosols were inherent soil C sinks during their respective periods of formation, when soil temperature and water content were precisely balanced to permit high soil C depositions and low organic matter decomposition. Although, in the face of disturbances like deforestation, drainage, plowing, liming, and burning, Histosols can become huge emitters of CO_2. In fact, evidence suggests disturbed Indonesian peat bogs may emit as much as 14% of the world's annual CO_2 emissions (Clover, 2005). While we should not expect all peats to emit CO_2 to the same magnitude as those in Indonesia, Histosols nonetheless are a major component of the global soil C reservoir and understanding their response to changing environmental conditions is essential.

Specifically, we decided to study temperature and moisture effects on one soil mapped as the Ponzer series (Loamy, mixed, dysic, thermic Terric Haplosaprists). Our soil of interest is one of many Saprists located in North Carolina, particularly the lower coastal plain and the centers of Carolina bays. Differences among many of the organic soils within the region are so subtle that results and applications from this study could probably be safely applied to many other similar soil series. While Ponzer soils are similar to many other organic soils in the region, it differs from many peats discussed in the literature, e.g., parent material and temperature regime. Differences can be so pronounced that comparisons across suborders may be inappropriate or unreliable. For these reasons, we focused our research on the soil discussed throughout the previous chapters.

The experiments we conducted shared a common theme of testing temperature and soil moisture effects on C mineralization. The first experiment was designed to balance control over

environmental conditions, commonly reserved for the laboratory, with intact soil, typically achievable only in a field setting. This greenhouse mesocosm experiment was useful for showing that reductions in total solar irradiance could decrease soil temperatures enough to cause measureable differences in C mineralization rates. In fact, average CO_2 efflux was reduced by 50% when sunlight reaching the soil surface was limited to 10% of ambient. Efflux under full sun averaged 4.1322 µmol m^{-2} s^{-1} and 2.0544 µmol m^{-2} s^{-1} under 90% shade. This difference was significant at α=0.05. There were also measureable differences in mineralization between unshaded mesocosms and those under 70% shade. Efflux was 16% lower under 70% shade compared to full sun, 3.4380 and 4.1322 µmol m^{-2} s^{-1}, respectively.

Our ability to show measureable differences in C mineralization was achievable under various shade treatments prompted the design of a similar experiment in a field setting. We selected Juniper Bay as our field site because it exemplified the potential transition from short term soil C loss under dry and hot agronomic production back to historic soil C storage as the water table is restored and vegetative establishment decreases soil temperatures via reductions in TSI.

During the Juniper Bay experiment, we demonstrated that sunlight attenuation caused reductions in soil temperature at 2.5 cm under field conditions. The sources of light reduction successful for reducing soil temperature included plant litter, herbaceous vegetation, and 70% light reducing shade cloth. Shade effects on soil temperature varied seasonally. The largest shade effect occurred under herbaceous vegetation in August when soil temperatures at 2.5 cm under herbaceous vegetation were 11°C cooler than soil exposed to full sun. At the same time, soil under 70% shade cloth was 8°C cooler than unshaded soil. The vegetation shade effect was lower in the spring when the previous year's plant litter was primarily responsible for reducing TSI. In May, soil under vegetation was only about 4° to 6°C cooler than unshaded soil. 70% shaded soil

temperatures ranged from 5° to 9°C cooler than unshaded soil during the same period.

Field CO_2 efflux measurements correlated well with soil temperatures temporally and between shade treatments. Efflux rates across treatments were low, < 3.0 µmol CO_2 m^{-2} s^{-1} during the first days of measurements but increased to over 7.0 µmol CO_2 m^{-2} s^{-1} on August 28. Between shade treatments, the highest rates of CO_2 efflux came from unshaded soil on all 16 d that measurements were taken. Efflux from unshaded soil was clearly higher than shaded treatments on most days, though high variability precluded statistical significance. On 14 of 16 d, 70% shaded soil showed the lowest CO_2 efflux rates.

CO_2 efflux also showed a strong temporal correlation with water table depth, increasing across treatments as the water table receded after June 19. A soil water retention curve showed macropore dewatering occurred from 0 to -10 kPa. Matric potential at 10 cm fell between this range when the water table dropped. It is likely that enhanced atmospheric gas exchange following macropore dewatering in the field created conditions more favorable for aerobic SOM decomposition, resulting in higher measured CO_2 efflux across treatments. Because soil water potential did not vary widely between shade treatments, efflux differences were likely due to temperature effects.

The experiment at Juniper Bay was successful for showing herbaceous vegetation in the form of forbs and graminoids can reduce soil temperature by decreasing TSI. In fact, soil temperature reduction via TSI attenuation was even more successful in the field than in the greenhouse. Consequently, we have every reason to believe that herbaceous vegetation establishment accompanying mitigation will reduce soil temperatures, but the effect will be greatest when the vegetative canopy is at peak density.

While shade effects on temperature and C mineralization seemed straightforward in the

greenhouse and field experiment, we still needed to determine precisely how the soil used for the previous two experiments responded to temperature and moisture controls in the absence of complicating factors. To do so, we conducted a series of incubations to measure C mineralization rates at two temperatures and three ranges of water content. Those incubations provided additional insight to temperature/moisture influences on mineralization that would have otherwise been lost.

A temperature/moisture interaction previously unseen manifested in the incubation data. Mineralization response to temperature, or Q_{10}, was positively correlated with soil water content. Q_{10} was lowest under dry soil moisture conditions (1.64 at 0.15-0.16 m^3 m^{-3}) and increased as water content increased (1.83 at 0.21-0.31 m^3 m^{-3}) reaching a peak of 2.55 at 0.40 m^3 m^{-3}. This was a particularly interesting development, because it suggested the soil at Juniper Bay may be more temperature sensitive than the literature suggests. Kirschbaum's (1995) synthesis of published Q_{10} values showed Q_{10} typically falls around 2.0 for our incubation temperatures (Fig. 2.3), and that was true when Q_{10} for all water conditions was averaged. But, at soil water potentials similar to those observed at Juniper Bay, Q_{10} was 2.55, 28% higher than the average for all water contents. The high Q_{10} under normal field conditions was additional evidence that (1) observed efflux differences in the greenhouse and field were probably due to shade controlled temperature effects and (2) there exists a high potential for reducing soil C loss from these soils by decreasing soil temperatures with surface shading.

The experiments discussed herein showed strong evidence that surface shading has profound effects on the rate of soil C loss from peatlands found in Carolina bays and possibly throughout the Atlantic coastal plain. Reduction of C mineralization was observed under as little as 70% light reduction, which was easily achievable with herbaceous vegetation. Although, seasonal variability in light reduction under herbaceous vegetation prohibited consistent reductions in temperature and CO_2 efflux throughout the growing season.

Proper maintenance of the water table to keep these soils saturated and anaerobic will certainly have the greatest effect for reducing soil carbon losses. Although, when precipitation input is low in dry years, the water table can drop during the warm summer months. As soils become aerobic C mineralization will increase. While soils are aerobic, the shading and cooling effect of vegetation will provide additional measures for effectively mitigating soil C losses. We conclude that further reductions in soil C loss can be reached with simple establishment of herbaceous vegetation, though more research is needed to determine whether greater reductions are possible with different plant communities.

REFERENCES:

Clover, C. 2005. Peat bog burning blamed for much of global warming. Daily Telegraph. Telegraph Media Group Limited, UK. http://www.telegraph.co.uk/news/uknews/1497501/Peat-bog-burning-blamed-for-much-of-global-warming.html. Accessed 12/1/09. Verified 12/1/09.

Kirschbaum, M.U.F. 1995. The temperature dependence of soil organic matter decomposition and the effect of global warming on soil organic C storage. Soil Biol. Biochem. 27: 753-760.

McDaniel, P. 2009. Global Distribution of Histosols. Soil Science Division, University of Idaho, Moscow, ID. http://soils.cals.uidaho.edu/soilORDERS/i/Histosols.jpg Accessed 12/1/09.

APPENDIX A

Redox Potential within Mesocosm Profiles

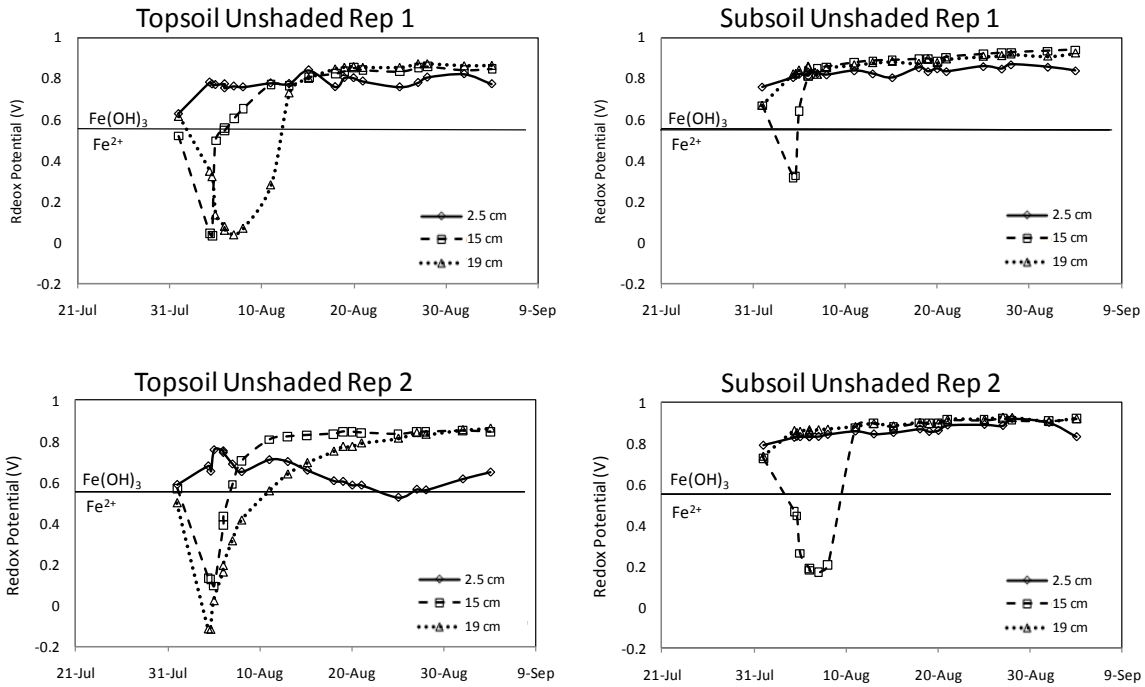

Figure A.1. Profile redox potential within topsoil and subsoil mesocosms under full sun.

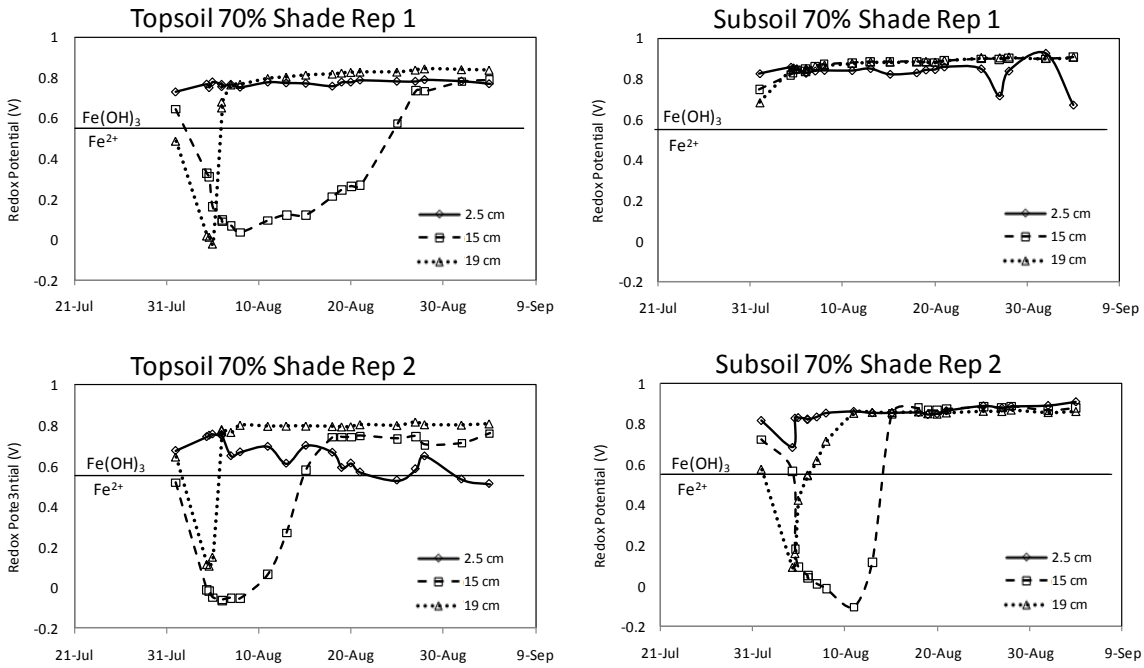

Figure A.2. Profile redox potential of topsoil and subsoil mesocosms under 70% shade.

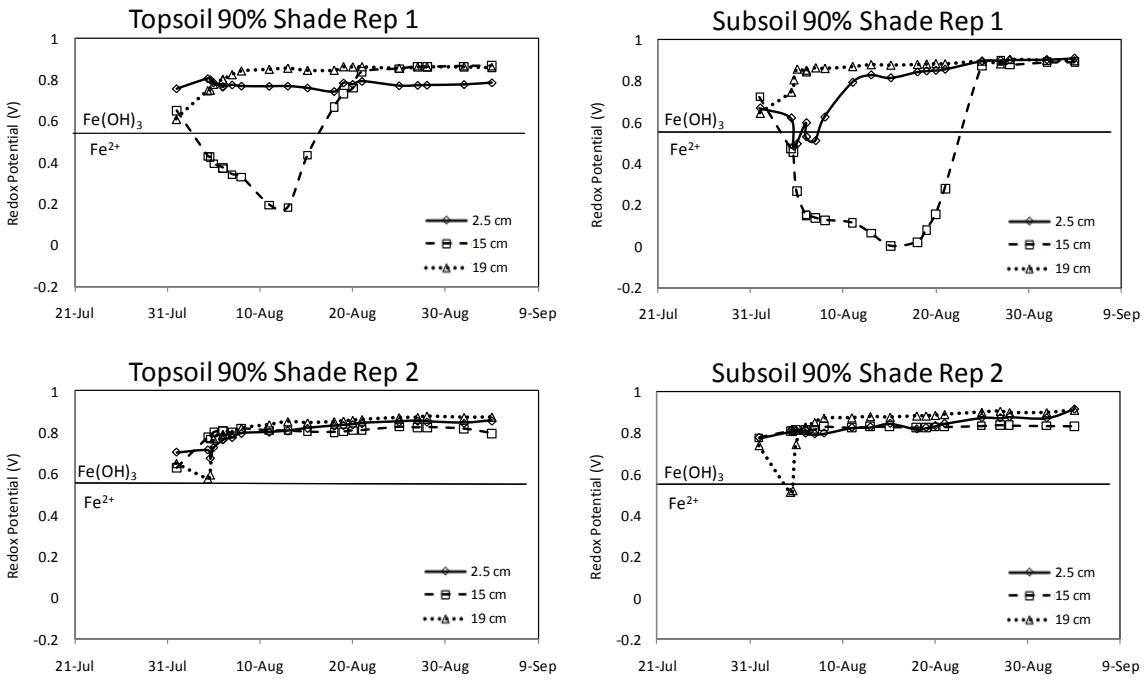

Figure A.3. Profile redox potential of topsoil and subsoil mesocosms under 90% shade.

APPENDIX B

Vegetation Photos at Juniper Bay Field Site

9 April 2009

26 May 2009

30 June 2009

17 August 2009

Figure B.1. Stages of vegetation growth at Juniper Bay field site.